

Copyright

By

Jeffrey Todd Cullen

2013

**The Thesis Committee for Jeffrey Todd Cullen**

**Certifies that this is the approved version of the following thesis:**

**Halogen chemistry and stable chlorine isotope composition of thermal  
springs and arc lavas in the Cascade arc**

**APPROVED BY  
SUPERVISING COMMITTEE:**

**Supervisor:**

\_\_\_\_\_  
Jaime D. Barnes, Supervisor

\_\_\_\_\_  
John Lassiter

\_\_\_\_\_  
Shaul Hurwitz

\_\_\_\_\_  
William P. Leeman

**Halogen chemistry and stable chlorine isotope composition of thermal  
springs and arc lavas in the Cascade arc**

**By**

**Jeffrey Todd Cullen, B.S.**

**Thesis**

Presented to the Faculty of the Graduate School of

The University of Texas at Austin

In Partial Fulfillment

of the Requirements

for the degree of

**Master of Science in Geological Sciences**

**The University of Texas at Austin**

**August 2013**

## **Dedication**

I would like to dedicate this thesis to the two most notable influences in my life thus far. To my magnificent parents, you have made the past two years of working on this project go by so much better through your motivation and understanding, especially of my frequent periods of unavailability due to being so busy. Also to my undergraduate research advisor Dr. Glenn Miller who, although is not exactly a geologist or even an isotope chemist, taught me how to approach scientific questions and allowed me to truly appreciate how fortunate we are as scientists to be able to do what we love pursuing research..

## Acknowledgements

I would not be where I am today without the guidance and support of my advisor Dr. Jaime Barnes. If it weren't for you I probably would not have ended up at UT; it was you that dug up my application from the pile of other hundreds, and recommended me for admission. Even after being admitted I was a little sluggish, and it took me over a semester to decide that I wanted you as an advisor and to work on stable isotopes, but looking back I am so happy I did. Your openness to pursue new ideas and accommodating nature helped me immensely over the past two years of this masters project. You are a superb scientist, teacher, and advisor; how you balance family and being a great mom I'll never know. If I someday become a professor, you have set the example I'll try to live up to. Thank you for everything and am so glad I have the opportunity to stay and work with you for another four years.

Mom, Dad, Kelley, and Justin thank you for all your love and encouragement, especially over the past 2 years as it really has been the first time I've properly been away from home. Eventhough you probably still have no idea what I do, your support in my decision to pursue a Ph.D. means so much. When I was trying to figure out what I wanted to do and where I wanted to go after undergrad, you told me to just do what I wanted to do and what felt best. That was good advice because I ended up in a pretty awesome place.

Thank you to my committee members John Lassiter, Shaul Hurwitz, and Bill Leeman for all your help and contributions to this project. Shaul, without you, Jaime and I would have never come up with the idea to look at hot springs and the samples you, Deb Bergfeld, and Jennifer Leweicki provided helped make this study more complete. Bill, the lavas samples you gave me were equally invaluable, and we really need to get more! I've thoroughly enjoyed our discussions and pondering the complexities of the Cascades and behavior of halogens in magmatic systems. To both of you, I hope we can continue such exchanges of ideas and conversations as I embark on my future Ph.D. work.

To the stable isotope group, Toti Larson, Miguel Cisneros, Nick Benz, Tim Prather, Edward Marshall IV, as well as Jay Santillan, thank you for all your help in the lab and in the field. It was always nice having some good banter to break up the day, especially during those, long, important times of non-stop writing.

Philip Guerrero is amazing, and if it were not for him I don't think any graduate student here would know what was going on and be able to graduate on time. Finally, all the good friends I've had the opportunity of making while at the Jackson School, thank you for giving me numerous great experiences and relationships I'll get to keep with me for the rest of my life. At one point or another we've all been in the same boat, and your understanding and advice has made life much easier over the past couple of years. It feels like we've become bit of a little geology family, and as we all start going our separate ways, try not to be a stranger

## **Abstract**

### **Halogen chemistry and stable chlorine isotope composition of thermal springs and arc lavas in the Cascade arc**

Jeffrey Todd Cullen, M.S. Geo. Sci

The University of Texas at Austin, 2013

Supervisor: Jaime Barnes

The stable isotope compositions (chlorine, oxygen, and hydrogen), major anion concentrations, and major/minor cation concentrations of 37 thermal (any spring water with temperature at least 6.5° C above mean ambient air temperature) and mineral springs from the Cascade Volcanic arc system were measured in order to better determine chlorine sources within the Cascades hydrothermal systems, and thus place better constraints on halogen flux through the subduction zone. Typically, most subduction zone flux calculations have been limited to the study of the erupted magmas and gases from fumarole vents, yet magmatic discharge through thermal springs may be

considerable, particularly those in the often ignored forearc. Additionally, 9 geochemically well characterized lavas from across the Mt. St. Helens/Mt. Adams region of the Cascade arc (Leeman et al. 2001, 2005) were analyzed for their halogen concentrations, as well as their Cl stable isotope composition. Cl concentrations in the springs range from 6 to 13,850 ppm and have  $\delta^{37}\text{Cl}$  values that range from -0.1‰ to +1.9‰ (average =  $+0.8 \pm 0.4\%$ ; error =  $\pm 0.2\%$ ), with no systematic variation along or across the arc. The slightly positive values ( $\sim -0.0$  to  $+0.9\%$ ) may be explained by fluid-rock interaction with underlying lithologic units, such as  $^{37}\text{Cl}$ -enriched volcanic sequences, and/or serpentinites or oceanic crust of accreted oceanic terranes. Another process possibly contributing to these positive  $\delta^{37}\text{Cl}$  values, particularly those with  $\delta^{37}\text{Cl} > 1\%$ , is magmatic HCl fractionation during degassing generating an enriched  $^{37}\text{Cl}$  vapor and mixing with thermal waters. We cannot completely rule out slab-derived altered oceanic crustal chlorine that has degassed into the springs, although most slab Cl is believed to have already been devolatilized from the slab before reaching subarc depths corresponding to longitudes where these springs are located at the surface.

Lavas from the arc transect exhibit highest Cl concentrations at the volcanic front compared to the forearc and backarc. Br, like Cl, exhibits highest concentrations along the volcanic front. F and I show a progressive decrease in concentration from forearc to backarc which may demonstrate the putative early surge of fluids/fluid mobile element loss early in subduction at relatively shallow depth.  $\delta^{37}\text{Cl}$  values range from -0.1 to +0.8‰ (error =  $\pm 0.2\%$ ) and may reflect a component of assimilation of crustal material,

or is derived from an enriched mantle, although we cannot completely rule out some isotopic fractionation and/or slab-derived chlorine.

# Table of Contents

|  |      |
|--|------|
| List of Tables.....  | xii  |
| List of Figures.....   | xiii |
| Chapter 1: Introduction.....                                       | 1    |
| Chapter 2: The Cascadia Subduction Zone.....                       | 10   |
| 2.1 Geologic Background.....                                       | 10   |
| 2.2 Cascade Thermal Springs and Previous Work.....                 | 15   |
| Chapter 3: Spring Sites, Sampling and Field Data.....              | 18   |
| 3.1 South Segment: northern California.....                        | 18   |
| 3.1.1 Sampling Sites.....  | 19   |
| 3.2 Central Segment: northern CA, southern and central Oregon..... | 21   |
| 3.2.1 Sampling Sites.....  | 22   |
| 3.3 Columbia Segment: northern Oregon & southern Washington.....   | 24   |
| 3.3.1 Sampling Sites.....  | 25   |
| 3.4 North Segment: northern Washington.....                        | 28   |
| 3.4.1 Sampling Sites.....  | 29   |
| Chapter 4: Methods.....  | 35   |
| 4.1 Field sampling techniques.....                                 | 35   |
| 4.2 Major element chemistry of thermal waters.....                 | 35   |
| 4.2.1 Alkalinity analysis.....                                     | 35   |
| 4.2.2 Anion analysis.....  | 36   |
| 4.2.3 Cation analysis.....   | 37   |
| 4.2.4 $\delta\text{D}$ and $\delta^{18}\text{O}$ analysis.....     | 37   |
| 4.2.5 $\delta^{37}\text{Cl}$ analysis.....                         | 37   |
| 4.3 Rock Geochemistry.....   | 39   |

|  |     |
|--|-----|
| Chapter 5: Results.....  | 40  |
| 5.1 Springwater Chemistry.....   | 40  |
| 5.1.1 Cl, O, and H stable isotopes.....                                      | 41  |
| 5.2 Halogen Chemistry and Stable Cl Isotopes of Volcanic Rock Powders.....   | 42  |
| Chapter 6: Discussion.....   | 50  |
| 6.1 Halogens in the Columbia Transect Lavas.....                             | 50  |
| 6.2 Potential Chloride Sources to the Thermal Springs .....                  | 68  |
| 6.3 Spatial Variability of Cl and $\delta^{37}\text{Cl}$ Along The Arc ..... | 80  |
| 6.4 Assessing Cl Transport Through the Cascade Subduction Zone.....          | 84  |
| Chapter 7: Conclusions.....  | 85  |
| APPENDIX A: THERMAL SPRINGWATER GEOCHEMICAL DATA.....                        | 88  |
| APPENDIX B: WHOLE ROCK MAJOR, TRACE, AND ISOTOPE<br>GEOCHEMISTRY .....       | 97  |
| REFERENCES.....  | 102 |

## List of Tables

|   |    |
|---|----|
| Table 1: Collected thermal springwater field data.....  | 31 |
| Table 2: Arc transect lavas from the Columbia Segment.....  | 34 |
| Table 3: Chemical data for thermal springwaters.....  | 46 |
| Table 4: Halogen concentration and stable Cl isotope composition of the Columbia<br>Transect lavas..... | 48 |
| Table A1: Geochemical data for thermal springwaters.....  | 89 |
| Table A1: Whole rock major, trace and isotope geochemistry.....   | 98 |

## List of Figures

|   |    |
|---|----|
| Figure 1: Range of $\delta^{37}\text{Cl}$ values of various Cl reservoirs .....   | 9  |
| Figure 2: Generalized geologic map of the Cascade Volcanic Arc .....  | 13 |
| Figure 3: Spring locations sampled from within the Cascades South Segment, northern<br>CA .....                                       | 20 |
| Figure 4: Spring locations sampled from within the Cascades Central Segment .....   | 23 |
| Figure 5: Spring locations sampled from within the Cascades Columbia Segment .....  | 26 |
| Figure 6: Lava sample locations sampled from the Columbia Transect of southwest<br>Washington.....                                    | 27 |
| Figure 7: Spring locations sampled from within the Cascades North Segment.....  | 30 |
| Figure 8: $\delta\text{D}$ Anion, Cation and Halogen ternary plots of select thermal springwaters and<br>Columbia Transect lavas..... | 43 |
| Figure 9: $\delta\text{D}$ vs. $\delta^{18}\text{O}$ plot of the 17 spring waters collected and analyzed by myself ....               | 44 |
| Figure 10: $\delta^{37}\text{Cl}$ vs. log concentration chloride for the 37 thermal spring waters .....                               | 45 |
| Figure 11: $\delta^{37}\text{Cl}$ value vs. west longitude across the Columbia Transect of the Cascade<br>Arc.....                    | 49 |
| Figure 12: (Cl, Br, F, and I)/Nb ratios of the 9 arc transect lavas .....   | 54 |
| Figure 13: Br vs. Cl concentration of the 9 arc transect lavas .....  | 56 |
| Figure 14: Cl Cl/Br ratio of lavas with plotted with respect to west longitude along the arc<br>transect .....                        | 57 |
| Figure 15: Ba/Nb ratio of the 9 cross-arc transect lavas plotted with respect to west<br>longitude along the arc transect .....       | 58 |
| Figure 16: Cl and Br vs. B concentrations of the 9 arc transect lavas .....   | 61 |

|   |    |
|---|----|
| Figure 17: Cl/B, Cl/Nb, and B/Nb*10 ratios for the 9 arc transect lavas plotted with respect to their west longitude along the transect ..... | 62 |
| Figure 18: $\delta^{37}\text{Cl}$ vs. Cl concentration for of the 9 arc transect lavas .....  | 65 |
| Figure 19: $\delta^{37}\text{Cl}$ value vs. west longitude across the Columbia Transect segment of the arc of the 9 lavas.....                | 66 |
| Figure 20: $\delta^{37}\text{Cl}$ value vs. Cl/Nb and B/Nb ratio of the 9 lavas from the Columbia Transect .....                              | 67 |
| Figure 21 $\delta\text{D}$ value vs. elevation of the thermal springs .....   | 72 |
| Figure 22: Na vs. Cl concentration of the measured thermal springwaters .....   | 73 |
| Figure 23: Cl vs. B and Cl vs. Br plots for the thermal springwaters .....  | 78 |
| Figure 24: $\delta^{37}\text{Cl}$ and Cl concentration variation in thermal springs plotted along full extent of the arc.....                 | 82 |
| Figure 25: $\delta^{37}\text{Cl}$ value vs. discharged water temperature of the thermal springs.....  | 83 |

## Chapter 1: Introduction

Subduction zones are Earth's recycling centers where sediments, oceanic crust, hydrothermally altered lithospheric mantle and even delaminated frontal-arc continental crust are conveyed back into the mantle (Stern, 2002; Tatsumi, 2005). However, volatiles, (i.e. H<sub>2</sub>O, CO<sub>2</sub>, H<sub>2</sub>S, SO<sub>2</sub>, HCl), and fluid mobile elements (FME, e.g., Cl, Br, B, F, S, Pb, As) are liberated from the slab in a subduction zone during metamorphic devolatilization reactions and largely returned to the surface (Manning, 2004; Peacock, 1990; Rüpke et al., 2004; Schmidt and Poli, 1998). Understanding the behavior of volatiles and FME in subduction zones is crucial for the accurate calibration of global elemental flux calculations used to predict long term climate forecasts (greenhouse gases discharge), understanding melt generation beneath volcanic arcs to better assess geohazards, and aid in the exploration of precious metal ore deposits formed as a by-product of subduction (Crowley, 2000; Grove et al., 2006; Hedenquist and Lowenstern, 1994; Nicholls and Ringwood, 1973; Robock, 2000; Schmidt and Poli, 1998).

Once volatiles are liberated from the slab, determination of their concentrations in fumarole discharge and the erupted volcanic material are the two primarily studied and conventional methods for calculating volatile elemental fluxes back to the surface. Much work has investigated gas emissions from volcanic centers across the world, as well as volatile contents of melt inclusions of primitive magmas in order to determine the flux of

volatiles through subduction zones (Fischer, 2008; Hilton et al., 2002; Wallace, 2005). However, less well studied and more poorly constrained is the flux of volatiles discharged into arc thermal springs. Furthermore, quantifying volatile budgets in subduction zones is very difficult. The many sinks and sources in the mantle and crust likely obscure pathways and reactions, resulting in considerable uncertainty in extrapolating surface observations (i.e., fluids, lavas) to specific processes at depth. However, by studying the chemistries of the thermal springs, I may be better able to assess whether their dissolved solutes are derived from a recycled subducted slab component, and are thus relevant to subduction flux calculations, or they reflect the incorporation of crustal material or pristine mantle and should not be considered in volatile flux calculations through the Cascades subduction zone.

A key constraint governing volatile behavior in subduction zones is the thermal regime. Numerous parameters must be taken into account when considering the thermal regime of a subduction zone, including slab dip, convergence rate, and slab age e.g. (Abers et al., 2006; Davies and Stevenson, 1992; Peacock, 1996; Syracuse et al., 2010). Cascadia is a unique case in that it is an anomalously warm end-member subduction zone compared to most others on Earth (Syracuse et al., 2010). This is a result of subduction of the very young Juan de Fuca, Explorer, and Gorda plates. (4-28 m.y., 2-8 m.y., and 10-26 m.y. respectively) (Wilson, 1988). A series of thermal models predict top of the slab temperatures between 387-438°C at 30 km depth for the Northern Cascades arc segment,

where in comparison the slab beneath southern Sumatra is predicted to only be as high as 218°C, and possibly as low as 98°C (Syracuse et al., 2010).

Based on such thermal models, as well as petrologic experimental results showing hydrous phase stability in P-T space, it is predicted that in Cascadia slab dehydration reactions initiate at very shallow depth (Bebout, 1996; Iwamori, 1998; Schmidt and Poli, 1998). Seismic imaging of the slab shows major fluid loss and resulting eclogitization of the slab to occur at approximately 40 km depth, and that perhaps as much as 98% H<sub>2</sub>O depletion has occurred from the initially hydrated sediments and oceanic crust by the time the Cascadia slab reaches subarc depths (Hacker et al., 2003; Rondenay et al., 2008). Progressive devolatilization of the subducting slab is also inferred from the geochemistry of primitive lavas spanning a transect in the Columbia region of SW Washington (Leeman et al., 2004). Boron, like the halogen elements, is a fluid mobile element in subduction zone settings and can be used, for example, to help gauge the extent of slab fluid addition to arc magmas. Boron concentrations along with  $\delta^{11}\text{B}$  values have been shown to decrease from forearc to back arc consistent with preferential release of <sup>11</sup>B from the slab (Hervig et al., 2002; Leeman et al., 2004; Palmer et al., 1992). Despite evidence for significant fluid and volatile loss from the slab before reaching sub-arc depths (~100km), some workers propose that part of the slab's volatile budget may be retained to greater depths; as much as 35% of the Cl measured in Central Oregon, Western Cascades hot springs could be derived from degassing of magma enriched in Cl from the devolatilization of the slab (Hurwitz et al., 2005). Additionally, Cl and H<sub>2</sub>O

contents of olivine-hosted melt inclusions in high-magnesium andesites and primitive basaltic andesites from Mt. Shasta range from 1590-2580 ppm Cl and 3.5-5.6 wt.% H<sub>2</sub>O (Ruscitto et al., 2011).

Cl and Br, and to a lesser extent F and I, are fluid mobile, “conservative”, incompatible elements that are often used as tracers for H<sub>2</sub>O cycling in subduction zones and to indirectly observe shallower process such as magma degassing (Bureau et al., 2000; Carroll and Webster, 1994; Kilinc and Burnham, 1972; Villemant and Boudon, 1999; Zajacz et al., 2012). Furthermore, the use of stable Cl isotopes have been used to study the migration of fluids in crustal environments, volatile recycling processes in subduction zones, and the interaction between oceanic lithosphere and seawater-derived hydrothermal fluids (Barnes and Sharp, 2006; Barnes et al., 2009; Bonifacie et al., 2008; Eggenkamp et al., 1995; Godon et al., 2004; John et al., 2010; John et al., 2011). Investigating the stable chlorine isotope composition of such fluids enables us to identify the primary chlorine source (i.e., magmatic, sedimentary saline pore fluids, Cl-bearing crustal minerals). Figure 1 shows the range of  $\delta^{37}\text{Cl}$  values for selected Cl bearing reservoirs.

Terrestrial  $\delta^{37}\text{Cl}$  values range from as low as -8‰ in marine pore waters to as high as +20‰ for high temperature fumarole gases from Mt. Etna (Ransom et al., 1995; Rizzo et al., 2013). MORB/upper mantle has a slightly negative value of  $-0.2 \pm 0.3\text{‰}$  (Sharp et al., 2007; Sharp et al., 2013). Marine sediments from the Pacific Ocean have  $\delta^{37}\text{Cl}$  values between  $-2.5$  and  $+0.7\text{‰}$  ( $n = 24$ ) with the majority of the samples having

negative values (Barnes et al., 2008; 2009), similar to marine and non-marine sediments from Chile ( $-2.6$  to  $+0.5\text{‰}$ , average =  $-0.6 \pm 1.0\text{‰}$ ; Arcuri and Brimhall, 2003). Marine pore waters are all distinctly negative ( $-7.8\text{‰}$  to  $+0.1$ ; Ransom et al., 1995; Spivack et al., 2002; Godon et al., 2004; Bonifacie et al., 2007). Nearly all deep formation waters are also limited to dominantly negative  $\delta^{37}\text{Cl}$  values between  $-3$  and  $\sim+0.5\text{‰}$  (Eastoe et al., 2001; Eggenkamp et al., 1995; Shouakar-Stash et al., 2007). Serpentinites range from  $-2.0$  to  $+1.6\text{‰}$  depending on the fluid source of hydration (Barnes and Sharp, 2006; Barnes et al., 2006; Barnes et al., 2008, 2009; Bonifacie et al., 2008a), with the majority of serpentinite samples hydrated by seawater and thus having slightly positive  $\delta^{37}\text{Cl}$  values ( $\sim +0.5\text{‰}$ ). Altered oceanic crustal rocks have values ranging from  $-1.6$  to  $+1.8\text{‰}$  with negative values in the clay-dominated low-temperature sections and positive values in the amphibole-dominated high-temperature sections of the crust (Bonifacie et al., 2007; Barnes and Cisneros, 2012). Cl isotope compositions measured in rocks from subduction zone settings vary, and can be quite heterogeneous even within a local area. Barnes et al. (2009) reports  $\delta^{37}\text{Cl}$  values from 23 volcanic centers in the Central American arc ranging from  $-2.6\text{‰}$  to  $+3.0\text{‰}$ .  $\delta^{37}\text{Cl}$  values of scoria ash samples from the Izu-Bonin Marianna Arc range from  $-2.0\text{‰}$  to  $0.0\text{‰}$ . (Barnes et al., 2008). However, 0-44 Ma air fall tephra from the Izu-Bonin Arc yield a large range of  $\delta^{37}\text{Cl}$  compositions from  $-2.1\text{‰}$  to  $+1.7\text{‰}$  (Barnes and Straub, 2010). Volcanic rocks collected from Mt. Etna define a narrower range,  $\delta^{37}\text{Cl} = \sim 0.0 \pm 0.7\text{‰}$  ( $n=5$ ) (Rizzo et al., 2013) as do basalts from the Aleutian Arc,  $\delta^{37}\text{Cl} = 0.2 \pm 0.6\text{‰}$  ( $n=11$ ) (Barnes, unpublished data). The cause

for the difference in  $\delta^{37}\text{Cl}$  values is believed to primarily be controlled by Cl source, but fractionation processes are another consideration.

Chlorine has been used as a fluid tracer, and is especially useful in high temperature systems, due to minimal to no Cl isotope fractionation occurring between minerals, melt/fluid, and vapor at high temperatures and during progressive subduction (Schauble et al., 2003; Liebscher et al., 2006; John et al., 2011; Barnes et al., 2006; Bonifacie et al., 2008). However, fractionation due to diffusion and/or ion membrane filtration in sedimentary pore fluids and other lithologies may effectively fractionate Cl isotopes during diagenesis under shallow zeolite facies conditions (Ransom et al., 1995).  $\delta^{37}\text{Cl}$  values as high as +19.7‰ have been reported for volcanic fumarole gases from the Central American Arc and Mt. Etna, and has been shown to be attributed to non-magmatic fractionation of HCl in a liquid/vapor system after gases were exsolved from the cooling magma, that is  $^{35}\text{Cl}$  and  $^{37}\text{Cl}$  have negligible fractionation as they initially degas from a magma (Barnes et al., 2009; Rizzo et al., 2013; Sharp et al., 2010). Also necessary for assessing Cl sources in the thermal springs is understanding Cl behavior in silicate melt during shallow crustal magma degassing. Cl behaves incompatibly during magma crystallization and its solubility in the melt is strongly controlled by pressure and  $\text{SiO}_2$  content where solubility increases with decreasing  $\text{SiO}_2$  content. It is removed from the melt by partitioning into a vapor phase, primarily hydrogen chloride, and to lesser extents NaCl, KCl, and  $\text{FeCl}_2$ , (Kilinc and Burnham, 1972; Zajacz et al., 2012).

The stable Cl isotope composition in thermal water should reflect the isotopic composition of the source from which it is derived, barring any subsequent fractionating reactions. Although stable isotope compositions of fluids have been well studied in deep formation brines, sediment pore fluids, and marine hydrothermal vents over oceanic ridges (Bonifacie et al., 2005; Bonifacie et al., 2007; Godon et al., 2004; Kaufmann et al., 1987; Kaufmann et al., 1993; Ransom et al., 1995; Spivack et al., 2002), little effort has been directed at investigating the stable Cl isotope composition of thermal springs, particularly arc-related springs (Barnes and Stefánsson, 2012; Eggenkamp et al., 1995; Kaufmann et al., 1984; Musashi et al., 2008; Zhang, 2004). In addition, previous studies do not address the halogen concentrations and Cl isotopic compositions of the volcanic rocks produced from within the arc, which may control the chemistries of the hot springs. This study uses chlorine stable isotopes and halogen concentrations to better constrain the source of Cl in arc thermal springs and halogen/Cl isotope behavior in the Cascades magmatic systems. Investigation of 9 well characterized lavas from the Columbia Transect in SW Washington will further allow us to identify any apparent coupled behavior between thermal springs and volcanic material in addition to identifying any across arc correlations in halogen chemistries and stable Cl isotope composition. Through these investigations I intend to address the following questions:

- 1) What are the sources of chlorine in the thermal springs in the Cascade arc?
- 2) Is there any observable spatial variability in Cl concentration and Cl isotope composition in the springs along and across the arc? What is responsible for the variability (or lack thereof)?

To address these questions, water samples from 37 springs were collected/provided for geochemical analysis. The 37 springs sampled are distributed over ~900 km of along strike arc distance, covering forearc, backarc, and volcanic arc axis regions. The scope of this sampling was to capture the entirety of the arc such that any large-scale geographic differences may be distinguished.

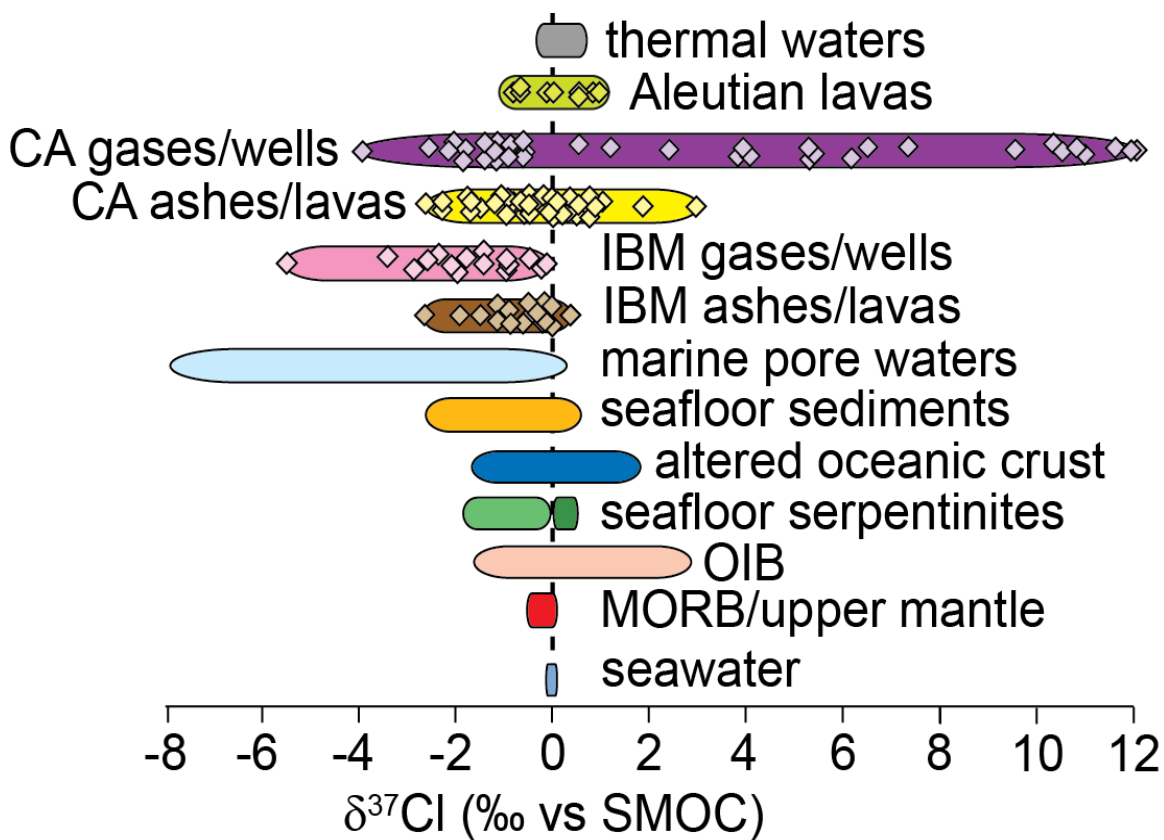


Figure 1: Range of  $\delta^{37}\text{Cl}$  values of various Cl reservoirs (modified from Barnes and Straub 2010) with previous data from the IBM system, volcanic front gases and geothermal wells, volcanic front ashes and lavas from (Barnes et al., 2008). Western Pacific seafloor sediments from (Barnes et al., 2008), serpentinites from (Barnes and Sharp 2006) and (Boniface et al., 2008) (n=88). Altered oceanic crust from (Boniface et al., 2008) (n=3); marine pore waters from (Boniface et al., 2007), (Godon et al., 2004), (Spivack et al., 2002), (Ransom et al., 1995), and (Hesse et al., 2000) (n=127). MORB from (Sharp et al., 2007, 2013). OIB from (John et al., 2010). Central American (CA) gases and geothermal wells, volcanic ashes and lavas from (Barnes et al., 2009). Aleutian lavas from (Barnes unpublished data). Thermal spring waters from (Kaufmann et al., 1984), (Vengosh 1991), (Eggenkamp 1994), (Zhang and Nordstrom 1994), and (Barnes and Stefansson 2012).

## **Chapter 2: The Cascadia Subduction Zone**

### **2.1 Geologic Background**

The Cascadia subduction zone and corresponding volcanic arc stretch approximately 1300 km from northern California to southern British Columbia and is the result of the eastward dipping convergence of the Juan de Fuca, Gorda, and Explorer plates beneath North America (von Huene and Scholl, 1991) (Figure 2). The convergence rate has decreased progressively from an initial rate of 16 cm/yr to the present rate of ~3.5 cm/yr (Duncan and Kulm, 1989; Verplanck and Duncan, 1987). By the time slab reaches the subduction trench it is a comparably very youthful 2-28 m.y. (Wilson, 1988, 2002). Because the slab is relatively young and has not had an extensive cooling history compared to most other subduction zones, it is globally characterized as having one of the warmest thermal regimes (Honda, 1985; Leeman et al., 2005; Syracuse et al., 2010), which has major implications regarding magma generation, elemental recycling, slab dehydration reactions, as well as seismicity due to the shallow, loss of water and other volatiles from the slab.

Volcanism has persisted to the present day where the ancestral arc has migrated west from the Idaho batholith and is currently building the High Cascades, erupting magmas spanning the compositional spectrum from minor amounts of rhyolite to substantial volumes of andesite, basaltic andesite, and basalt (du Bray and John, 2011; Gaschnig et al., 2010; Hildreth, 2007) The primary basaltic magmatism in the Cascades,

in comparison to other arc settings, is unusually large (Green and Harry, 1999; Leeman et al., 2004), 2005). Of the total estimated 6749 km<sup>2</sup> covered by 2 to 7 million year old arc volcanic rocks, 4930 km<sup>2</sup> is basalt-basaltic andesite in composition (approximately 70%). Over the complete history of the Cascades (2-45 My) basalt-basaltic andesite accounts for roughly 43% (du Bray and John, 2011; Sherrod and Smith, 2000; Smith, 1993).

The arc itself and regional volcanism is influenced by a range of different tectonic factors such as Basin and Range impingement in the south as well as clockwise rotation of western Washington, and models have been developed to relate the distribution of volcanism to the regional tectonic framework (Magill et al., 1982). Guffanti and Weaver (1988) partitioned the arc into six sections based on the spatial distribution of roughly 4000 volcanic vents formed since 16 Ma. More recently, Schmidt et al. (2008) refined this segmentation and divide the arc into four regions based on the distribution of primitive magmas with respect to their <sup>87</sup>Sr/<sup>86</sup>Sr and <sup>143</sup>Nd/<sup>144</sup>Nd isotopic ratios. Each of these four segments corresponds to a different tectonic environment within the arc. The four segments are the South Segment (from Mt. Shasta to Lassen Peak), the Central Segment (from the Three Sisters to Medicine Lake), the Columbia Segment (from Mt. Rainier to Mt. Jefferson), and the North Segment (from Mt. Meager to Glacier Peak). For example, the South Segment, is characterized by the highest <sup>87</sup>Sr/<sup>86</sup>Sr and Ba/Ce ratios with lower Ce/Yb ratios of calc-alkaline basalts compared to other types of abundant ambient basalts; these features may signify a relatively high degree of fluid fluxing and melting beneath this part of the arc. (Cameron et al., 2003; Schmidt et al., 2008) In

contrast, the Northern Segment is distinguishable from the rest of the arc by lower  $^{87}\text{Sr}/^{86}\text{Sr}$  and Ba/Ce ratios-consistent with lower degrees of flux melting and evidence for melting of an enriched mantle (Schmidt et al., 2008).

Further evidence for the variable amounts of slab contributions to arc magmatism, geochemical stratification of melt regions, and domains of different heat is provided by the large variation in the composition of well characterized basalts from a transect across the southern Washington arc (Leeman et al., 2005; Leeman et al., 2004). Basalts fall into two compositional groups: one representative of typical arc calc-alkaline lavas with a subducted slab signature characterized by enrichment in fluid-mobile elements (e.g. high B/Nb ratios) in the forearc and decreasing to the backarc across the transect (“Group 2” lavas); and the other resembling a relatively unmodified OIB-MORB source (Group 1 lavas), both groups to be discussed later (Leeman et al., 2004). Samples from this transect were analyzed as part of this study for their stable Cl isotope composition and halogen concentration in an attempt to better constrain melt source and Cl behavior across this lateral transect of the arc. I assign the 37 springs analyzed in this study into one of the four regions mentioned above and outlined in Schmidt et al. (2008) based on their geographic locations. The regional geology of these regions will be briefly discussed in section 2.3

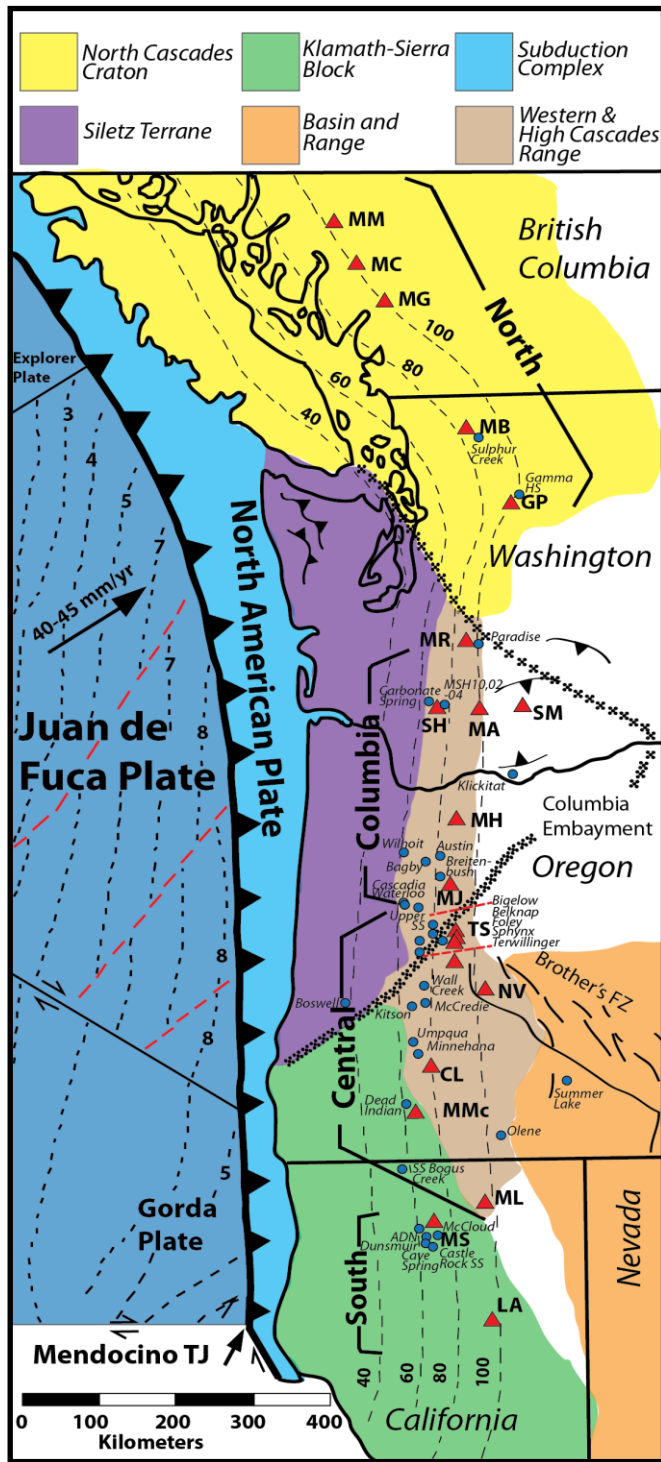


Figure 2: Generalized geologic map of the Cascade Volcanic Arc.

Figure 2 cont: Important terranes are colored (Couch and Riddihough, 1989; Trehu et al., 1994). Dashed contours for the depths to the slab are in km (Weaver and Baker, 1988). Dashed lines on oceanic plates are magnetic anomalies (Wilson, 1988). Segmentation is based on  $^{87}\text{Sr}/^{86}\text{Sr}$  and  $^{143}\text{Nd}/^{144}\text{Nd}$  ratios from Schmidt et al., 2008. Major volcanoes illustrated as red triangles. Abbreviations: (LA) Lassen, (MS) Mt. Shasta, (ML) Medicine Lake, (MMc) Mt. McLaughlin, (CL) Crater Lake, (NV) Newberry Volcano, (TS) Three Sisters, (MJ) Mt. Jefferson, (MH) Mt. Hood, (SH) Mt. St. Helens, (MA) Mt. Adams, (SM) Simcoe, (MR) Mt. Rainer, (GP) Glacier Peak, (MB) Mt. Baker, (MG), Mt. Garibaldi, (MC). Mt. Cayley, (MM) Mt. Meager. Springs sampled as part of this study are labeled and indicated by blue circles. Modified from Schmidt et al. (2008).

## 2.2 Cascade Thermal Springs and Previous Work

This study is further partly motivated by the previous work of Mariner et al. (2003) and Hurwitz et al. (2005) who used water chemistry and isotopic composition of thermal waters in the Cascades to identify the source of several solutes associated with volcanism and hydrothermal activity. Mariner et al. (2003) contends that excess  $N_2$  dissolved in the springs is derived from an early Tertiary marine unit and that the chlorine is likely associated with this excess  $N_2$  as well. Hurwitz et al. (2005) investigate many of the same thermal springs and, based on mass balance considerations, halogen element ratios, and constraints from radiogenic  $^{129}I/I$  and  $^{36}Cl/Cl$  data concluded that halogens discharged through the springs are most likely derived from magmatic degassing.

Thermal springs in the Cascades have been previously described by numerous other workers whose investigations were largely motivated by the region's geothermal potential (Blackwell and Steele, 1985; Blackwell et al., 1990; Brook et al., 1979; Ingebritsen et al., 1989; Ingebritsen et al., 1991; Mariner et al., 1990; Mariner et al., 1981; Waring et al., 1965). These studies, in particular focusing on the central region of the Cascades in Oregon, have produced an extensive database of thermal water data. ~2.5 Ma basalts, basaltic andesites and pyroclastic flows in the region have a modeled estimated bulk permeability of  $\sim 10^{-14} \text{ m}^2$ , or 10 md and thermal groundwater flow is believed to be driven by a gravimetric potential (Ingebritsen et al., 1991). Flow modeling calculations yield path lengths varying from 10 to 40 km and an average topographic

gradient of 0.1% from recharge to discharge points. Calculations based off of the kinetics of sulfate-water ( $\text{SO}_4\text{-H}_2\text{O}$ ) oxygen-isotope equilibrium imply a minimum residence time of 40 to 2,000 years, with the time needed to reach isotopic equilibrium decreasing with increasing reservoir temperature. With maximum residence times unable to be in excess of 10,000 years (Ingebritsen et al., 1991). These thermal springs were initially thought to transport approximately 1 megawatt of heat per km of arc from the younger more active eastern Quaternary arc to the Western Cascades. Subsequently, Ingebritsen and Mariner (2010) reported significant additional components of heat discharge through non-“hot”, “slightly thermal” springs (~660 MW in the U.S. Cascades) and fumaroles (~160 MW). They suggest a nearly steady state hydrothermal heat discharge in the Cascades over the past ~25 years excluding transient events involving Mt. Baker and Mt. St. Helens in the mid 70’s and 1980, respectively.

Geochemical and isotopic studies of geothermal systems are relatively common. Stable isotope methods have been used in order to better understand fluid-rock interactions and magmatic processes affecting the chemistries of thermal springs principal species; however, these studies are primarily limited to oxygen, hydrogen, carbon, nitrogen, and boron isotopes (Giggenbach, 1992; Hilton et al., 1993; James et al., 1999; Mariner et al., 2003; Pinti et al., 2012; Saar et al., 2005; Vengosh et al., 1991). Only a small number of thermal waters have been characterized for their stable Cl isotope composition. Three values are reported by Kaufmann et al. (1984) for Morgan Hot Spring, CA, Crater Lake, New Zealand, and El Chichon crater, Mexico and are all

approximately  $+0.43 \pm 0.02\text{‰}$ . Vengosh et al. (1991) reports one value from Ein Gedy hot spring, Israel, of  $+0.5\text{‰}$ .  $\delta^{37}\text{Cl}$  values for Indonesian volcanic springs reported by Eggenkamp (1994) range from  $-0.28$  to  $+0.43\text{‰}$  ( $n=17$ ). Most recently Barnes and Stefansson (2012) describe thermal waters from Iceland with  $\delta^{37}\text{Cl}$  values between  $-0.3$  to  $+0.3\text{‰}$ . Stable chlorine isotope compositions were determined from four different thermal areas in Yellowstone and ranged from  $-0.13 \text{‰}$  to  $+0.42\text{‰}$  ( $n=16$ ) (Zhang and Nordstrom, 2004). Chloride in the Yellowstone waters was interpreted as being derived from either mixing of a small amount of magmatic brine with the parent water and/or leaching of the rhyolitic wall rock, (albeit the Cl isotope composition of the host rhyolite was not determined in that study) (Zhang and Nordstrom 2004).

## Chapter 3: Spring Sites, Sampling and Field Data

The informal segmentation of the Cascade Arc based on  $^{87}\text{Sr}/^{86}\text{Sr}$  and  $^{143}\text{Nd}/^{144}\text{Nd}$  ratios of primitive lavas described in Schmidt et al. (2008) divides the arc into four discrete segments as discussed in Chapter 2. I group the 37 springs sampled in this study into these four segments (Table 1): the South Segment, the Central Segment, the Columbia Segment and the North Segment and outline the regional geology of each, as their non-uniformity may affect the chemistry of the springs in each region differently.

### 3.1 South Segment: northern California

The South Segment extends from near Lassen Peak, in northern California, northward to Mt. Shasta and is approximately 120 km in length. This sector is associated with subduction of the Gorda plate and the Blanco Fracture Zone that has been postulated to introduce anomalous volumes of altered oceanic lithosphere and fluids beneath the Shasta region. Despite the presence of several conspicuous stratovolcanoes (Shasta, Lassen), much of the Cascades arc in this region is dominated by late Pliocene and Quaternary intermediate-mafic flows from short lived composite or monogenetic cones and nearly all volcanism is younger than 7 Ma (Clynne, 1984; Clynne and Muffler, 2010). Here the arc sits atop accreted terranes of the Klamath Mountains which formed by the accretion of allochthonous oceanic terranes during early Paleozoic to Cretaceous times (Irwin, 1972, 1985; Norris and Webb, 1990; Snoke and Barnes, 2006). These

underlying accreted terranes consist of the early Paleozoic Trinity Ophiolite to late Mesozoic shales, conglomerates and limestones (Clynne, 1984).

### **3.1.1 Sampling Sites**

Spring waters were collected from five locations in the South Segment, all within a 20 km radius of Mt. Shasta (Figure 3). Relative to the volcanic arc as a whole, the springs are situated in a “frontal arc” position, as is Mt. Shasta. Aqua de Ney spring was collected in August 2012, whereas the neighboring Cave Spring, Upper Soda Spring Dunsmuir, Soda Spring South McCloud, and Castle Rock Soda Spring were collected in September 2012 by Jennifer Lewicki of the USGS in Menlo Park, CA.

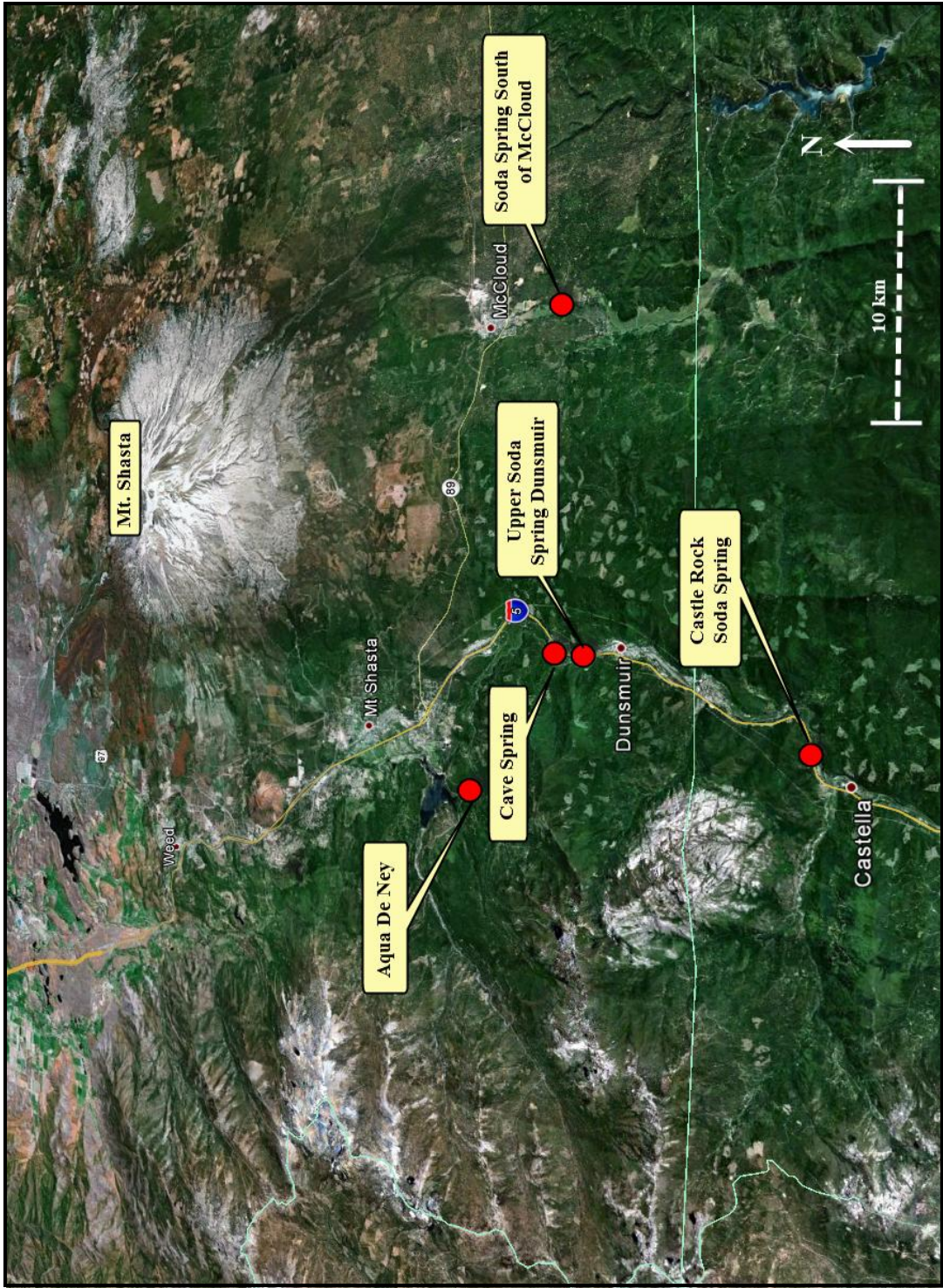


Figure 3: Spring locations sampled from within the Cascades South Segment, northern CA.

### **3.2 Central Segment: northern CA, southern and central Oregon**

The Central Segment extends ~320 km from the Medicine Lake area in northern California to the Three Sisters area of central Oregon. In contrast to the other 3 segments where all sample sites are on or very near the arc crest, the spring waters collected in the Central Segment span roughly a 280 km cross-arc transect: sampling both the forearc and backarc regions. The southern and central Oregon portions of the Central Segment of the volcanic arc are primarily associated with subduction of the Juan de Fuca Plate. Collected springs sample several distinct geographic areas as follows: the Cascade Range, the Basin-Range, the High Lava Plains and the Willamette Valley. Additionally, the Cascade Range can be divided into the Western Cascades and the High Cascades on the eastern edge. The Western Cascades are primarily altered basalt, andesite and dacite flows of Miocene age ranging from 10-42 m.y. (Hildreth, 2007; McBirney, 1978; Taylor, 1990). The High Cascades are the product of the eastern migration of the volcanic arc, are younger than 10 m.y., and form the prototypical belt of prominent stratovolcanoes stretching from Crater Lake in the south to Mt. Hood in the north (Hildreth, 2007; Priest, 1990).

The Basin-Range east of the Cascades is largely made up of Miocene to Recent volcanic flows, pyroclastic beds and alluvial sediments. The basement structure of the area is not well constrained, but comprises accreted oceanic and island arc terranes of Paleozoic to Cretaceous age as well as volcanic-plutonic rocks of Cretaceous to Oligocene age which have been deformed multiple times (Crider, 2001; Donath, 1962).

The High Lava Plains directly north of the Basin-Range Province are a relatively undeformed region of Miocene-Pleistocene volcanic rocks with cinder cones scattered throughout (Baldwin, 1981). To the west, the Willamette Valley is a deep forearc basin which separates the Oregon Coast Range from the Cascade Range. Oceanic basalts and basaltic sedimentary rocks dated between  $58.1 \pm 1.5$  to  $50.7 \pm 3.1$  Ma form the basement of this region and are part of the accreted Siletz River Volcanics and other coast range terrane. Collectively, these rocks form much of the larger Columbia Embayment which are believed to be part of an ancient oceanic plateau (du Bray and John, 2011; Duncan, 1982). Overlying the Paleocene-Eocene volcanics are deltaic clastic sediments of middle Eocene age, and arkosic sandstones, siltstones, minor volcanoclastics, and basaltic andesite flows of late Eocene to Early Miocene age (Yeats et al., 1996).

### **3.2.1 Sampling Sites**

19 springs were sampled from each of the aforementioned regions of the Central Segment: two from the Basin-Range, one from the High Lava Plains, one from the Willamette Valley, and 15 from the Cascade Range (Figure 4). In most cases springs were found as clusters of discharge points out of a hillside rock face or stream/river bank in which case the hottest was chosen for collection. At Terwillinger, Foley, Boswell, and Kitson springs, only a singular discharge point was observed and sampled.

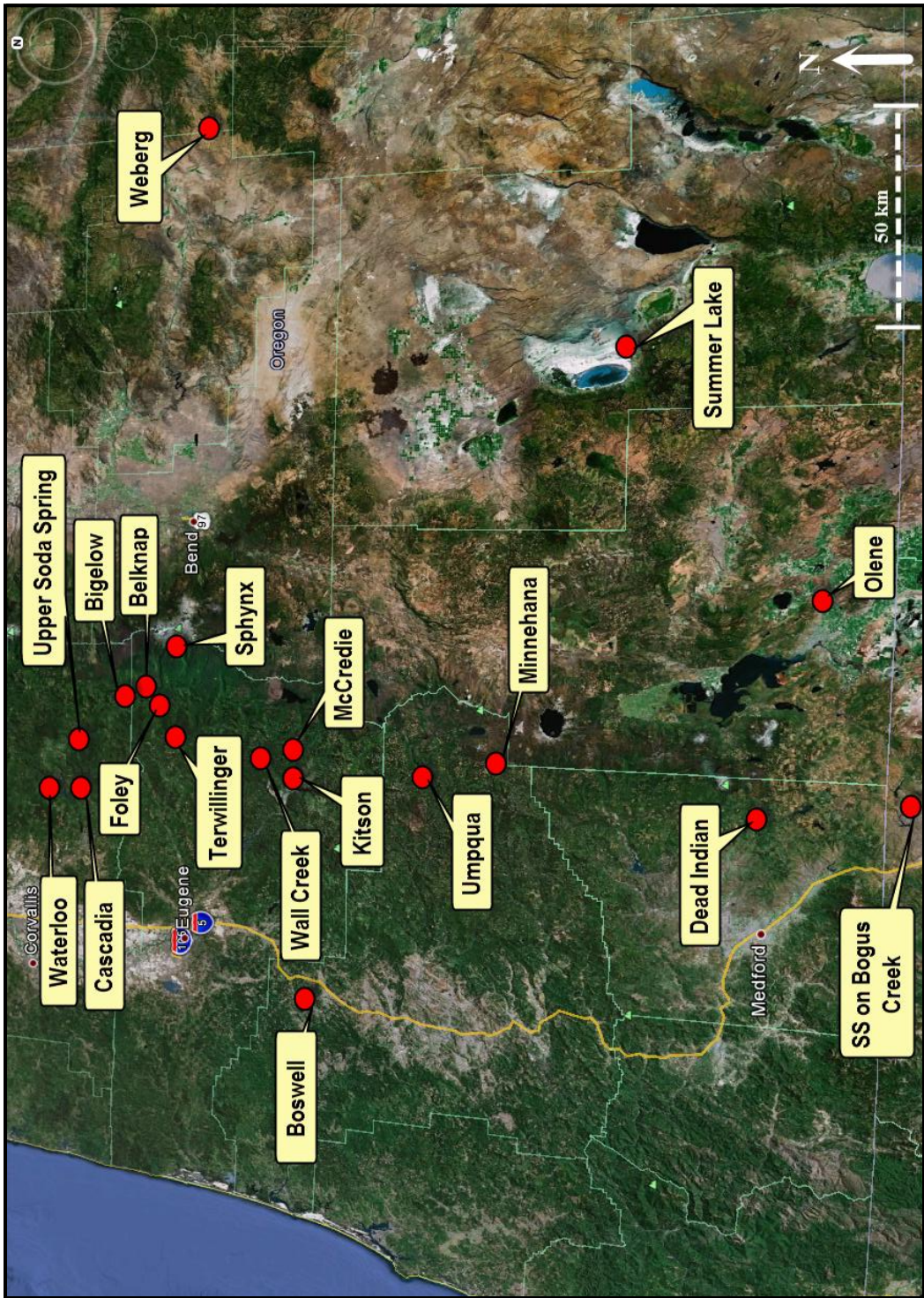


Figure 4: Spring locations sampled from within the Cascades Central Segment.

### **3.3 Columbia Segment: northern Oregon & southern Washington**

The Columbia Segment stretches ~240 km from Mount Jefferson north to Mount Rainer. This region, and especially the “back-arc” Simcoe Volcanic field, is distinguished from the rest of the arc by the common occurrence of “intra-plate like” basalts (IPBs), which lack depletion in HFSEs that is usually observed in most arc magmas (Hildreth, 2007; Leeman et al., 1990; Schmidt et al., 2008). The high Nb concentrations (often >20 ppm) are coupled with low  $\text{Al}_2\text{O}_3/\text{TiO}_2$  ratios (4-11) (Bacon et al., 1997; Conrey et al., 1997; Leeman et al., 2005; Schmidt et al., 2008). Magma generation in this large region is complex, and the geochemical signatures of erupted lavas are influenced by many factors; including tapping an accreted enriched domain, melting of a geochemically stratified upper mantle, possibly even varied degrees of flux induced melting. (Leeman et al., 2005; Reiners et al., 2000; Rowe et al., 2009; Schmidt et al., 2008).

The arc in this northern Oregon area, and extending into southern Washington is built upon basement crust of the Columbia Embayment and Siletz terrane, believed to be composed of accreted igneous rocks of oceanic origin (Miller, 1989). A portion of the overlying rocks above the Siletz basement, near the Columbia River Gorge is the Columbia River Basalt, a large volume flood basalt with an estimated total volume of  $175,000 \text{ km}^3$  which erupted very rapidly during the middle Miocene (Hooper, 1997). The extent of marine sediments beneath the arc in northern Oregon and southern Washington is not well constrained, as no wells have been drilled to sufficient depth as to break through the thick Tertiary volcanic units. However, it is likely that pre-Oligocene marine

sedimentary rocks are present beneath the arc based on field outcrop correlations and geophysical data (Stanley et al., 1987).

### **3.3.1 Sampling Sites**

Ten water samples were collected from the Columbia Segment, four from northern Oregon and six from southern Washington (Figure 5). Klickitat, Bagby, Austin, and Breitenbush springs were sampled by myself, while all the others were samples provided by USGS colleagues. Samples MSH10-02, 03, and 04 come from thermal springs in Loowit and or Step Canyons as well as creeks that drain the crater of Mt St Helens. For detailed site descriptions refer to Bergfeld et al. 2008. In conjunction with the 37 spring waters analyzed, nine volcanic rock samples from southern Washington Cascades transect were provided by Dr. William P. Leeman of Rice University (Figure 6) and (Table 2).

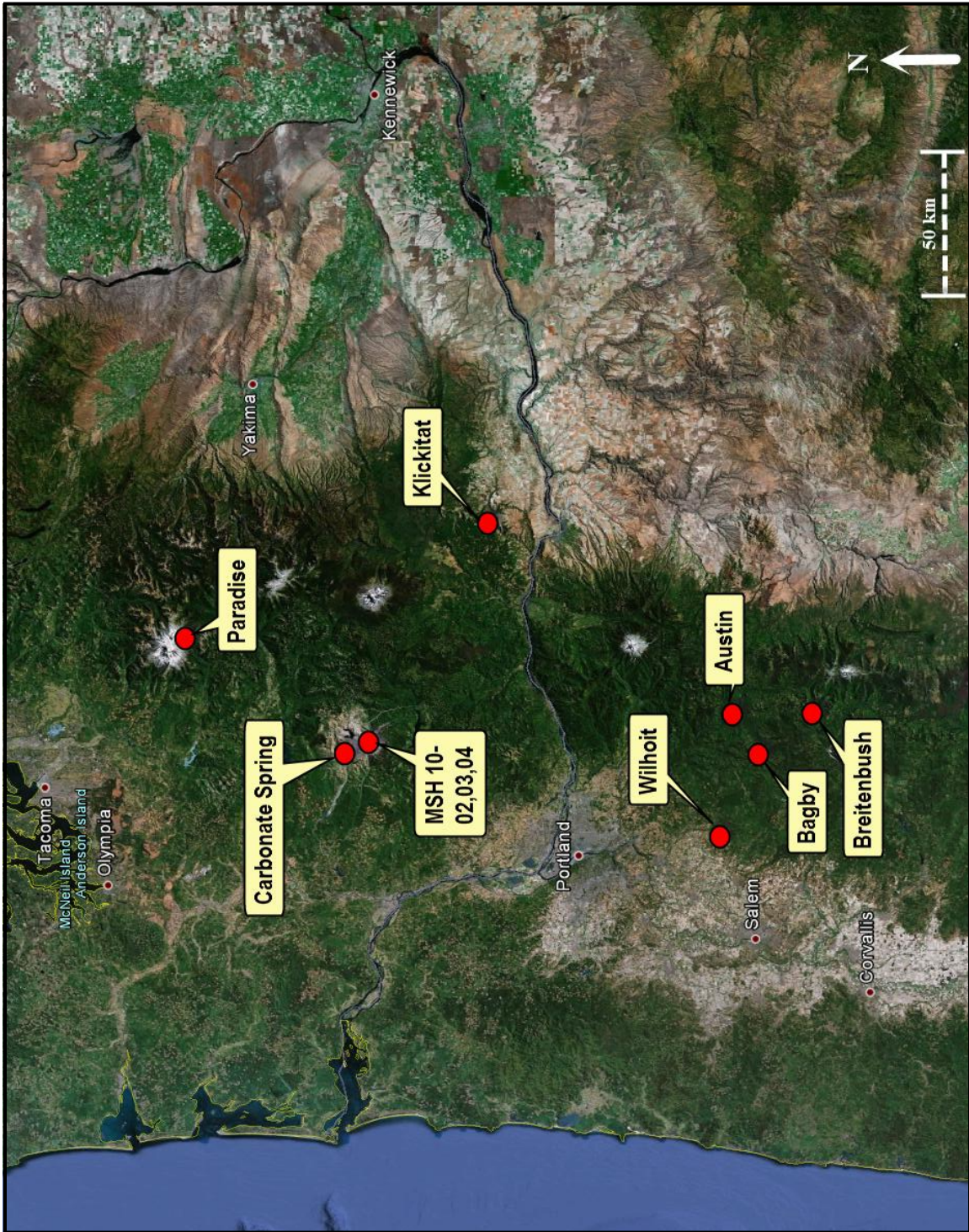


Figure 5: Spring locations sampled from within the Cascades Columbia Segment.

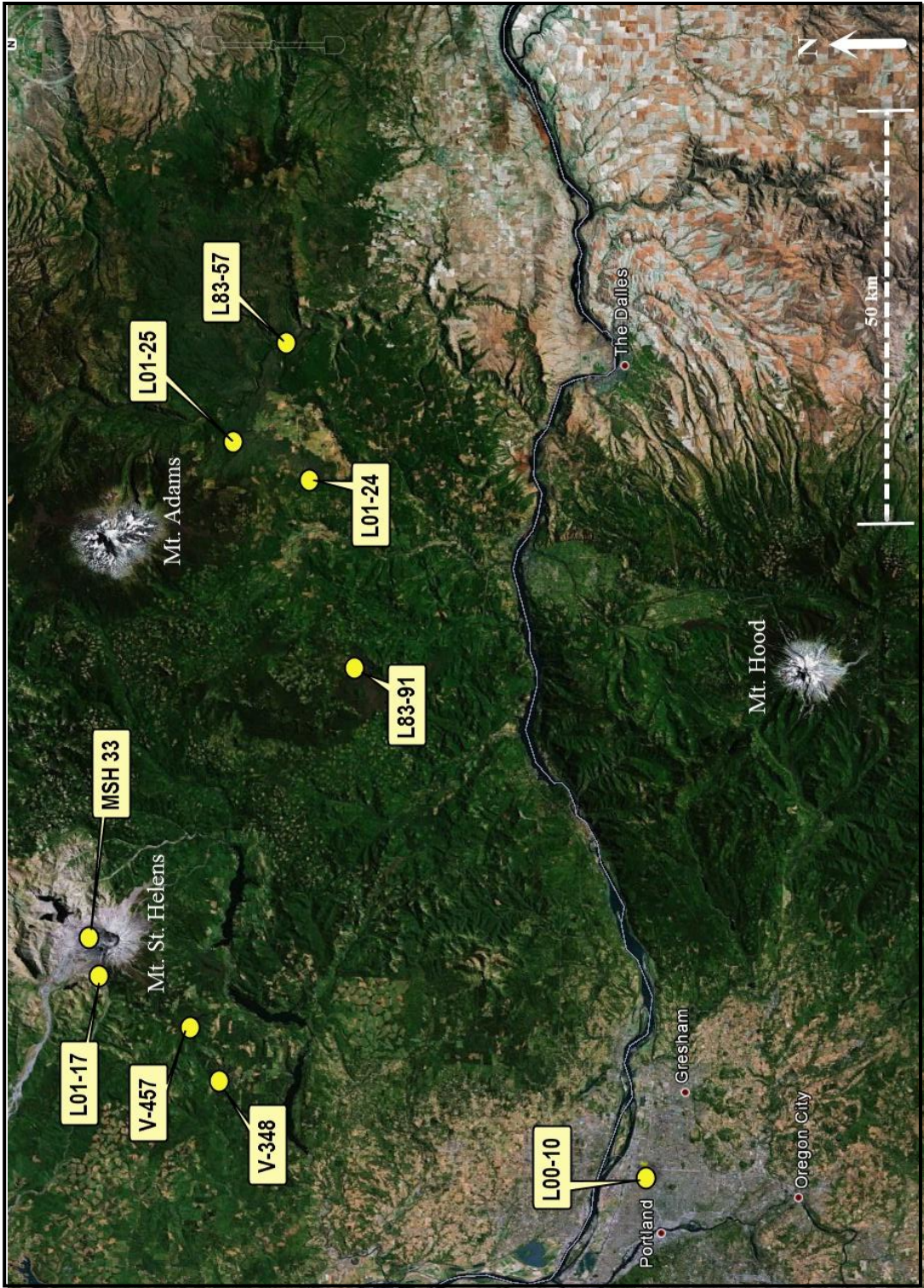


Figure 6: Lava sample locations sampled from the Columbia Transect of southwest Washington.

### 3.4 North Segment: northern Washington

The North segment stretches from Glacier Peak in northern Washington to Mount Meager in British Columbia. This segment of the arc is dominated by calc-alkaline basaltic magmatism with higher  $^{143}\text{Nd}/^{144}\text{Nd}$  ratios and lower  $^{87}\text{Sr}/^{86}\text{Sr}$  ratios than in any other segment (Schmidt et al., 2008). The increasing  $^{87}\text{Sr}/^{86}\text{Sr}$  ratio from the northern arc to the southern arc has been interpreted to reflect an increase in fluid flux melting in the south which may suggest that flux melting is not the primary form of melt generation in the northern part of the Cascades (Hildreth, 2007; Schmidt et al., 2008).

The North segment of the arc has been assembled upon two major thrust sheets composed of marine metasedimentary and metavolcanic rocks of Paleozoic age (Miller et al., 1997). The lower sheet is likely Devonian to Permian volcanoclastic silts/sandstone, basaltic breccias and tuffs, with the upper part containing fragments of serpentinized peridotites (Miller et al., 1997). The upper sheet is metamorphosed MORB affinity basalts of the Shuksan Greenschist and the Darrington Phyllite (Brown, 1987). Above the thrust sheets, the overlying sediments are primarily fluviatile arkosic sandstones, silts, and shales of Eocene age roughly 5-6 km thick. The volcanic arc rocks are also Eocene to recent in age and are primarily andesitic to dacitic pyroclastic lithologies (Hildreth, 2007). The volcanism in this region is confined to widely spaced, prominent stratovolcanoes and has been attributed to a much more compressional crustal regime as opposed to the southern arc where clockwise extensional rotation is believed to occur (Hildreth, 2007; Wells, 1990)

### **3.4.1 Sampling Sites**

Two springs were sampled from the Northern Segment, both corresponding to the arc front (Figure 7): one on the flank of Glacier Peak and the other on the flank of Mt. Baker. Neither spring water was collected as part of this study and no site descriptions are available, were samples provided by USGS colleagues.

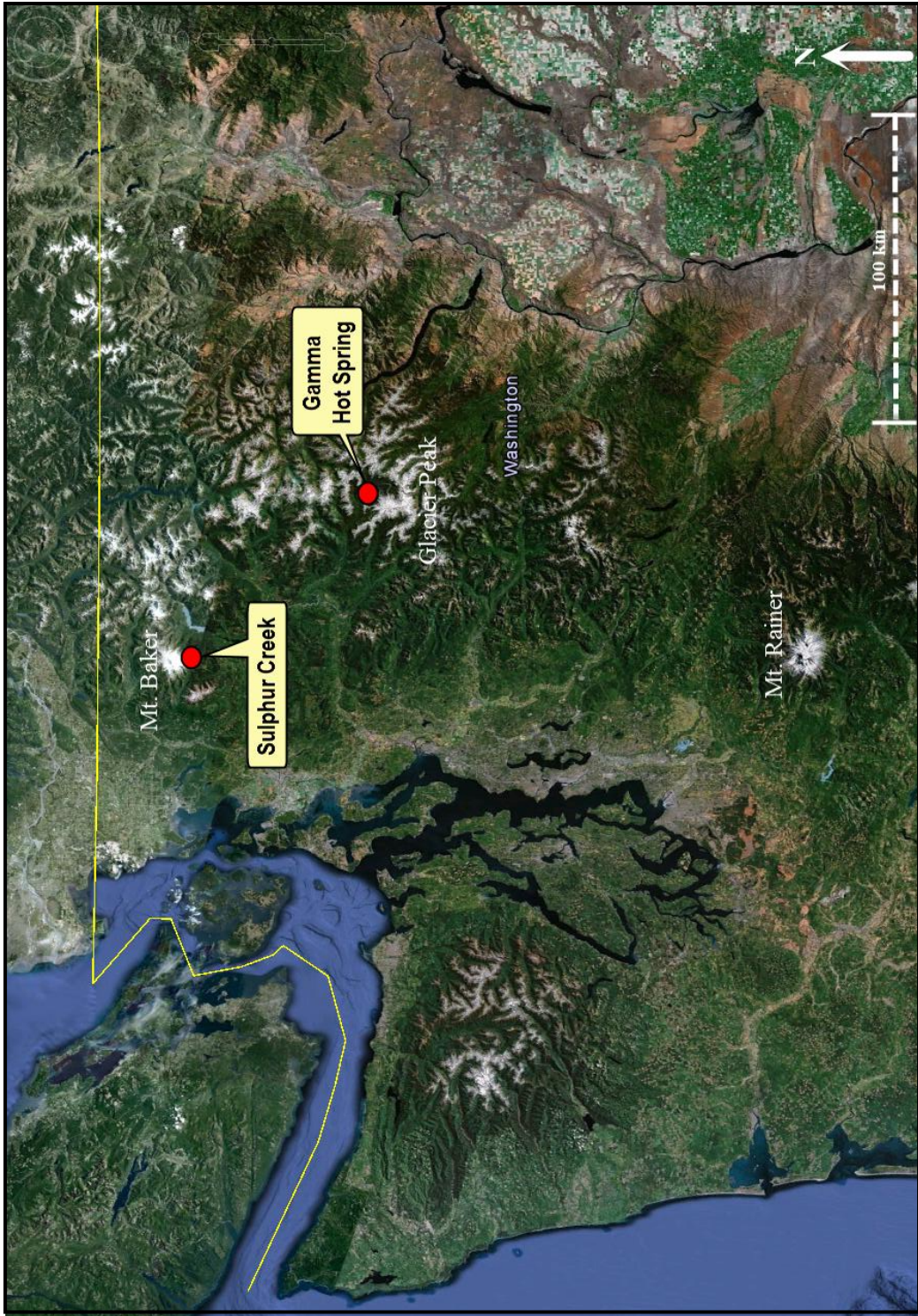


Figure 7: Spring locations sampled from within the Cascades North Segment.

Table 1: Collected thermal springwater field data.

| <b>Spring Name</b>               | <b>Segment</b> | <b>Province</b>   | <b>Sampled by</b> | <b>Location</b>                 | <b>pH</b> | <b>t (°C)</b> | <b>Specific Conductance (µS)</b> |
|----------------------------------|----------------|-------------------|-------------------|---------------------------------|-----------|---------------|----------------------------------|
| Cave Spring                      | South          | Cascades          | USGS              | 41°13'29.90''<br>122°16'36.10'' | 6.0       | 11.9          | 2860                             |
| Upper Soda Spring<br>Dunsmuir    | South          | Cascades          | USGS              | 41°13'18.82''<br>122°16'36.24'' | 5.9       | 12.3          | 2660                             |
| Soda Spring<br>South<br>McCloud  | South          | Cascades          | USGS              | 41°13'38.52''<br>122°8'20.52''  | 6.0       | 9.3           | 1348                             |
| Castle Rock<br>Soda Spring       | South          | Cascades          | USGS              | 41°8'59.97''<br>122°18'27.06''  | 6.4       | 14.4          | 5830                             |
| Aqua de Ney                      | South          | Cascades          | Myself            | 41°15'41.86''<br>122°19'54.91'' | 11.       | 15.1          | 36480                            |
| Soda Spring<br>on Bogus<br>Creek | Central        | N. CA<br>Cascades | USGS              | 41°55'15.21"<br>122°22'15.29"   | 6.6       | 23.2          | 15530                            |
| Olene                            | Central        | Basin-Range       | Myself            | 42°10'20.82"<br>121°37'8.51"    | 7.9       | 39.5          | 645.0                            |
| Summer<br>Lake 1                 | Central        | Basin-Range       | Myself            | 42°43'31.19"<br>120°38'47.80"   | 8.3       | 48            | 1812                             |
| Summer<br>Lake 2                 | Central        | Basin-Range       | Myself            | 42°43'31.19"<br>120°38'47.80"   | 8.5       | 43            | 2033                             |
| Dead Indian                      | Central        | Cascade<br>Range  | USGS              | 42°19'57.50"<br>122°26'59.70"   | 5.9       | 14            | 2660                             |
| Minnehana                        | Central        | Cascade<br>Range  | USGS              | 43°4'31.60"<br>122°16'31.80"    | 6.3       | 9.3           | 3040                             |
| Umpqua                           | Central        | Cascade<br>Range  | Myself            | 43°17'48.48"<br>122°21'18.32"   | 6.1       | 43.5          | 12000                            |
| Kitson                           | Central        | Cascade<br>Range  | Myself            | 43°41'24.50"<br>122°22'30.25"   | 7.5       | 39            | 9430                             |
| McCredie                         | Central        | Cascade<br>Range  | Myself            | 43°42'21.20"<br>122°17'16.19"   | 7.2       | 71            | 7570                             |
| Wall Creek                       | Central        | Cascade<br>Range  | Myself            | 43°48'24.77"<br>122°18'39.74"   | 7.8       | 38            | 2372                             |
| Terwillinger                     | Central        | Cascade<br>Range  | Myself            | 44°4'59.32"<br>122°14'25.27"    | 8.4       | 43.8          | 2884                             |
| Foley                            | Central        | Cascade<br>Range  | Myself            | 44°9'14.04"<br>122°5'53.24"     | 6.0       | 79.2          | 4780                             |

Table 1 cont.

|                   |          |                           |        |                               |      |      |       |
|-------------------|----------|---------------------------|--------|-------------------------------|------|------|-------|
| Sphynx            | Central  | Cascade Range             | USGS   | 44° 4'50.50"<br>121°50'50.30" | 8.4  | 4.9  | 143   |
| Bigelow           | Central  | Cascade Range             | Myself | 44°14'19.68"<br>122° 3'32.26" | 6.9  | 36.3 | 3987  |
| Belknap           | Central  | Cascade Range             | Myself | 44°11'37.14"<br>122° 3'2.52"  | 7.5  | 86.5 | 4295  |
| Waterloo          | Central  | Cascade Range             | USGS   | 44°29'44.60"<br>122°28'48.50" | 6.1  | 15.4 | 6300  |
| Cascadia          | Central  | Cascade Range             | USGS   | 44°23'57.50"<br>122°28'49.00" | 6.0  | 15.7 | 9500  |
| Upper Soda Spring | Central  | Cascade Range             | USGS   | 44°24'18.98"<br>122°17'4.32"  | 6.0  | 12.2 | 12530 |
| Boswell           | Central  | Willamette Valley         | Myself | 43°38'29.94"<br>123°17'54.42" | 8.6  | 14.2 | 45470 |
| Weberg            | Central  | High Lava Plains          | Myself | 44° 0'5.94"<br>119°38'59.52"  | 6.7  | 42.5 | 2651  |
| Breitenbush       | Columbia | Cascade Range             | Myself | 44°46'52.65"<br>121°58'34.61" | 7.6  | 66.5 | 3791  |
| Bagby             | Columbia | Cascade Range             | Myself | 44°56'7.26"<br>122°10'21.54"  | 9.0  | 53.8 | 266   |
| Austin            | Columbia | Cascade Range             | Myself | 45° 1'9.52"<br>122° 0'1.44"   | 7.5  | 86.5 | 1631  |
| Wilhoit           | Columbia | Willamette Valley         | USGS   | 45° 3'8.30"<br>122°34'6.30"   | 6.1  | 10.7 | 9800  |
| Klickitat         | Columbia | S.<br>Washington Cascades | Myself | 45°49'23.70"<br>121° 6'57.72" | 5.8  | 25.4 | 1479  |
| MSH10-02          | Columbia | S.<br>Washington Cascades | USGS   | 46°12'39.53"<br>122°11'17.07" | n.d. | n.d. | n.d.  |
| MSH10-03          | Columbia | S.<br>Washington Cascades | USGS   | 46°12'39.53"<br>122°11'17.07" | n.d. | n.d. | n.d.  |
| MSH10-04          | Columbia | S.<br>Washington Cascades | USGS   | 46°12'39.53"<br>122°11'17.07" | n.d. | n.d. | n.d.  |
| Carbonate Spring  | Columbia | S.<br>Washington Cascades | USGS   | 46°15'11.29"<br>122°13'16.07" | 6.7  | 18.1 | 790   |
| Paradise          | Columbia | S.<br>Washington Cascades | USGS   | 46°48'10.24"<br>121°43'8.49"  | 6.3  | 22.4 | 893   |

Table 1 cont.

|                  |       |                              |      |                               |      |      |      |
|------------------|-------|------------------------------|------|-------------------------------|------|------|------|
| Gamma Hot Spring | North | N.<br>Washington<br>Cascades | USGS | 48°9'9.36"<br>121°3'48.24"    | n.d. | n.d. | n.d. |
| Sulfur Creek     | North | N.<br>Washington<br>Cascades | USGS | 48°42'24.67"<br>121°48'57.46" | 6.2  | 5.1  | 187  |

(n.d.) not determined

Table 2: Arc transect lavas from the Columbia Segment.

| <b>Sample</b> | <b>Rock Type</b>                   | <b>Location</b>               | <b>Geographic Locale</b>         |
|---------------|------------------------------------|-------------------------------|----------------------------------|
| <b>L83-57</b> | Low K<br>Theolite                  | 46° 0'14.40"<br>121° 9'7.20"  | Mt. Adams                        |
| <b>L01-24</b> | OIB-like<br>Basalt                 | 45°58'12.00"<br>121°23'24.00" | Mt. Adams                        |
| <b>L01-25</b> | OIB-like<br>Basalt                 | 46° 3'36.00"<br>121°19'48.00" | Mt. Adams                        |
| <b>L01-17</b> | OIB-like<br>Basalt                 | 46°12'36.00"<br>122°15'0.00"  | Mt. St.<br>Helens                |
| <b>L00-10</b> | High K calc-<br>alkaline<br>Basalt | 45°32'24.00"<br>122°33'36.00" | Portland<br>Basin<br>Frontal Arc |
| <b>L83-91</b> | OIB-like<br>Basalt                 | 45°54'28.80"<br>121°42'39.60" | Simcoe VF<br>Back Arc            |
| <b>V-348</b>  | Calc-<br>Alkaline<br>Basalt        | 46° 3'46.80"<br>122°25'51.60" | Frontal Arc                      |
| <b>V-457</b>  | High K calc-<br>alkaline<br>Basalt | 46° 5'52.80"<br>122°20'31.20" | Frontal Arc                      |
| <b>MSH 33</b> | Dacite                             | 46°13'12.00"<br>122°11'13.20" | Mt. St.<br>Helens                |

## Chapter 4: Methods

### 4.1 Field sampling techniques

Spring waters found as pools were collected using tygon tubing lowered into the pool and attached to a peristaltic pump to ensure collection of pristine water. In cases where there were multiple discharge points for a single spring, the hottest water was collected. Samples were collected into four polyethylene Nalgene vessels for anion analysis, cation analysis, stable chlorine isotope analysis, and alkalinity analysis and one glass bottle fitted with a Teflon cap for hydrogen and oxygen isotope analysis. The waters collected for cation analysis were collected into HNO<sub>3</sub> rinsed polyethylene bottles then acidified in the field using dilute HNO<sub>3</sub>. All water samples were filtered through a 0.35 μm membrane. GPS coordinates were taken using a handheld GPS device. pH and temperature measurements were taken using a Scientific Instruments ISFET IQ probe. Calibrations at pH of 4, 7, and 10 were made daily. Conductivity data was collected using a Myron L GPIIFCE ultrameter, calibrated using a 700 μS solution.

### 4.2 Major element chemistry of thermal waters

**4.2.1 Alkalinity analysis:** Alkalinity measurements could not be made in the field, and for the 18 springs sampled by myself, total alkalinity was measured using an acid titration on a METROHM 702 SM Titrino auto-titrator at the University of Texas-Austin Jackson School of Geosciences. Time between collection and analysis was within

14 days and pH was not re-measured in the lab before titrations. 25 mL of sample fluid was titrated to pH 4.5 using 0.1N H<sub>2</sub>SO<sub>4</sub>. Total mili-equivalents alkalinity is reported as mg/L bicarbonate.

**4.2.2 Anions analysis:** All 37 spring water samples were analyzed for their major anions using high performance liquid chromatography (HPLC) on a Waters HPLC unit with a model 430 conductivity detector and Waters 486 tunable absorbance detector at the University of Texas-Austin Jackson School of Geosciences aqueous geochemistry lab. Cl<sup>-</sup>, SO<sub>4</sub><sup>2-</sup>, Br<sup>-</sup>, PO<sub>4</sub><sup>3-</sup>, and F<sup>-</sup> concentrations were determined using conductivity measurements relative to the conductivity of known standards of various concentrations between 0.1 ppm and 200 ppm, which were prepared from NaCl, NaF, NaNO<sub>3</sub>, NaSO<sub>4</sub>, NaPO<sub>4</sub>, and NaBr salts. NO<sub>3</sub><sup>-</sup> concentrations were determined using UV absorbance at 210 nm. The column used was a Waters IC-Pak Anion HC Column, 4.6x150mm with Na/Li Borate Gluconate-Acetonitrile-1 Butanol eluent at a flow rate of 1.5 ml/min. Check standards were within ±5% of the calibration with a minimum detection limit of 0.2 ppm. Large dilutions were necessary to accommodate the high chloride contents in the water samples. As a result, Br<sup>-</sup>, PO<sub>4</sub><sup>3-</sup>, NO<sub>3</sub><sup>-</sup>, and F<sup>-</sup> were diluted to below their limits of detection and a means to separate Cl<sup>-</sup> from solution and re-analyze the undiluted samples for Br<sup>-</sup>, PO<sub>4</sub><sup>3-</sup>, NO<sub>3</sub><sup>-</sup>, and F<sup>-</sup> were not available. The, Br, F, and I data in this study comes from Hurwitz et al. (2005) and Lewicki (unpublished data).

**4.2.3 Cations analysis:** From the 18 spring waters run for cation analysis, aliquots were diluted accordingly and were run on an Agilent 7500ce Quadrupole ICP-MS in the Isotope Geochemistry lab at the Department of Geosciences at UT-Austin. NIST 1643e “trace elements in water certified reference standard” of multiple dilutions was used as the primary reference standard in the analysis. Analytical detection limits of the measured analytes and complete cation data can be found in (Table A1) of Appendix A. Analytical uncertainties were between 1 and 3 percent.

**4.2.4  $\delta\text{D}$  and  $\delta^{18}\text{O}$  analysis :** For each of each of the 18 water samples collected by myself, 1 mL were equilibrated with  $\text{CO}_2$  for 24 hrs at  $25^\circ\text{C}$  in Labco exetainer vials for oxygen isotope analysis by continuous-flow mass spectrometry. Internal lab standards were calibrated by applying a stretching factor that resulted in a value of  $-55.5\text{‰}$  for SLAP (Standard Light Antarctic Precipitation) relative to SMOW (Standard Mean Ocean Water) (Coplen et al., 1983). Error is  $\pm 0.04\text{‰}$ . 10  $\mu\text{L}$  of water samples were reduced to  $\text{H}_2$  gas on glassy carbon using a TCEA (thermo conversion elemental analyzer) coupled to a ThermoElectron MAT 253 for hydrogen isotope analysis. Error is  $\pm 3\text{‰}$  and values are reported in standard per mil notation relative to SMOW. Sample data are reported as the average of 9 individual analyses with similar errors mentioned above.

**4.2.5  $\delta^{37}\text{Cl}$  analysis:** All 37 water samples were analyzed for their  $\delta^{37}\text{Cl}$  values following the procedures of Eggenkamp (1994) as modified by Barnes and Sharp (2006) and Sharp et al. (2007). The raw filtered spring waters were first diluted to chloride

concentrations ranging between 40-100 mg/L. Aliquots corresponding to roughly 75  $\mu\text{g}$   $\text{Cl}^-$  were dispensed into 18 M $\Omega$  deionized water rinsed 50 mL glass beakers. 8 mL of 8M  $\text{HNO}_3$  was added and the mixture then heated for two hours on a hot plate to drive off any sulfur-containing species present in the sample. Chlorine was precipitated out of solution as  $\text{AgCl}$  with the addition of  $\text{AgNO}_3$  and  $\text{KNO}_3$ . The precipitate was filtered and rinsed with 1%  $\text{HNO}_3$  and dried and placed in 0.5 cm x 20cm pyrex glass tubes. The tube was brought to vacuum and 10  $\mu\text{L}$  methyl iodide was syringed in. The tubes were sealed using a propane torch and the methyl iodide was allowed to react with the silver chloride for 48 hours at 80°C. The methyl chloride in each sample was subsequently analyzed for its  $^{37}\text{Cl}/^{35}\text{Cl}$  ratio using isotope ratio mass spectrometry.  $\delta^{37}\text{Cl}$  values were determined using a ThermoElectron MAT 253 mass spectrometer and reported in standard per mil notation vs. SMOC (Standard Mean Ocean Chloride ( $\delta^{37}\text{Cl}_{\text{SMOC}} = 0\text{‰}$ )). Analytical precision is  $\pm 0.2\text{‰}$  based on long-term precision of in house seawater standards and one in-house rock standard. Check replicates from the identical water sample vessels were rerun on 9 samples weeks later to test for repeatability.  $\delta^{37}\text{Cl}$  values are within  $\pm 0.3\text{‰}$  for 6 of the 9 samples however, 3 are significantly beyond this range. These outliers may have been the result of imperfect sample preparation, but the analytical chromatograms did not give reason to discard the data therefore the data are included and reported as the average of the two values.

### 4.3 Rock Geochemistry

The 9 rock powders, (8 basalts and 1 dacite) from the Cascade Columbia Segment transect have been previously analyzed for bulk rock, trace, and stable Li and B and radiogenic Sr, Nd, and Pb isotope geochemistry in (Leeman et al., 2005; Leeman et al., 2004) (Table B1) in Appendix B. Halogens were extracted from the rock powders using a pyrohydrolysis technique of Schnetger and Muramatsu (1996). Released halogens and water vapor were collected as a condensate in a trapping solution containing NaOH (0.05 N) and Na<sub>2</sub>SO<sub>3</sub> (0.005 N). F<sup>-</sup> concentrations were determined by ion chromatography following the same method outlined in section 4.2.2 above using HPLC electrical conductivity detection. The LOD is 200 ppb. Cl<sup>-</sup>, Br<sup>-</sup>, and I<sup>-</sup> concentrations were determined using a ThermoFinnigan Element 2 ICP-MS at the University of Bremen following methods described by Bu et al. (2003) . Limits of detection are 16, 0.4, and 0.06 ppb, respectively.  $\delta^{37}\text{Cl}$  values of the rock powders were determined using the condensate solution and the same procedure as in section 4.2.5.

## Chapter 5: Results

### 5.1 Springwater Chemistry

Selected geochemical data for all springs analyzed are presented in (Table 3). Complete geochemical data are presented in (Table A1) of Appendix A. Charge balance calculations were made for 31 springs with adequate data, and have a balance within  $\sim\pm 5\%$  error, with the exception of Aqua de Ney, Sphynx, and Boswell, with a charge imbalances of -5.9%, 8.0%, and 13.6% respectively. This may be caused by, the presence of other charged species not analyzed, poor sample preparation, or alkalinity lost as carbonate through degassing after collection, or in the form of  $\text{OH}^-$ , which is likely the case with Aqua de Ney. Percent imbalances and species used in the calculation can be found in (Table 3). Aqua de Ney spring is unique with a pH of 12, and its chemistry is believed to be controlled by the strong interaction with an underlying serpentinized body (Barnes and O'Neil, 1969), the data from Aqua de Ney Spring are omitted from subsequent plots, as it does not reflect the same processes occurring in the rest of the thermal springs.

Cl concentrations in spring waters range dramatically from 6.6 ppm to 13,848.5 ppm. In most cases, Cl provides the majority of negative charge balance. However, bicarbonate is the dominant anion in Klickitat, Cave Spring, Castle Rock, Minnehana, and Weberg. Aqua de Ney has the highest alkalinity of any of the samples (17348 total bicarbonate), but is noteworthy because this high alkalinity is likely due to the presence

of hydroxide ions and not bicarbonate as suggested by the unusually high pH of 11.9. The major cations, B, Na, Mg, Si, K, and Ca, concentrations range between 0.07-251 ppm, 52-10513 ppm, <.065-111 ppm, <13.3-897 ppm, 1.1-142.6 ppm, and 2-6890 ppm respectively. Figure 8 shows ternary plots of selected chemical data for the thermal springwaters as well as the Columbia Transects basalts.

### 5.1.1 Cl, O, and H stable Isotopes

$\delta D$  values for the 17 analyzed springs range from -121‰ to -15‰ with corresponding  $\delta^{18}O$  values ranging from -14.6‰ to -2.3‰ (Table 3). No local meteoric waters were collected, so estimated meteoric water isotope compositions were calculated using the sample's coordinates, elevation, and the Bowen (2003) Online Isotope Precipitation Calculator, ver. 2.2 software ([wateriso.utah.edu/waterisotopes/index.htm](http://wateriso.utah.edu/waterisotopes/index.htm)). Confidence intervals from the calculation estimate are within approximately  $\pm 5\%$  and  $\pm 1\%$  for hydrogen and deuterium respectively.  $\delta D$  and  $\delta^{18}O$  data are plotted in conjunction with the calculated local meteoric water line,  $\delta D = 8.5 \times \delta^{18}O + 10$  (Figure 9) and global meteoric water trend,  $\delta D = 8 \times \delta^{18}O + 10$  (Craig, 1961). No geographical dependence is observed, however samples show slight deviations from the meteoric trends and will be discussed later in Chapter 6.

Stable chlorine isotope analyses were performed on all 37 samples and range from -0.1 ‰ to +1.9‰ with a mean value +0.8‰ ( $1\sigma = \pm 0.4\%$ ) (Table 3). There is no significant correlation between  $\delta^{37}Cl$  value and Cl concentration ( $p = 0.11$ ) (Figure 10).

## 5.2 Halogen Chemistry and Stable Cl isotopes of Volcanic Rock Powders

Halogen concentrations and  $\delta^{37}\text{Cl}$  values were determined for the 9 rock powders (Table 4). Previously published geochemical data are presented in Appendix B (Table B1). Cl concentrations are highest at the volcanic front (140-157 ppm) compared to the forearc (17-82 ppm) and the backarc (19-65 ppm). Br shows a similar trend to Cl with the highest concentrations at the volcanic front (152-308 ppb) compared to the forearc (78-131 ppb) and the backarc (<60 ppb). In contrast, F concentrations are highest in the forearc (144-600 ppm) decreasing to 136-197 ppm at the volcanic front and 75-164 ppm in the backarc. Iodine concentrations are highest in the forearc (26 to 99 ppb) to <30 ppb at the volcanic front and backarc.  $\delta^{37}\text{Cl}$  values range from -0.1‰ to 0.8‰ with a mean value of 0.4‰ ( $\pm 0.3$ ). There is no apparent geographic dependence on  $\delta^{37}\text{Cl}$  values as samples have both the highest and lowest values from the volcanic front (Figure 11). Moreover, there is no significant correlation of  $\delta^{37}\text{Cl}$  value with Cl concentration or Cl/Br ratio.

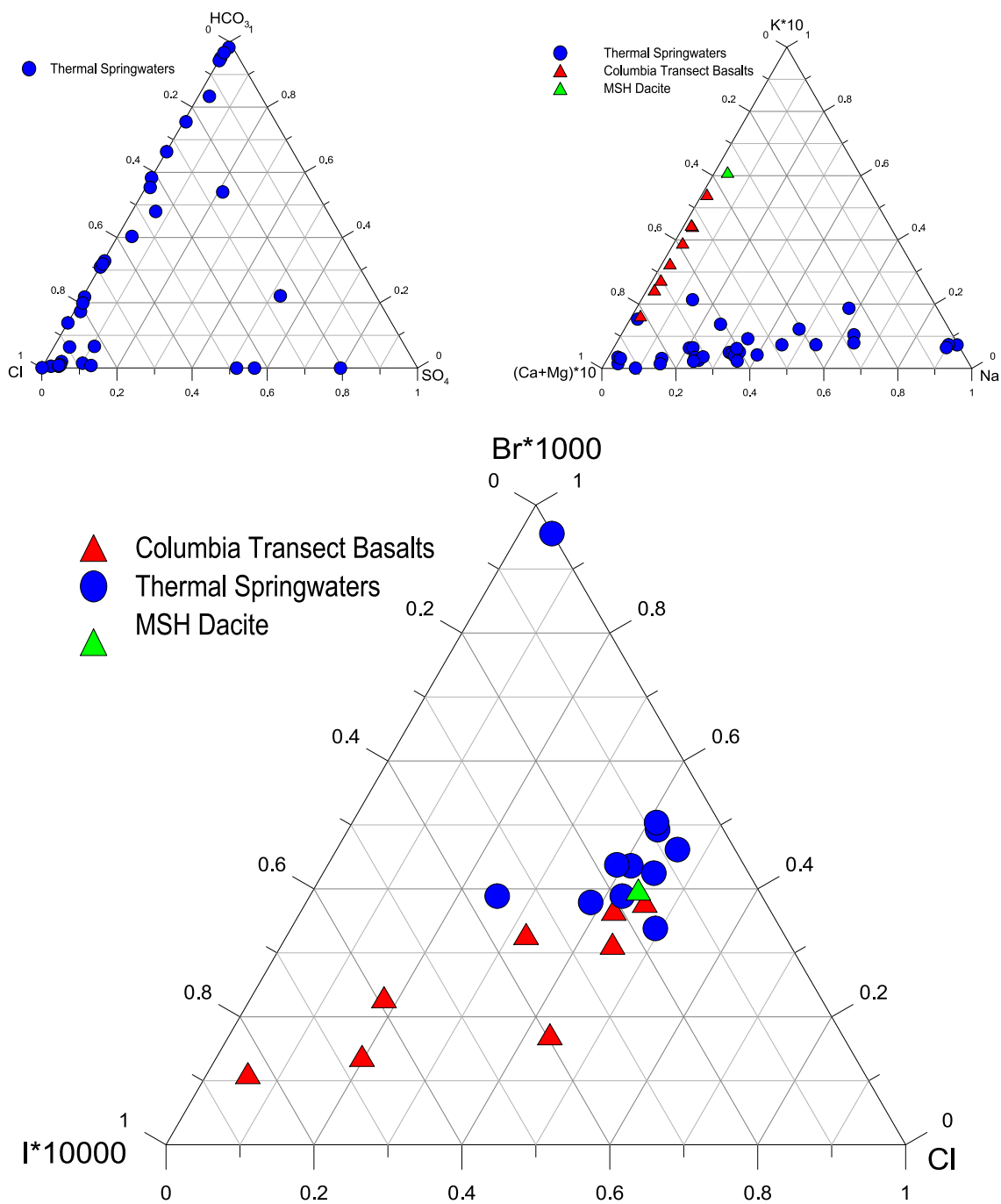


Figure 8: Ternary plots showing molar ratios of anions, cations, and halogens of the measured thermal springwaters and arc transect lavas. Br and I data comes from Mariner et al (2003).

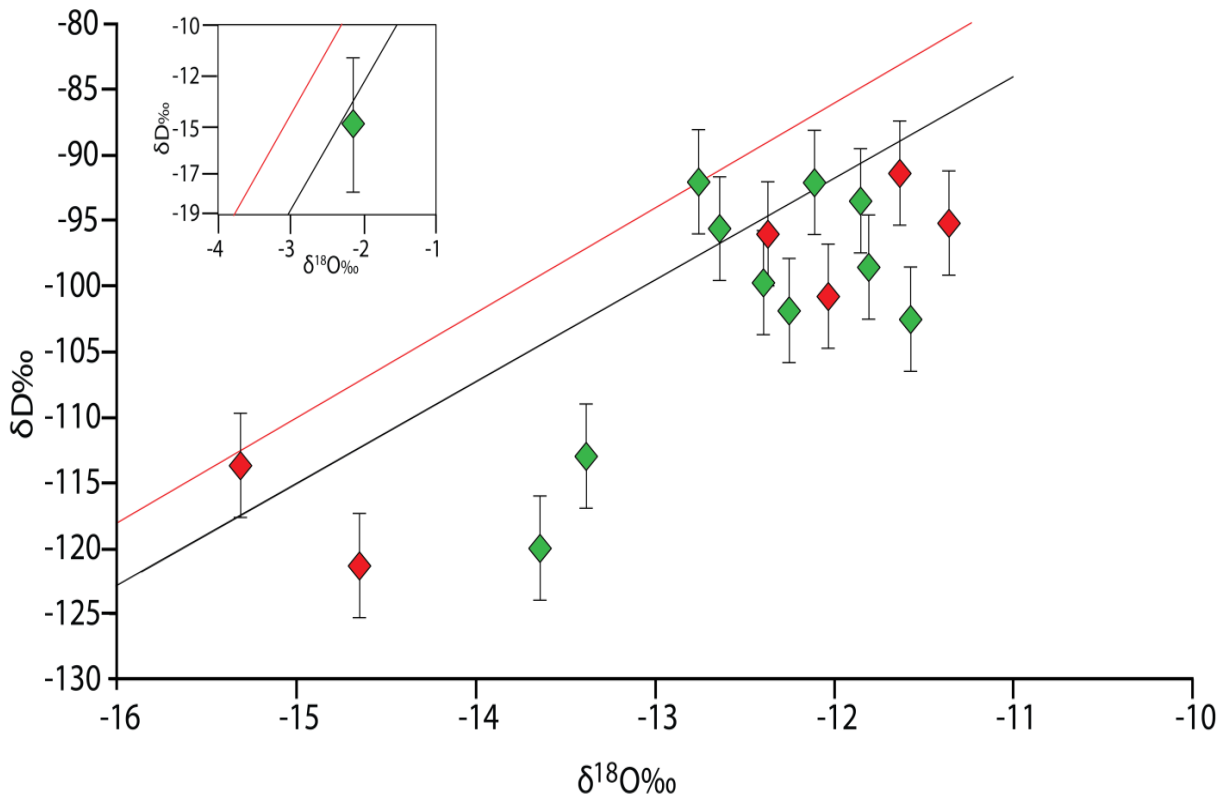


Figure 9:  $\delta D$  vs.  $\delta^{18}O$  plot of the 17 spring waters collected and analyzed by myself. Local meteoric water line (black) calculated using Online Isotope Precipitation Calculator (Bowen 2003). Global meteoric water line shown in red. Red points indicate thermal springwaters with  $pH < 7.5$ . Green points are waters with  $pH > 7.5$ . Boswell Spring shown in inset.

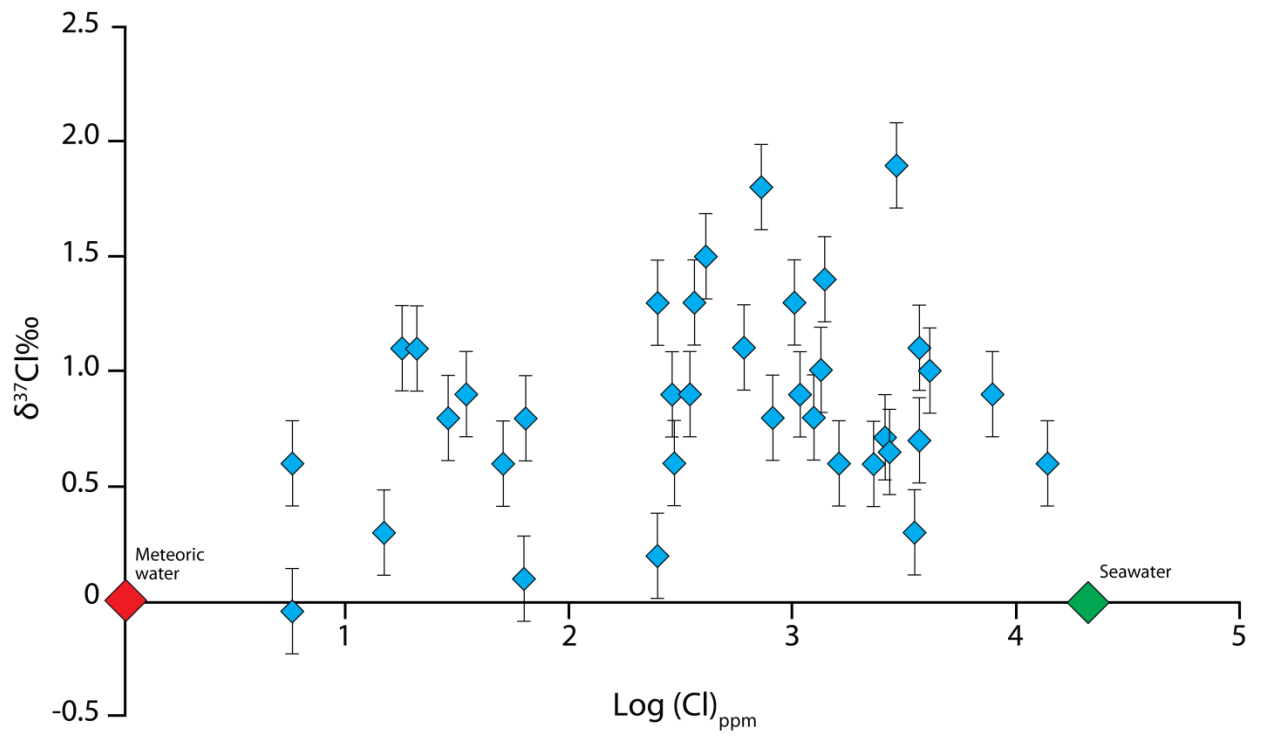


Figure 10:  $\delta^{37}\text{Cl}$  vs. log concentration chloride for the 37 spring waters as well with meteoric water and seawater.

Table 3: Chemical data for thermal and mineral springs in this study. (concentrations are in mg/L).

| Spring Name    | B     | Na    | Mg    | Si  | K   | Ca  | Fe    | HCO <sub>3</sub> <sup>a</sup> | Cl     | Br <sup>b</sup> | F <sup>b</sup> | SO <sub>4</sub> | δ <sup>37</sup> Cl | δ <sup>18</sup> O | δD   | Charge Imbalance <sup>c</sup> |
|----------------|-------|-------|-------|-----|-----|-----|-------|-------------------------------|--------|-----------------|----------------|-----------------|--------------------|-------------------|------|-------------------------------|
| Cave Spring    | 19.8  | 399   | 82.1  | 36  | 21  | 113 | 7.10  | 1260                          | 371.5  | 1               | 0.2            | 1               | 1.2,1.4            | n.d.              | n.d. | -0.9                          |
| Upper Dunsuir  | 18.4  | 386   | 77.7  | 38  | 20  | 98  | 4.87  | 1032                          | 373.3  | 0.96            | 0.1            | 1               | 0.7, 0.7           | n.d.              | n.d. | 2.3                           |
| SS McCloud     | 1.6   | 59    | 41.2  | 33  | 4   | 204 | 18.68 | 992                           | 29.8   | 0.12            | 0.1            | 1               | 0.8                | n.d.              | n.d. | -0.5                          |
| Castle Rock SS | 43.5  | 914   | 197.4 | 41  | 23  | 172 | <0.03 | 2461                          | 1020.4 | 2.86            | 0.4            | 1               | 1.3                | n.d.              | n.d. | -3.0                          |
| Aqua de Ney    | 251.3 | 10513 | b.d.1 | 897 | 143 | 6   | b.d.1 | 17348                         | 7905.1 | 13              | 2.0            | 562             | 0.9                | n.d.              | n.d. | -5.9                          |
| SS Bogus Creek | 97.4  | 3484  | 55.4  | 35  | 99  | 166 | <0.15 | 3202                          | 4135.2 | 5               | 0.0            | 16              | 1                  | n.d.              | n.d. | -0.8                          |
| Olene          | 0.5   | 100   | 2.0   | 33  | 5   | 25  | 0.06  | 53                            | 35.5   | n.d.            | n.d.           | 196             | 0.9                | -11.6             | -103 | -0.8                          |
| Summer Lake 1  | 7.3   | 453   | 0.1   | 41  | 6   | 2   | 0.01  | 529                           | 292.4  | n.d.            | n.d.           | 109             | 0.9                | -13.4             | -113 | 2.0                           |
| Summer Lake 2  | 6.9   | 391   | 0.1   | 43  | 5   | 3   | 0.01  | 416                           | 334.3  | n.d.            | n.d.           | 61              | n.d.               | -13.6             | -120 | -0.6                          |
| Dead Indian    | 17.4  | 435   | 156.8 | 41  | 16  | 169 | 2.84  | 1892                          | 347.4  | 0.28            | 0.1            | 24              | 0.3, 1.5           | -12.5             | -98  | -0.7                          |
| Minnehaha      | 0.2   | 116   | 261.7 | 35  | 27  | 305 | 8.17  | 2435                          | 15.2   | 0.03            | .01            | 24              | 0.3                | -14.3             | -110 | 2.3                           |
| Umpqua         | 40.8  | 2244  | 41.1  | 38  | 63  | 347 | 1.92  | 1308                          | 3546.7 | 5.5             | 1.0            | 194             | 0.3                | -12.0             | -101 | -2.3                          |
| Kitson         | 19.7  | 1189  | 2.0   | 18  | 21  | 601 | 0.01  | 30                            | 2919.7 | 7               | 2.5            | 174             | 1.9                | -11.9             | -94  | -2.4                          |
| McCredie       | 17.9  | 984   | 0.9   | 31  | 24  | 474 | 0.01  | 24                            | 2333.4 | 5               | 2.5            | 280             | 0, 1.2             | -12.4             | -96  | -3.5                          |
| Wall Creek     | 6.5   | 331   | 0.2   | 29  | 9   | 113 | 0.03  | 43                            | 615.2  | 2.7             | 8.6            | 147             | 1.1                | -12.7             | -96  | -2.1                          |
| Terwillinger   | 5.2   | 389   | 0.1   | 21  | 6   | 212 | 0.01  | 24                            | 818.7  | 1.82            | 0.8            | 253             | 0.9, 0.7           | -12.1             | -92  | -1.9                          |
| Foley          | 8.5   | 531   | 0.1   | 28  | 9   | 514 | 0.01  | 22                            | 1400.3 | 3.54            | 0.4            | 557             | 1.4                | -11.6             | -91  | -2.5                          |
| Sphinx         | 0.2   | 22    | 3.1   | 13  | 2   | 4   | <0.03 | 61                            | 6.6    | 0.03            | 0.2            | 3               | -0.1, 0            | -13.5             | -96  | 8.0                           |

Table 3 cont.

| Spring Name             | B           | Na          | Mg           | Si           | K         | Ca          | Fe           | HCO <sub>3</sub> <sup>a</sup> | Cl             | Br <sup>b</sup> | F <sup>b</sup> | SO <sub>4</sub> | δ <sup>37</sup> Cl | δ <sup>18</sup> O | δD          | Charge Imbalance <sup>c</sup> |
|-------------------------|-------------|-------------|--------------|--------------|-----------|-------------|--------------|-------------------------------|----------------|-----------------|----------------|-----------------|--------------------|-------------------|-------------|-------------------------------|
| <b>Bigelow</b>          | <b>6.3</b>  | <b>662</b>  | <b>0.3</b>   | <b>41</b>    | <b>16</b> | <b>219</b>  | <b>0.02</b>  | <b>24</b>                     | <b>1354.6</b>  | <b>3.6</b>      | <b>1.2</b>     | <b>172</b>      | <b>1</b>           | <b>-11.8</b>      | <b>-99</b>  | <b>-1.4</b>                   |
| <b>Belknap</b>          | <b>5.6</b>  | <b>634</b>  | <b>0.9</b>   | <b>32</b>    | <b>16</b> | <b>191</b>  | <b>0.03</b>  | <b>20</b>                     | <b>1251.3</b>  | <b>2.6</b>      | <b>3.2</b>     | <b>145</b>      | <b>0.8</b>         | <b>-11.4</b>      | <b>-95</b>  | <b>-2.5</b>                   |
| <i>Waterloo</i>         | <i>27.4</i> | <i>1200</i> | <i>62.5</i>  | <i>35</i>    | <i>22</i> | <i>190</i>  | <i>8.98</i>  | <i>1385</i>                   | <b>1636.2</b>  | <i>5</i>        | <i>1.0</i>     | <b>20</b>       | <b>0.6</b>         | <i>-8.3</i>       | <i>-68</i>  | <i>-1.2</i>                   |
| <b>Cascadia</b>         | <b>39.5</b> | <b>1598</b> | <b>99.6</b>  | <b>17</b>    | <b>32</b> | <b>348</b>  | <b>24.42</b> | <b>1348</b>                   | <b>2794.8</b>  | <b>9</b>        | <b>1.0</b>     | <b>47</b>       | <b>0.5, 0.8</b>    | <i>-8.6</i>       | <i>-72</i>  | <i>-2.6</i>                   |
| <b>Upper Soda</b>       | <b>28.1</b> | <b>2155</b> | <b>48.2</b>  | <b>20</b>    | <b>69</b> | <b>601</b>  | <b>6.88</b>  | <b>1618</b>                   | <b>3726.5</b>  | <b>8</b>        | <b>1.0</b>     | <b>117</b>      | <b>1.1</b>         | n.d.              | n.d.        | <i>-1.7</i>                   |
| <b>Boswell</b>          | <b>6.8</b>  | <b>3922</b> | <b>0.4</b>   | <b>b.d.l</b> | <b>11</b> | <b>6890</b> | <b>0.04</b>  | <b>27</b>                     | <b>13848.5</b> | <b>48</b>       | <b>0.0</b>     | <b>0</b>        | <b>0.5, 0.7</b>    | <b>-2.3</b>       | <b>-15</b>  | <b>13.6</b>                   |
| <b>Weberg</b>           | <b>17.7</b> | <b>707</b>  | <b>8.3</b>   | <b>40</b>    | <b>39</b> | <b>38</b>   | <b>0.09</b>  | <b>1823</b>                   | <b>63.0</b>    | n.d.            | n.d.           | <b>2</b>        | <b>0.1</b>         | <b>-14.6</b>      | <b>-121</b> | <b>4.0</b>                    |
| <b>Breitenbush</b>      | <b>3.9</b>  | <b>681</b>  | <b>0.9</b>   | <b>69</b>    | <b>30</b> | <b>101</b>  | <b>0.07</b>  | <b>135</b>                    | <b>1085.1</b>  | <b>3</b>        | <b>3.8</b>     | <b>137</b>      | <b>0.9</b>         | <b>-12.3</b>      | <b>-102</b> | <b>-0.3</b>                   |
| <b>Bagby</b>            | <b>0.1</b>  | <b>52</b>   | <b>0.1</b>   | <b>36</b>    | <b>1</b>  | <b>4</b>    | <b>0.44</b>  | <b>67</b>                     | <b>18.6</b>    | n.d.            | <b>0.7</b>     | <b>41</b>       | <b>1.1</b>         | <b>-12.8</b>      | <b>-92</b>  | <b>1.0</b>                    |
| <b>Austin</b>           | <b>2.6</b>  | <b>300</b>  | <b>0.1</b>   | <b>38</b>    | <b>7</b>  | <b>37</b>   | <b>0.01</b>  | <b>56</b>                     | <b>406.6</b>   | <b>20</b>       | <b>1.3</b>     | <b>142</b>      | <b>1.5</b>         | <b>-12.4</b>      | <b>-100</b> | <b>-1.7</b>                   |
| <i>Wilhoit</i>          | <i>34.9</i> | <i>1800</i> | <i>110.7</i> | <i>32</i>    | <i>20</i> | <i>369</i>  | <i>11.20</i> | <i>2142</i>                   | <b>2648.4</b>  | <i>4.5</i>      | <b>1.0</b>     | <b>25</b>       | <b>0.3, 1.1</b>    | <i>-8.2</i>       | <i>-72</i>  | <i>-1.7</i>                   |
| <b>Klickitat</b>        | <b>0.1</b>  | <b>67</b>   | <b>110.9</b> | <b>74</b>    | <b>11</b> | <b>133</b>  | <b>14.51</b> | <b>1096</b>                   | <b>21.4</b>    | n.d.            | n.d.           | <b>2</b>        | <b>1.1</b>         | <b>-15.3</b>      | <b>-114</b> | <b>2.3</b>                    |
| <b>MSH10-02</b>         | n.d.        | n.d.        | n.d.         | n.d.         | n.d.      | n.d.        | n.d.         | n.d.                          | <b>250.5</b>   | n.d.            | n.d.           | n.d.            | <b>1.3</b>         | n.d.              | n.d.        | n.d.                          |
| <b>MSH10-03</b>         | n.d.        | n.d.        | n.d.         | n.d.         | n.d.      | n.d.        | n.d.         | n.d.                          | <b>300.3</b>   | n.d.            | n.d.           | n.d.            | <b>0.6</b>         | n.d.              | n.d.        | n.d.                          |
| <b>MSH10-04</b>         | n.d.        | n.d.        | n.d.         | n.d.         | n.d.      | n.d.        | n.d.         | n.d.                          | <b>250.5</b>   | n.d.            | n.d.           | n.d.            | <b>0.2</b>         | n.d.              | n.d.        | n.d.                          |
| <b>Carbonate Spring</b> | n.d.        | n.d.        | n.d.         | n.d.         | n.d.      | n.d.        | n.d.         | n.d.                          | <b>51.3</b>    | n.d.            | n.d.           | <b>180</b>      | <b>0.6</b>         | n.d.              | n.d.        | n.d.                          |
| <b>Paradise Spring</b>  | <i>0.9</i>  | <i>13</i>   | <i>32.5</i>  | n.d.         | <i>18</i> | <i>43</i>   | n.d.         | n.d.                          | <b>64.4</b>    | n.d.            | n.d.           | <b>188</b>      | <b>0.8</b>         | n.d.              | n.d.        | <i>0.9</i>                    |
| <b>Gamma Spring</b>     | n.d.        | n.d.        | n.d.         | n.d.         | n.d.      | n.d.        | n.d.         | n.d.                          | <b>736.4</b>   | n.d.            | n.d.           | n.d.            | <b>1.8</b>         | n.d.              | n.d.        | n.d.                          |
| <b>Sulphur Creek</b>    | <i>0.1</i>  | <i>13</i>   | <i>6.5</i>   | <i>20</i>    | <i>3</i>  | <i>9</i>    | n.d.         | n.d.                          | <b>6.2</b>     | n.d.            | n.d.           | <b>62</b>       | <b>0.6</b>         | n.d.              | n.d.        | n.d.                          |

(n.d.) not determined.

(b.d.l) below detection limit.

Bolded values are data acquired myself at the University of TX. Italicized data were acquired by USGS

<sup>a</sup> Total alkalinity as bicarbonate<sup>b</sup> Values in bold from Mariner et al. 2003<sup>c</sup> Charge balance calculated using the anions Cl<sup>-</sup>, SO<sub>4</sub><sup>2-</sup>, Br<sup>-</sup>, HCO<sub>3</sub><sup>-</sup>, and the cations Na<sup>+</sup>, Mg<sup>2+</sup>, K<sup>+</sup>, Ca<sup>2+</sup>, Fe<sup>2+</sup>and the equation 
$$\left[ \frac{\sum mEq_{cations} - \sum mEq_{anions}}{\sum mEq_{cations} + \sum mEq_{anions}} \right] \times 100 \%$$

Table 4. Halogen concentration and stable Cl isotope composition of the 9 lava samples.

| <b>Sample</b> | <b>Description</b>              | <b>Cl<sub>(ppm)</sub></b> | <b>Br<sub>(ppb)</sub></b> | <b>F<sub>(ppm)</sub></b> | <b>I<sub>(ppb)</sub></b> | <b>δ<sup>37</sup>Cl‰<sub>(SMOC)</sub></b> |
|---------------|---------------------------------|---------------------------|---------------------------|--------------------------|--------------------------|---|
| <b>V457</b>   | Forearc                         | 16.761                    | 78.2                      | 599.9                    | 91.9                     | +0.0                                      |
| <b>V348</b>   | Forearc                         | 81.468                    | 131.2                     | 143.7                    | 99.4                     | n.d.                                      |
| <b>L00-10</b> | Portland Basin                  | 65.931                    | 152.4                     | 317.1                    | 25.5                     | +0.6                                      |
| <b>L01-17</b> | Mt. St. Helens                  | 141.210                   | 264.7                     | 136.3                    | 18.0                     | +0.5                                      |
| <b>L01-25</b> | Mt Adams                        | 139.582                   | 221.9                     | 155.5                    | 26.7                     | -0.1                                      |
| <b>L01-24</b> | Mt. Adams                       | 156.727                   | 308.2                     | 197.2                    | 28.0                     | +0.7                                      |
| <b>L83-91</b> | Backarc                         | 18.792                    | 54.7                      | 164.1                    | 22.1                     | +0.5                                      |
| <b>L83-57</b> | Backarc                         | 64.718                    | 58.5                      | 75.1                     | 21.1                     | +0.1                                      |
| <b>SH-33</b>  | Mt. St. Helens,<br>crustal melt | 119.130                   | 244.4                     | 120.6                    | 15.7                     | +0.8                                      |

(n.d.) not determined

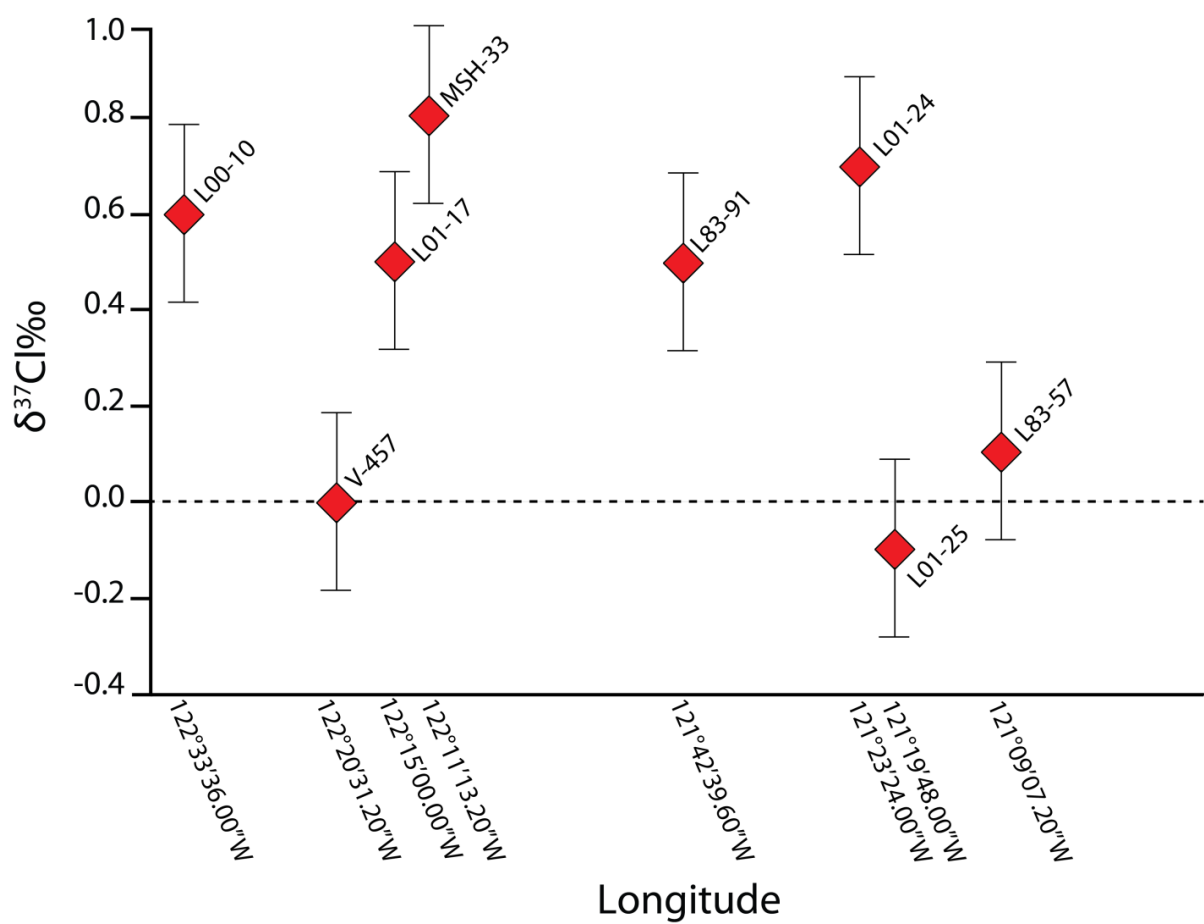


Figure 11:  $\delta^{37}\text{Cl}$  value vs. west longitude across the Columbia Transect of the Cascade Arc.

## Chapter 6: Discussion

Previous work has suggested that across the central Oregon Cascades the majority of chloride in thermal springs is either derived from an organic-bearing, early Tertiary marine unit underlying late Tertiary and Quaternary lava flows (Mariner et al., 2003) or, based on  $^{36}\text{Cl}$  and  $^{129}\text{I}$  data, is due to degassing of magmatic intrusions (Hurwitz et al., 2005). Below, through the presentation of new stable Cl isotope data, I aim to better constrain the Cl sources in the springs across the Cascades and illustrate any systematic spatial variability in Cl chemistry throughout the Cascade Arc springs which may be linked to the subducting slab Cl devolatilization processes. In order to do this, newly acquired halogen concentration and stable Cl isotope data for nine well-characterized cross-arc lavas are used to constrain the  $\delta^{37}\text{Cl}$  values and Cl concentrations of the volcanic rocks hosting the springs and quantify how much Cl is lost across the arc, and thus the available Cl that could be incorporated into the spring waters. Correlating  $\delta^{37}\text{Cl}$  values between the thermal springs and lavas may provide better understanding of the relationship between the two.

### 6.2 Halogens in the Columbia Transect lavas.

The halogen and chlorine stable isotope data gathered in this study on the nine lavas from the Columbia Transect supplement results from Leeman et al. (2004; 2005), which asserts that distinct mantle sources and variable slab contributions exist between the

two groups of lavas. Group 1 lavas (n=5) (L01-17, 24, 25, and L83-57, 91), which have stronger affinities to MORB-OIB, were produced from mantle decompressional melting, and group 2 lavas (n=3) (V-348, 457, and L001-10) exhibit chemical signatures reflective of strong interaction with slab-derived components i.e. elevated volatile elements, high LILE/HFSE ratios etc.. Following the criteria and classification from Leeman (2004, 2005), the 9 lavas analyzed from the Columbia Transect are evaluated with consideration to their respective groups outlined above.

The halogen chemistries of the lavas show spatial relationships along the arc. Figure 12 illustrates halogen ratios across the Columbia transect normalized to Nb concentrations, where Nb should be unaffected by any slab contributions as it is an incompatible, fluid immobile element. It is immediately seen that the MSH-33 dacite sample is a highly differentiated magma and its halogen composition does not directly derive from the mantle; being likely affected by higher order processes such as fractional crystallization, crustal assimilation, and perhaps magma mixing. I and F are systematically higher in group 2 samples, consistent with the premise of modest slab fluid contribution in the forearc. Contrary to what is expected for the observation of any slab contribution in the forearc, Cl and Br do not show a similar spatial trend to I and F. It should be noted that variations in halogen concentrations in the lavas across the arc transect may not elucidate subduction processes altogether. Magmatic degassing has likely overprinted the original halogen compositions to different degrees. Cl concentrations in the whole rocks range from 16.76-156.72 ppm, whereas Cl concentrations in Mt. Shasta melt inclusions have

been found to be as high as 1200 ppm with Cl/Nb ratios between 37-190 (Ruscitto et al., 2010). Significant Cl and to varying extents Br, F, and I have probably been lost from the parental melts before having cooled.

Chlorine and bromine concentrations correlate very well with one another within individual samples across the transect (Figure 13). This complementary behavior is predicted as the two have the most similar atomic radii of all the halogens (79 and 94 pm respectively, differing by 15%, in comparison to F (42 pm) and I (115 pm) (Cotton et al., 1988). Although Cl and Br concentrations exhibit a coupled behavior from within individual samples, the Cl/Br ratios show poor systematic spatial dependence along the arc transect and are non-uniform (Figure 14). Cl, with a higher fluid melt partition coefficient will preferentially be lost as HCl over HBr during magma degassing. Variable extents of degassing between each sample's parental magmas could account for this variability as highly degassed magmas will likely have lower Cl/Br ratios compared to less degassed magmas, assuming relatively similar starting Cl and Br compositions between the two. Because of the effects of degassing, the array in Cl/Br ratios probably do not strongly reflect processes occurring within the slab during progressive devolatilization reactions. Group 1 backarc samples ratios', where little slab contribution is believed to effect magma composition, are rather comparable to forearc sample ratios. It is also interesting that the highest Cl/Br ratio comes from the sample furthest east in the backarc where slab contribution is thought to be negligible. The elevated Cl with respect to Br here may be

derived from a lower degree of degassing, although initial melt source composition or the later addition of other Cl and Br bearing material cannot be discounted.

Unlike the halogens, Ba composition of the lavas is much less susceptible to alteration by degassing processes yet is also fluid mobile which can be used to reveal the addition of slab component. (Figure 15) shows Ba/Nb ratios of the lavas with respect to their longitudinal collection location. The same systematic that is observed with F and I across the transect is also seen with Ba where Ba/Nb ratios are unequivocally higher in the group 2 forearc lavas compared to the group 1 back arc lavas. This observation is consistent with the suggestion that slab contributions to lavas are minimal in the backarc, yet high enough in the forearc that the systematic decrease moving towards the backarc can be identified.

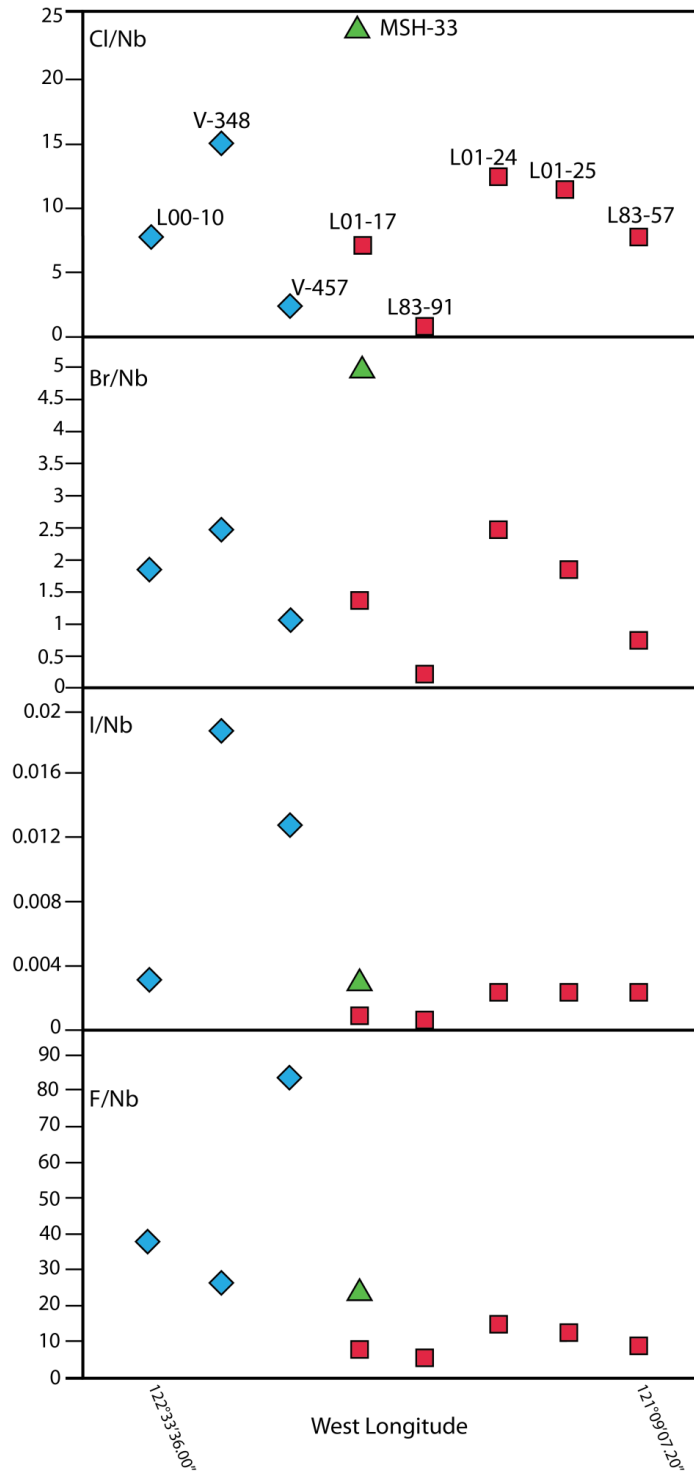


Figure 12: (Cl, Br, F, and I)/Nb ratios of the 9 arc transect lavas.

Figure 12 cont: plotted with respect to west longitude along the transect. Blue diamonds represent the group 2 lavas. Red squares represent group 1 lavas. Green triangle shows MSH-33 dacite.

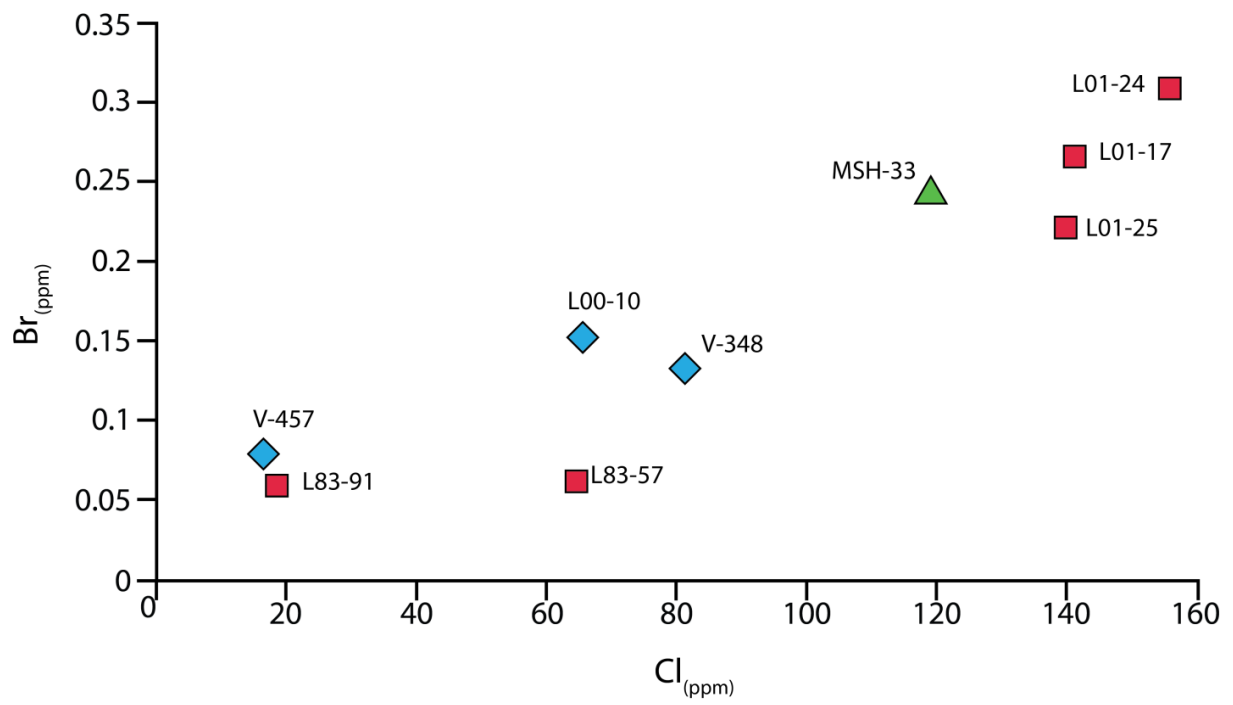


Figure 13: Br vs. Cl concentration of the 9 arc transect lavas. Blue diamonds represent the group 2 lavas. Red squares represent group 1 lavas. Green triangle shows MSH-33 dacite.

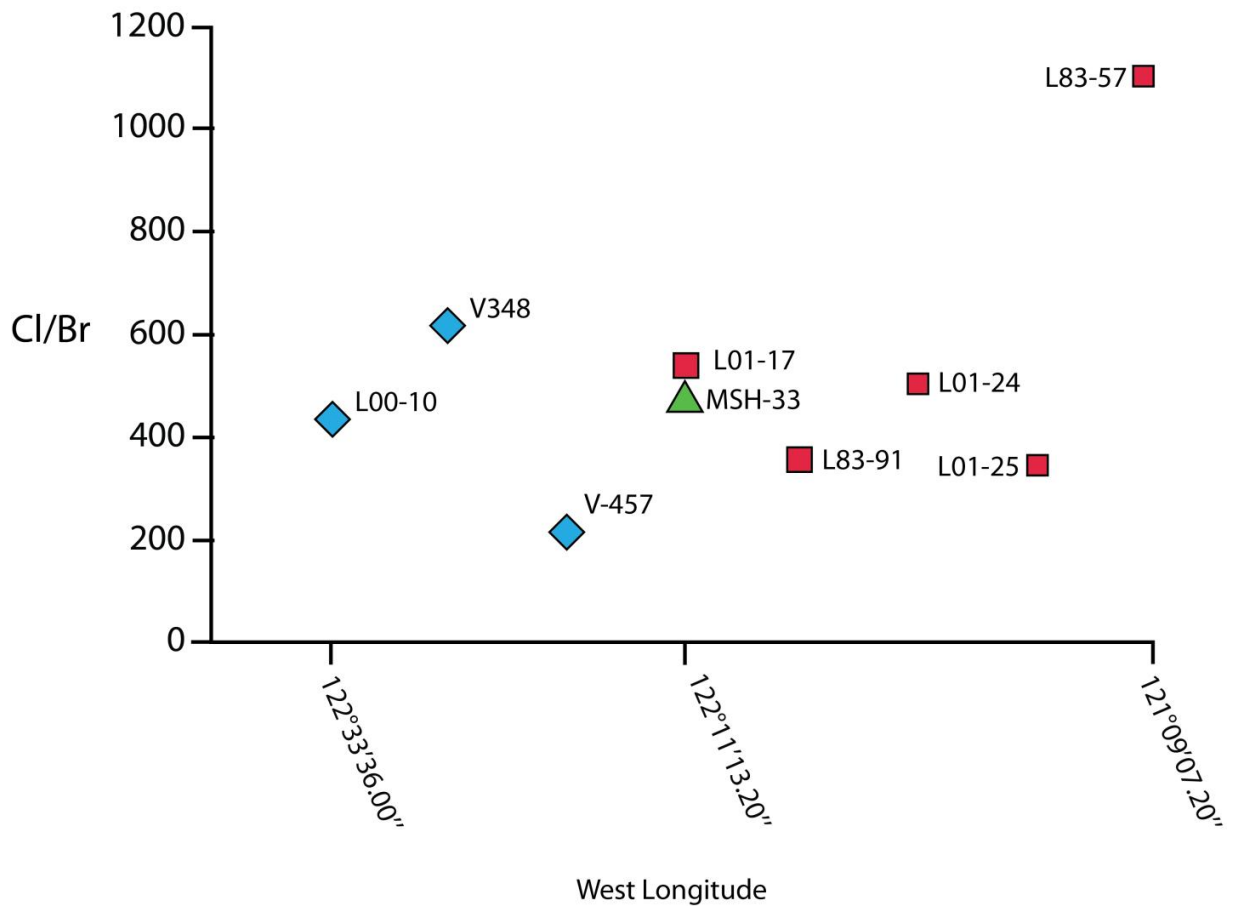


Figure 14: Cl/Br ratio of lavas with plotted with respect to west longitude along the arc transect. Blue diamonds represent the group 2 lavas. Red squares represent group 1 lavas. Green triangle shows MSH 33 dacite.

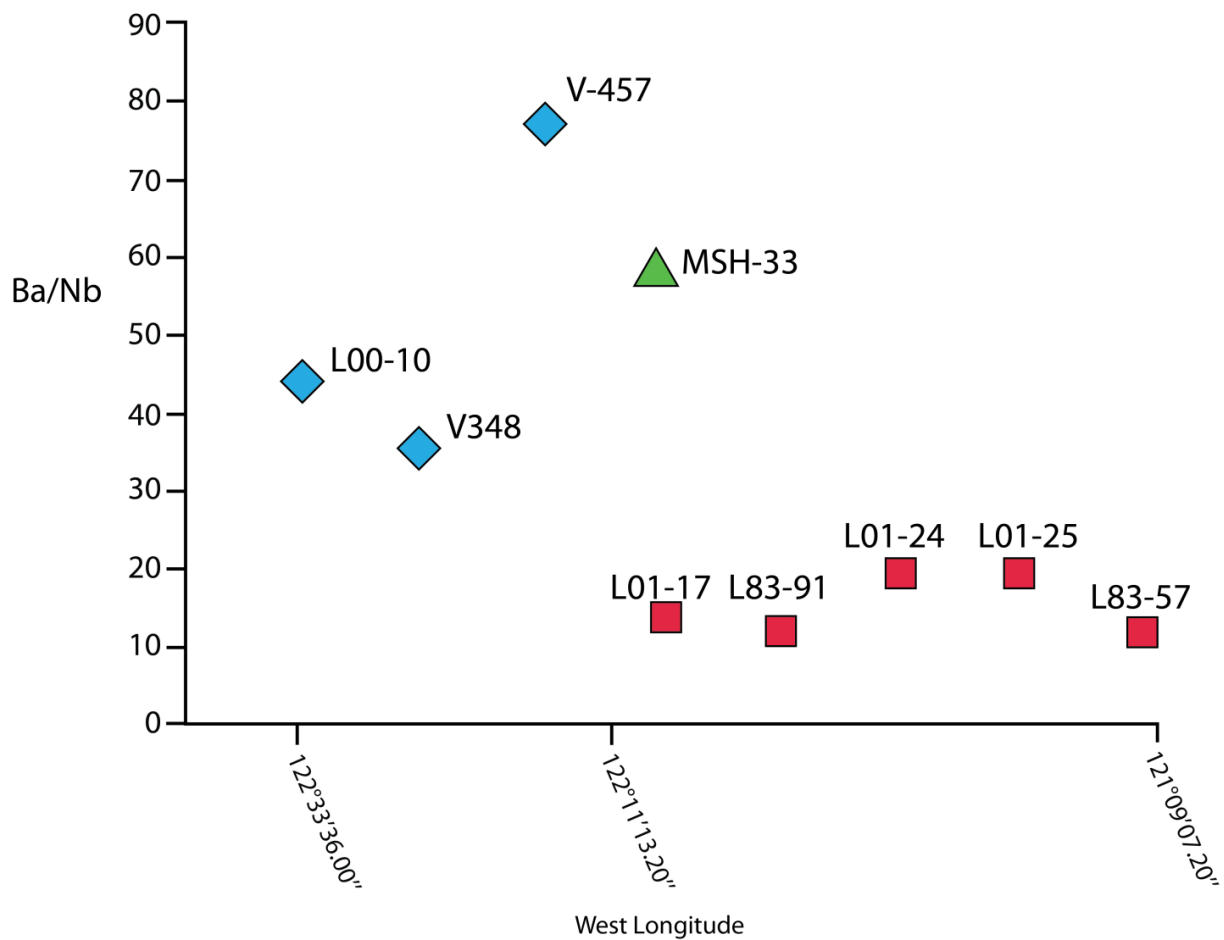


Figure 15: Ba/Nb ratio of the 9 cross-arc transect lavas plotted with respect to west longitude along the arc transect. Blue diamonds represent the group 2 lavas. Red squares represent group 1 lavas. Green triangle shows MSH 33 dacite.

Cl and Br concentrations correlate extraordinarily well with B concentrations within the group 1 backarc lavas,  $R^2 = .87$  and  $.67$   $P = .006$  and  $.046$  respectively (Figure 16). Slab signature in these backarc group 1 lavas is not believed to be present, and the good agreement between Br and Cl to B concentrations likely reflects processes that affect B similarly i.e. non flux induced partial melting and subsequent degassing. If however a portion of the Cl, Br, and B in these lavas is slab derived, this trend may be indicative of equal, cogenetic slab contributions to the lavas. It is also curious why this correlation is only observed in the group 1 lavas. It may be that the amount of Cl, Br, and B in group 2 lavas is significantly larger, from early devolatilization off the subducting slab, than in group 1 lavas and that they are highly fractionated from the subducting slab during these devolatilization reactions. However, it is noteworthy that despite the good correlation between Cl and B and apparent universal similar behavior, the Cl/B ratio is highly non-uniform across the arc (Figure 17). Furthermore, despite the established interpretation that slab contributions should be highly attenuated in the backarc, absolute abundance of Cl and B are overall higher in 3 of the 5 back arc lavas. This anomaly may just be a result of the very limited sample set, or larger extents of degassing in the fore-arc lavas construe the early, pre-eruptive concentrations. Although previous enrichment of these 3 backarc samples' mantle sources much earlier in the subduction history of the Cascades is another possible explanation to reconcile this peculiarity. Whereas B/Nb ratios are generally characterized by higher values in the group 2 forarc lavas and lower in group 1, consistent with a greater slab component from the shallow loss from the slab, Cl/B ratios are

sporadic across the arc and suggest that should Cl and B be derived from the dehydrating slab, Cl concentrations are being subsequently altered to various degrees in relation to B, perhaps by fractional crystallization or degassing processes. Figure 17 shows the similar behavior of Cl and B in conjunction with the complex nature of Cl/B ratios across the arc.

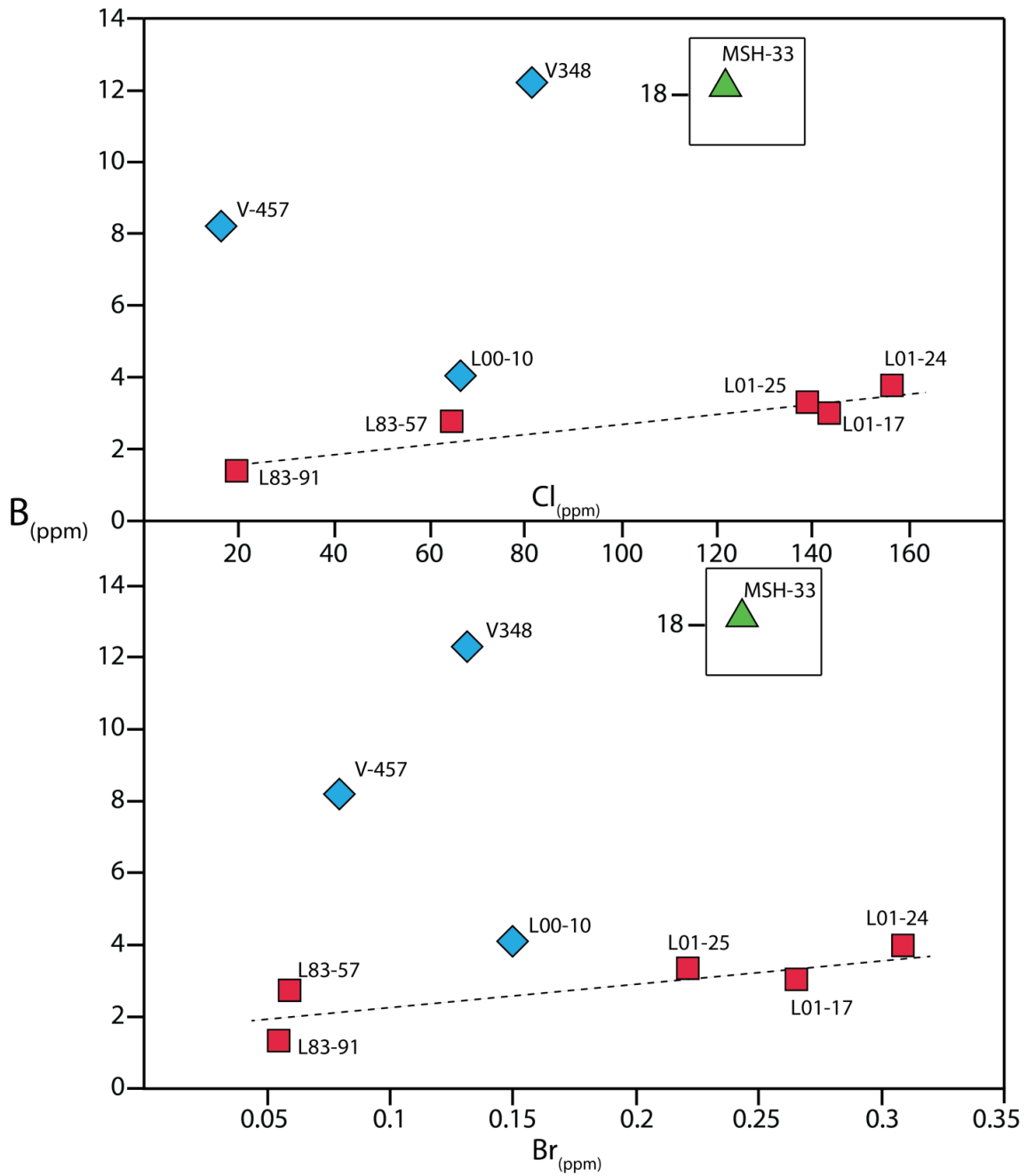


Figure 16: B concentrations vs. Cl and Br concentrations of the 9 arc transect lavas. Blue diamonds represent the group 2 lavas. Red squares represent group 1 lavas. Mt. St. Helens dacite shown as green triangle.

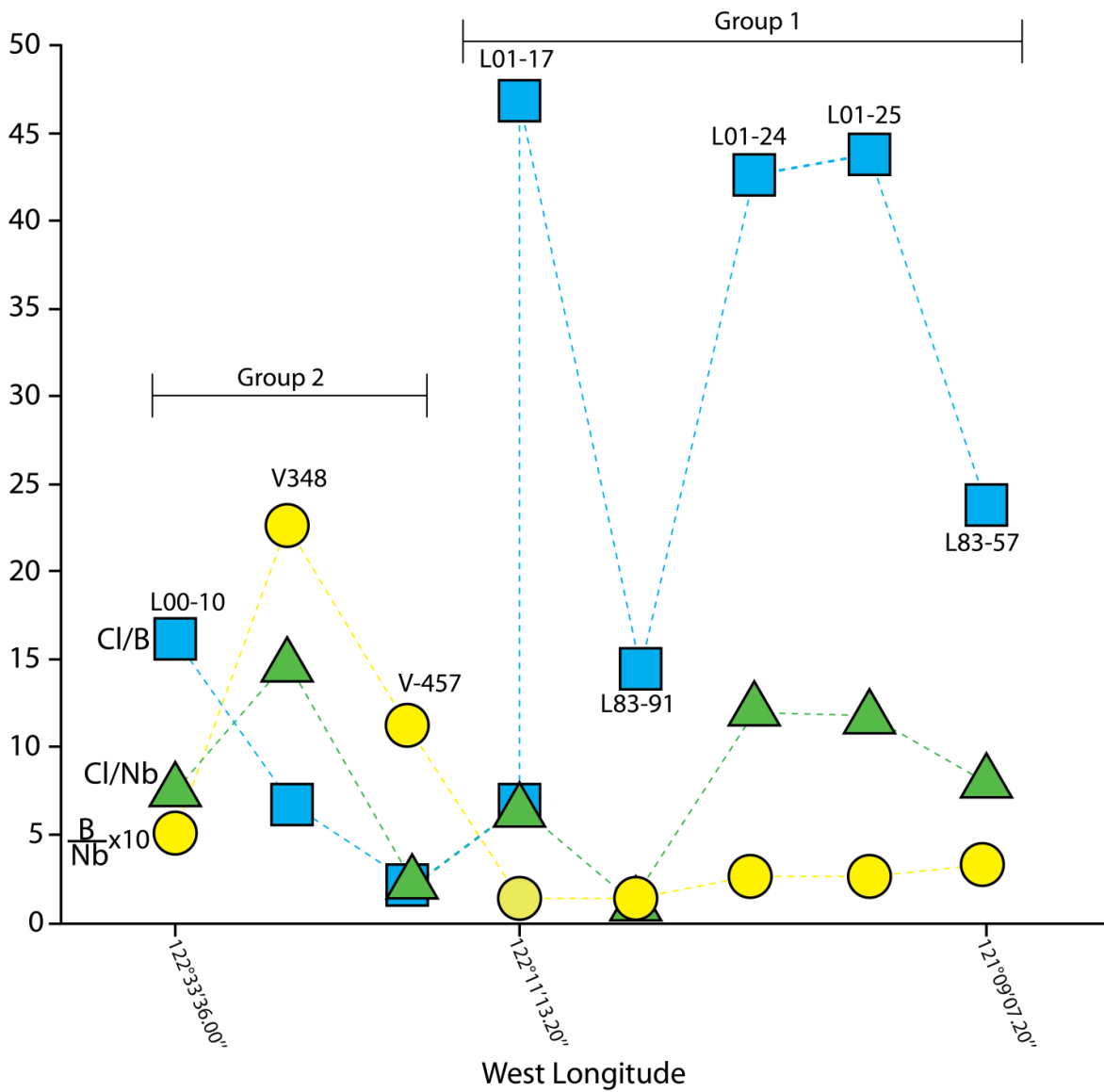


Figure 17: Cl/B, Cl/Nb, and B/Nb\*10 ratios for the 9 arc transect lavas plotted with respect to their west longitude along the transect. Cl/B ratio shown as blue squares, Cl/Nb ratio shown as green triangles, and B/Nb x 10 ratios shown as yellow circles.

Cl isotope ratios are independent of location along the transect as well as their inferred mantle sources. Only two  $\delta^{37}\text{Cl}$  values were obtained for the group 2 lavas, one of which is 0.0‰. This  $\delta^{37}\text{Cl}$  value is consistent with the near 0‰ of the mantle ( $-0.2 \pm 0.3\%$ , Sharp et al., 2007, 2013) supporting the premise that group 2 lavas are decompression melts of unmodified lithosphere. However, one sample is insufficient to base this interpretation on and more  $\delta^{37}\text{Cl}$  analyses of samples from the backarc are required in order to establish any variation between group 1 and group 2 lavas. Furthermore,  $\delta^{37}\text{Cl}$  values of the lavas are independent of their respective Cl concentrations (Figure 18), an observation in agreement with the notion that Cl isotopes do not fractionate in magmatic systems. Additionally, no relationship exists between  $\delta^{37}\text{Cl}$  value and spatial location across the arc transect (Figure 19). If Cl isotope fractionation was occurring either during loss of Cl from the slab or during the evolution of a parental magma (e.g., degassing), one would expect to see a dependence of  $\delta^{37}\text{Cl}$  value on either Cl concentration and/or its erupted location across the arc, but no such relationships exist.

The variation in  $\delta^{37}\text{Cl}$  values among the samples plausibly stems from heterogeneities in the mantle source or variation in crustal contamination. However, these samples have previously been modeled to have high melt temperatures, and show no indices of fractionation or incorporation of evolved or altered material (Leeman et al., 2005; Leeman et al., 2004). The  $>0\%$   $\delta^{37}\text{Cl}$  values of these basalts then suggest that the mantle source of the Cl is similar in composition to the magma. With NMORB mantle constrained to  $\delta^{37}\text{Cl}$  values of  $-0.2 \pm 0.3\%$ , Sharp et al. (2007, 2013), one explanation to

reconcile the  $\delta^{37}\text{Cl}$  values of the basalts is the existence of a  $^{37}\text{Cl}$  enriched local mantle beneath this transect of the Cascades. Based on previous work that suggests a limited slab component in the Cascades, particularly the Central Cascades (Leeman et al., 1990, 2004, Ruscitto et al., 2010), I suggest that the slightly higher than mantle  $\delta^{37}\text{Cl}$  values are due to the combination of a slightly modified mantle and minor assimilation of basement mafic and ultramafic rock, as has been proposed in the Shasta region (Streck et al., 2007), with minimal to moderate slab-derived component. In particular, the high  $\text{SiO}_2$  content and elevated outlying B/Nb and Cl/Nb ratios in sample MSH-33 are explained by the incorporation of evolved crustal material. MSH-33 also has the highest  $\delta^{37}\text{Cl}$  value in the sample set (+0.8‰) possibly reflecting the assimilation of  $^{37}\text{Cl}$ -enriched material (amphibole- and/or serpentine-bearing) from within the crust. Figure 20 shows, with the exception of sample L01-25 from group 2, lower Cl/Nb ratios coincide with lower  $\delta^{37}\text{Cl}$  values. A less pronounced trend is also seen with B/Nb versus  $\delta^{37}\text{Cl}$  value (Figure 20). Assimilation of Cl, and/or B, into a melt from crustal sources enriched in  $^{37}\text{Cl}$  following the initial input from the slab is capable of producing this mixing trend. Although at the moment these trends are categorized as statistically non-significant, further analysis of more samples may help refine this trend.

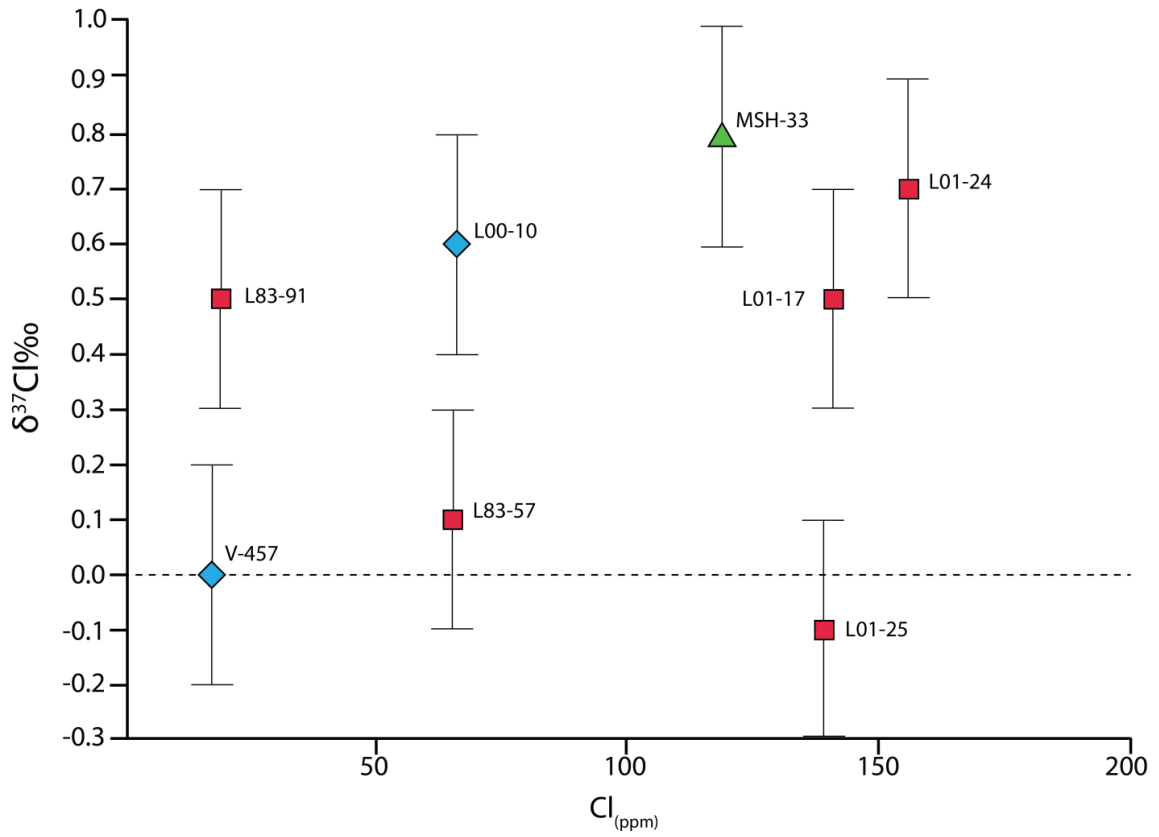


Figure 18:  $\delta^{37}\text{Cl}$  value vs. Cl concentration for of the 9 arc transect lavas. Blue diamonds represent the group 2 lavas. Red squares represent group 1 lavas. Green triangle shows MSH-33 dacite.

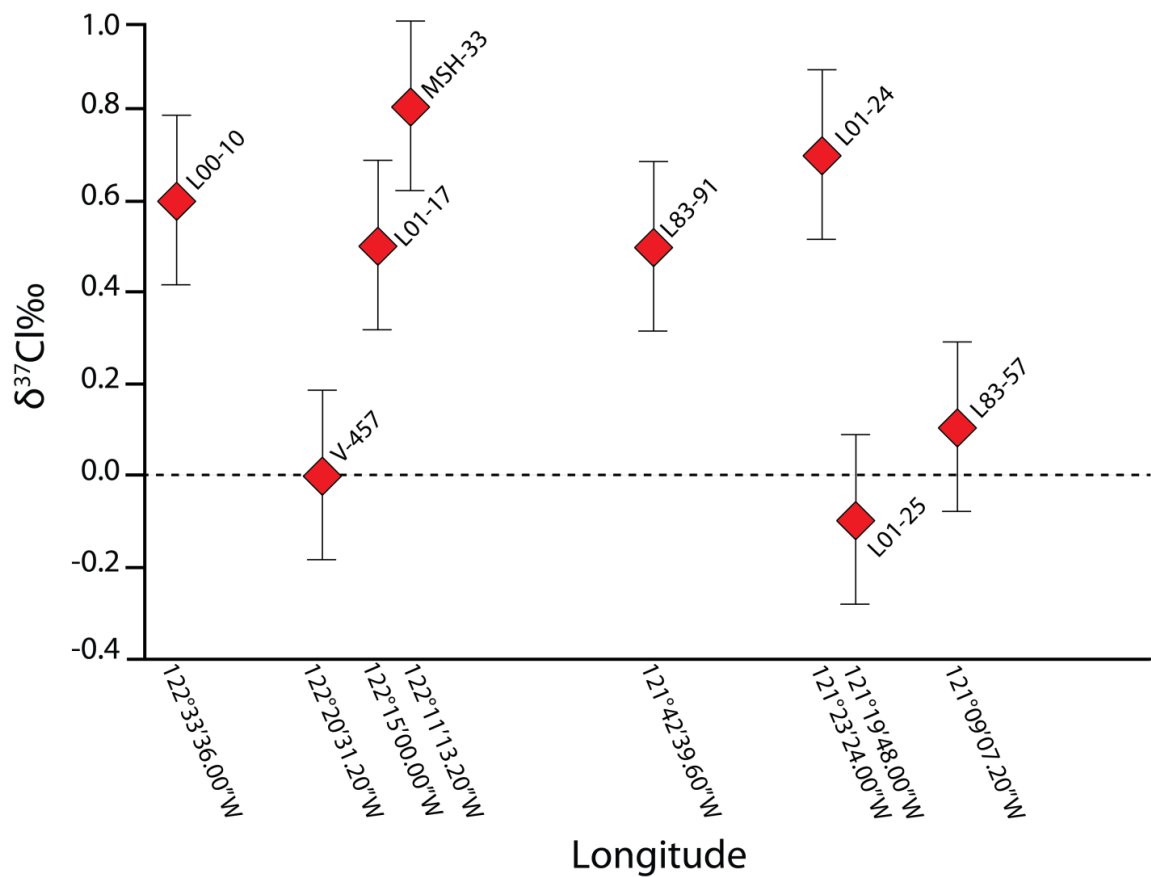


Figure 19:  $\delta^{37}\text{Cl}$  value vs. west longitude across the Columbia Transect segment of the arc of the 9 lavas sampled from within.

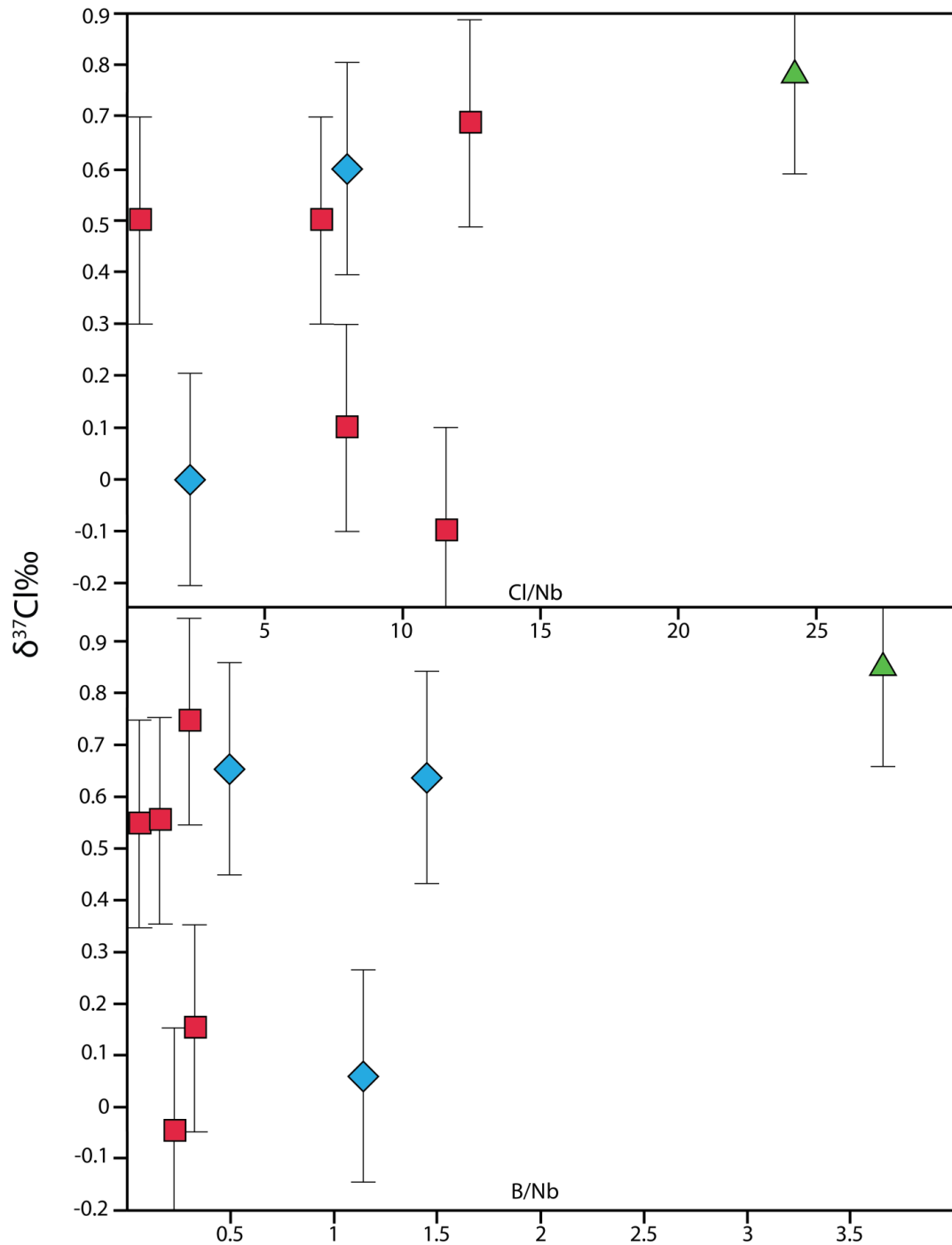


Figure 20:  $\delta^{37}\text{Cl}$  value vs. CI/Nb and B/Nb ratio of the 9 lavas from the Columbia Transect. Blue diamonds represent the group 2 lavas. Red squares represent group 1 lavas. Green triangle shows MSH-33 dacite

### 6.3. Potential chloride sources to the thermal springs

Oxygen and hydrogen isotope data show the majority of spring waters fall, on or very near, the local meteoric water line (Figure 7). The source precipitation for the springs likely originates at altitudes comparable to, or slightly higher in elevation (~200-400 m) (Figure 21), to the spring's elevations, consistent with conclusions made by Ingebritsen et al. (1994), however, a few exceptions exist. Klickitat, to the west of the Quaternary arc, at 170 m elevation appears to be sourced from precipitation originating at much higher <1500 m elevation. Additionally, Boswell Spring may reflect some seawater component, either by infiltration from the Pacific Ocean landward into the neighboring forearc, or preexisting seawater derived pore water as evidenced by the much higher  $\delta D$  and  $\delta^{18}O$  values (-2.3‰ and -15‰, respectively) than the local meteoric water, as well as a high Cl/Br ratio of 289, identical to that of seawater (Barnes, 1954; Riley and Chester, 1971). This interpretation is consistent with Hurwitz et al. (2005) who state that the water discharged from Boswell Spring is locally derived from a subterranean reservoir unlike the rest of the springs which are recharged with meteoric water originating from higher elevations. Constraining the actual deviations in D and  $^{18}O$  values from the meteoric trend in hopes to better quantify the degree of water rock interaction is difficult for a number of reasons: The “true” meteoric trend is not firmly defined. With many of the samples, the deviation in D is within the limits of analytical uncertainty, and water vapor loss during subsurface boiling or addition of magmatic hydrogen and oxygen bearing gasses also alter the  $^{18}O$  and D composition of the waters.

With the exception of Sphynx, all the springs exhibit positive  $\delta^{37}\text{Cl}$  values. The major predominance of  $\delta^{37}\text{Cl}$  values  $>0\text{‰}$  is not consistent with a sedimentary-derived fluid Cl source as most sedimentary materials and pore fluids have negative  $\delta^{37}\text{Cl}$  values (Ransom et al., 1995; Shouakar-Stash et al., 2007; Stewart and Spivack, 2004). In fact,  $\delta^{37}\text{Cl}$  values of the springs generally overlap well with values obtained from lavas from the Columbia Transect. Additionally, saline brines from the Gulf Coast Basin and Palo Duro Basin have predominantly negative to near zero  $\delta^{37}\text{Cl}$  values (-1.9 to 0.6‰) (Eastoe et al., 2001; Eastoe et al., 1999). It should be noted however, high saline brines with Cl concentrations ranging from 44,000-242,000 mg/l and  $\delta^{37}\text{Cl}$  values as high as +1.54‰ have been documented in deep groundwaters of the Siberian Platform of Russia (Shouakar-Stash et al., 2007). Halite precipitated in equilibrium with evaporating seawater has a  $\delta^{37}\text{Cl}$  values of +0.3‰ (Eggenkamp et al., 1995), and globally halite associated with the evaporation of seawater is characterized by  $\delta^{37}\text{Cl}$  values from +0.2‰ to +0.5‰ (Eastoe et al., 2001; Eastoe et al., 2007). Halite with  $\delta^{37}\text{Cl}$  values as high as +0.8‰ can be generated by multiple evaporitic cycles by the congruent dissolution of halite with  $\delta^{37}\text{Cl} >0\text{‰}$  and recrystallization from  $^{37}\text{Cl}$  enriched brine (Eastoe and Peryt, 1999). Slow dissolution of halite, or mixing of residual high salinity brines with an uncommonly high  $\delta^{37}\text{Cl}$  value could partially contribute to the high Cl content of many of the springs. Hurwitz et al. (2005) calculates that for a sedimentary unit with a thickness of 2 km over an area of  $1.3 \times 10^4 \text{ km}^2$  (260 km  $\times$  50 km) with a porosity of 5%, that was initially saturated with seawater and has released Cl at a constant rate similar to that needed to

support the current Cl discharge ( $5 \times 10^6$  kg/yr), it would take only 5 m.y. to discharge all the Cl; a fraction of the time since active volcanism in the Cascades commenced ~44 Ma. In order for this Cl mass balanced to be satisfied for the same 44 m.y. duration, an initial Cl concentration of 169,000 ppm is necessary. A basinal brine of this concentration is unlikely to be found in a subduction zone active margin setting. If halite were the sole-dominant chloride source, congruent dissolution of NaCl into the meteoric waters should produce Na/Cl ratios near 1, and if seawater were a major contributor Na/Cl values should lie along a line with a slope of 0.86 (Figure 22). The positive deviation from the 1:1 line is indication that halite dissolution is unlikely the principal chloride contributor to the springs.

Aerosols from the Pacific Ocean and meteoric water do not likely contribute much Cl to the springs as well, as the springs are on average ~150km from the coast. These sources also only carry a relatively marginal Cl load compared to the high concentrations in many of the thermal springs. Cl isotope fractionation and loss of  $^{35}\text{Cl}$  with underlying organic chlorinated solvents is not likely an explanation in this case as the necessary depths to reach an organic rich marine sedimentary layer beneath the volcanic cover are greater than average estimated circulation depth. Furthermore isotopic equilibrium between water and organic Cl bearing material would have previously been reached assuming these springs have been active for at least a few million years (Hurwitz et al., 2005), and the elevated water temperatures in the subsurface do not favor significant fractionation. The radical variability in Cl concentrations, and almost freshwater character

of some springs further suggest that a high Cl reservoir such as sedimentary connate water or evaporate deposits are not prolific Cl sources to these thermal springs.

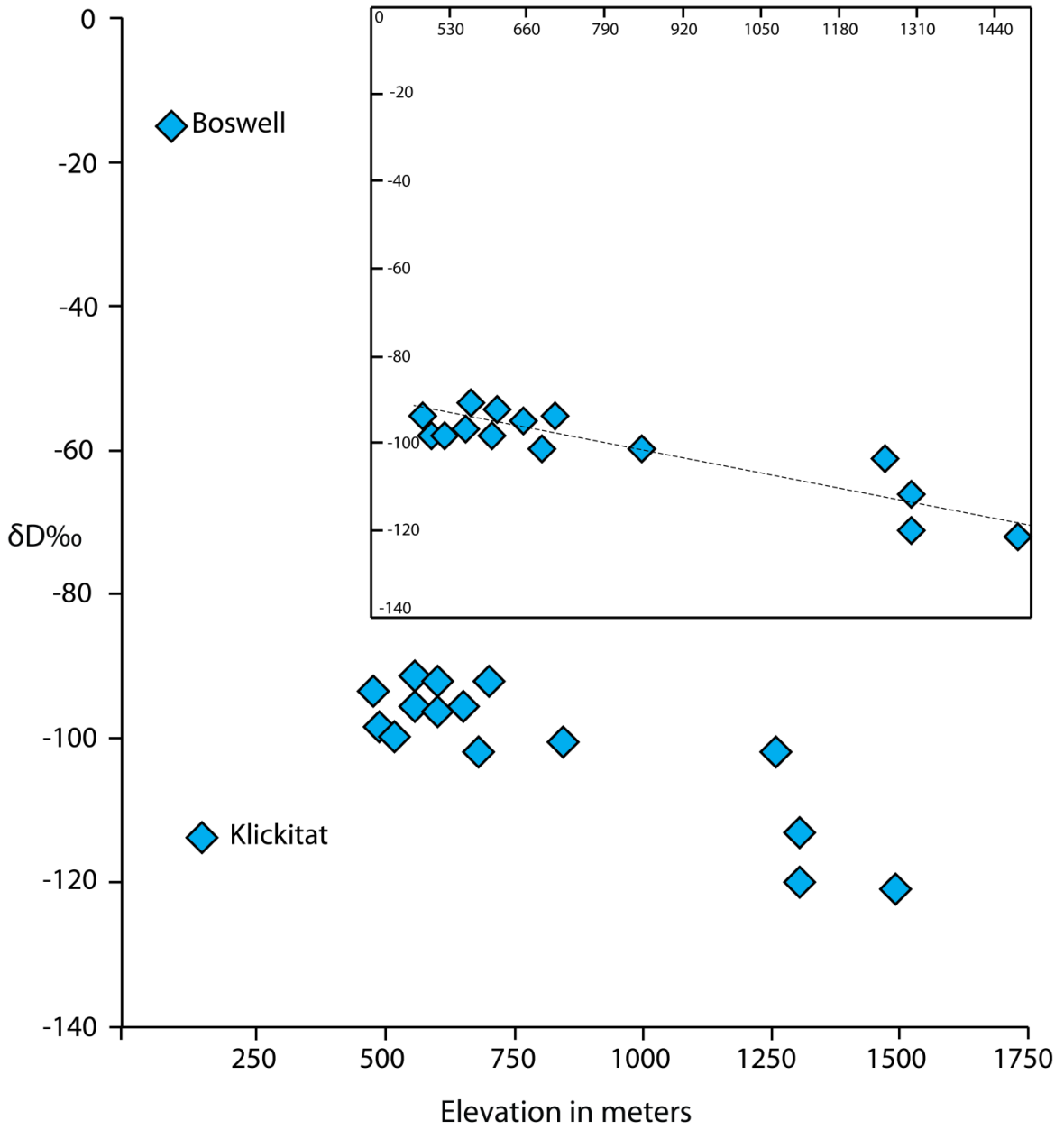


Figure 21:  $\delta D$  value vs. elevation of the thermal springs.

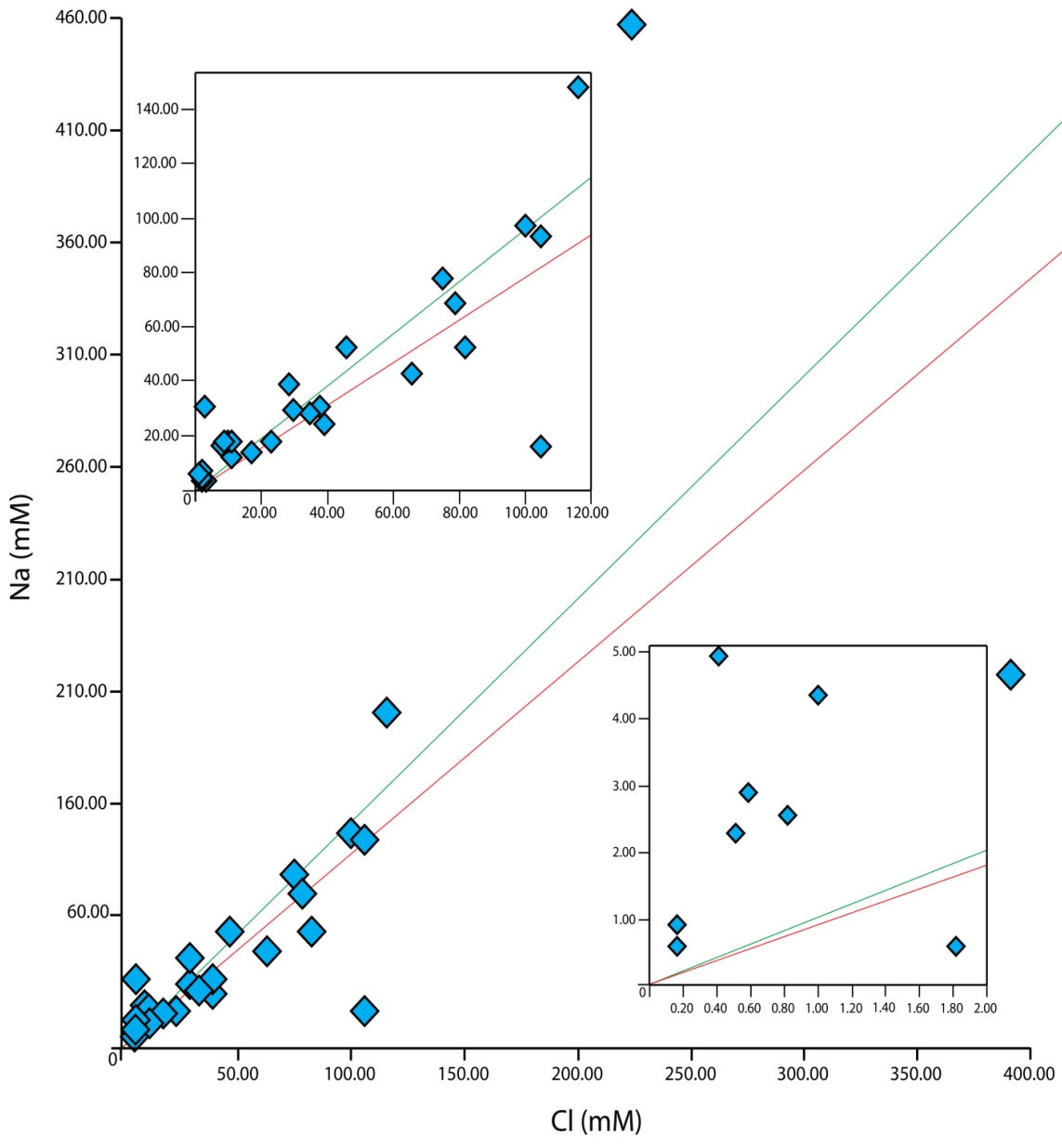


Figure 22: Na vs. Cl concentration in millimolars of the measured thermal springwaters. Green line indicates 1:1 Na/Cl ratio (dissolution/precipitation of halite), and red line indicates 0.86:1 ratio of seawater.

Much of the study area lies on exotic accreted oceanic terranes including the Siletz Terrane in central Oregon and the Trinity Ophiolite in northern California/southern Oregon. Thermal water interaction with altered oceanic crust of Siletz basement rocks and possibly serpentinites from the Trinity Ophiolite, likely both characterized by  $\delta^{37}\text{Cl}$  values  $>0\text{‰}$ , may also contribute to the positive  $\delta^{37}\text{Cl}$  values of some of the thermal waters. No Cl data is available from rocks of the Siletz Terrane or the Trinity Ophiolite, so assessing the potential influence of these underlying basement rocks on the  $\delta^{37}\text{Cl}$  composition and Cl concentrations of the springs is difficult. However, serpentinites from the Coast Range Ophiolite in northern California have  $\delta^{37}\text{Cl}$  values of  $+0.4$  to  $+1.7\text{‰}$  ( $n = 3$ ) (Barnes et al., 2013). Based on the likely chlorine isotope composition of the underlying basement rocks and the  $\delta^{37}\text{Cl}$  values of the springs, there is reasonable overlap to imagine some Cl contribution from the underlying material. It seems that the extent to which these basement rocks contribute to the Cl chemistries of the springs is probably minor, by virtue of the fact that only springs with circulation pathways penetrating the entire thickness of the sedimentary cover are capable of interacting with the basement rock units.

$\delta^{37}\text{Cl}$  values for the majority of spring waters also overlap the range of  $\delta^{37}\text{Cl}$  values obtained for the volcanic rocks ( $\sim 0$  to  $+0.8\text{‰}$ ). The preferred explanation in this study is that the stable Cl isotope compositions of most thermal springwaters are consistent with interaction between meteoric water and thick volcanic sequences. Assuming flow paths of 10-40 km, residence times between  $10^2$  to  $10^4$  years, and rock permeabilities of 1-100  $\mu\text{D}$  (Ingebritsen et al., 1991) it is plausible that the majority of

dissolved chloride is derived from the surrounding wall rock. However, leeching of wall rock has been previously disregarded as the major Cl source based on mass balance calculations of Ingebritsen (1991). Ingebritsen (1991) calculates an intrusion rate of about 70 km<sup>3</sup> of volcanic rock intruded every kilometer of arc length per million years with an average Cl concentration of 160 ppm in the volcanic rock so as to sustain the current flux of Cl from these springs in the central Oregon region. The necessary 70 km<sup>3</sup>/km arc length/m.y. is at least 10 times greater than estimates by Sherrod and Smith (1990) of between 3-6 km<sup>3</sup>/km arc length/m.y. based on thermal discharge calculations. Hurwitz et al (2005) examine the viability of volcanic material as the principal Cl source. Using the estimated intrusion rate of 6 km<sup>3</sup>/km arc length/m.y. and assuming complete leaching of partially degassed igneous rocks having Cl contents less than initial concentration in the melt (<1000 ppm Cl), also produces a Cl flux far less than that currently carried by the springs. To attain a more reasonable mass balance requires intrusion rates on the order of 9-33 km<sup>3</sup>/km arc length/m.y. (Ingebritsen et al., 1989) and/or higher Cl concentrations in the undegassed melts (1590-2580 ppm) (Ruscitto et al., 2011). For example, Cl concentrations of the bulk igneous pile interacting with the meteoric waters at depth are likely more evolved and have higher Cl concentrations than the primitive basalts sampled from the surface, perhaps more on the order of ~1000 ppm while maintaining an intrusion rate of 6 km<sup>3</sup>/km arc length/m.y. there is adequate supply of Cl to account for Cl output from the springs. Furthermore, should the Cl flux through the springs not be in a stable, long term steady state, or the assumption that the springs' inception coincides with the

initiation of Cascades volcanism ~44Ma is invalid, the Cl bearing volcanic rock reservoirs may be less depleted from ongoing water rock interaction than initially presumed. Whether these springs have actually been active over the entire lifespan of the Cascade arc is uncertain, but constraining the approximate age of the springs would help settle whether there is sufficient Cl in the surrounding volume of rock to sustain current Cl discharge from the springs. This possibly could be achieved by analyzing Umpqua hot spring travertine deposits by U-Pb isotope dating. Additionally, as mentioned previously, Cl contribution from meteoric water and Pacific aerosols probably have negligible effect on the mass balance constraints when using similar Cl concentrations found for rainwater and aerosols at monitoring stations from Lake Ozette WA, 3.5ppm and 390 ng/m<sup>3</sup> respectively (Vong et al., 1988).

An additional line of evidence for interaction with the host volcanic rock is based on Cl/B and Cl/Br ratios. Molar Cl/B ratios of the volcanic rocks of the Columbia Transect range from 4-10 (average = 7), overlapping reasonably with the ratios observed in the spring waters (Figure 23). Additionally, the average Cl/Br ratio for the volcanic rocks is ~1200, which overlaps well with Cl/Br ratios of the thermal springwaters (Figure 23). Both of these observations suggest hydrothermal interaction of the spring waters with the host volcanic material or some contribution from magmatic degassing. For springs whose  $\delta^{37}\text{Cl}$  values are higher (up to +1.9‰) than  $\delta^{37}\text{Cl}$  values observed in the volcanic rocks, it is possible that minor liquid/vapor phase fractionation of HCl at high temperature from degassing magma produces a <sup>37</sup>Cl rich vapor and is incorporated into the

groundwater. Alternatively, volcanic rocks with comparably high  $\delta^{37}\text{Cl}$  values are interacting with the waters, but are not represented in the limited sample set.

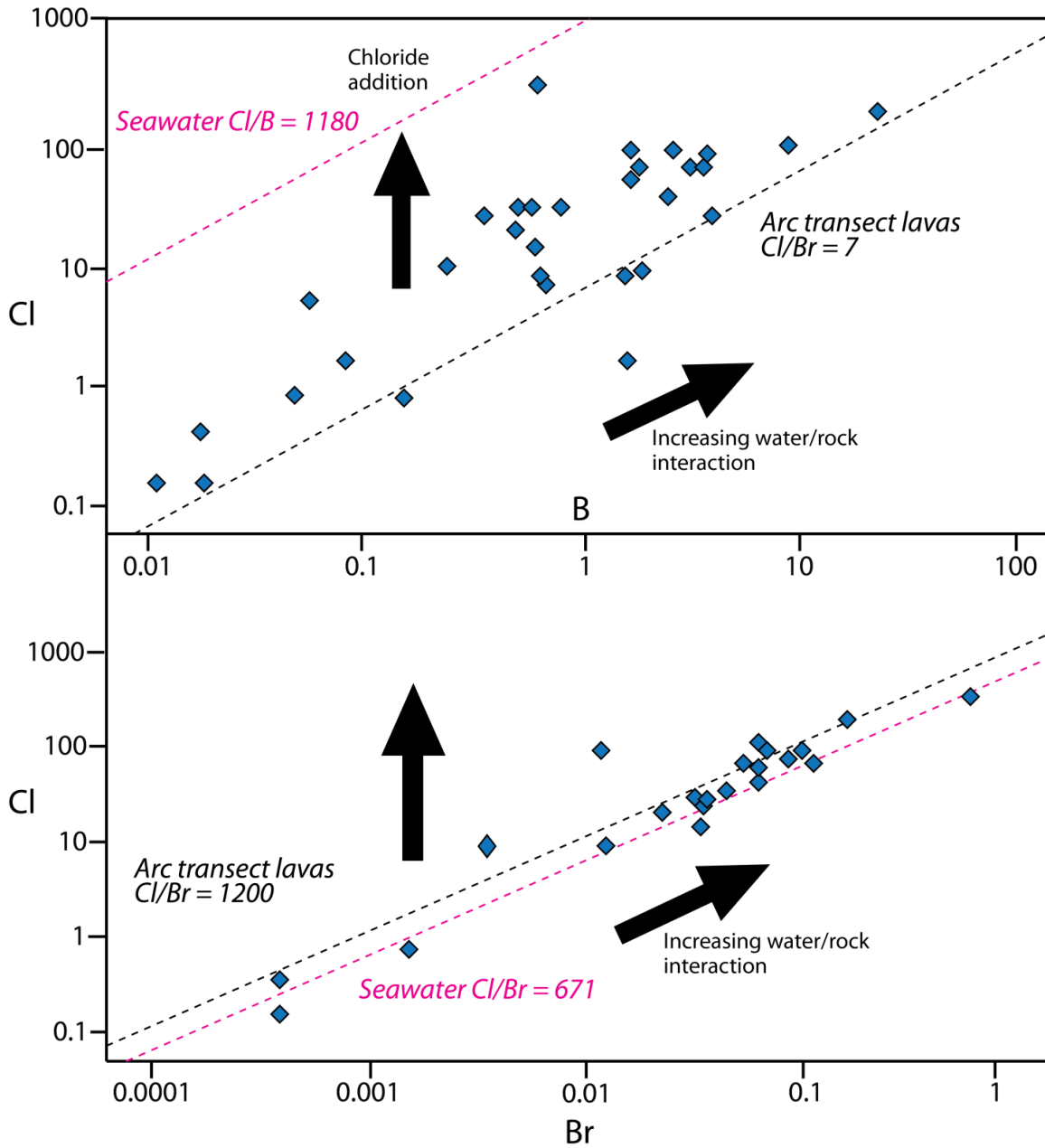


Figure 23: Cl vs. B and Cl vs. Br plots for the thermal springwaters. Dashed black line indicates constant Cl/B ratio of 7 (average ratio from measured lavas) and constant Cl/Br ratio of 1200. Dashed pink line indicates constant Cl/B ratio of 1180 (ratio of seawater) and constant seawater Cl/Br ratio of 671.

$\delta^{37}\text{Cl}$  data for Cascadia thermal springs do not yield a singular explanation as to what the chloride source is, however  $\delta^{37}\text{Cl}$  values are relatively well defined  $+0.9 \pm 0.3\text{‰}$  with the exception of 3 outliers ( $-0.1\text{‰}$ ,  $+1.8\text{‰}$ ,  $+1.9\text{‰}$ ) which suggest a fairly homogenous source. Small variations in  $\delta^{37}\text{Cl}$  values with large variations in Cl concentration may be caused by differing water/rock ratios from spring to spring which can vary as a function of groundwater circulation distance, rock permeability, and volume of meteoric water recharge. Some slight Cl fractionation may also occur in geothermal groundwater systems. Interaction with the volcanic units is a probable source for much of the chlorine measured in the springs whereas dissolution of evaporites, interaction with underlying sedimentary units, and incorporation of high salinity pore water is not consistent with the stable Cl isotope and cation data. However,  $\delta^{37}\text{Cl}$  values alone cannot eliminate the possible contribute of Cl in the springs from assimilation of or interaction with chlorine bearing lower crustal gabbros and/or serpentinites of the Siletz Terrane or Trinity ophiolite or from the dehydration of similar lithologies within the subducting slab. I suggest that slab derived Cl contributions to the springs are likely negligible based on the lack of correlation between the spatial position of the spring and its Cl concentration, as will be further discussed shortly, consistent with conclusions that the majority of Cl bearing materials will likely have devolatilized at shallower, forearc depths due to the anomalously warm thermal regime of the subduction zone. A possible contribution of slab-modified mantle suggested by Hurwitz et al (2005) cannot be discounted if the slab component is derived from serpentinites and/or amphibole-rich altered oceanic crust. It is

feasible that the Cl in the springs is dominantly from interaction with the host volcanic rock, whose hosted Cl is from  $^{37}\text{Cl}$  enriched mantle with perhaps a minor contribution from a slab-modified mantle.

### **6.3 Spatial variability of Cl and $\delta^{37}\text{Cl}$ along the arc.**

Figure 24 illustrates the Cl concentration and stable Cl isotope composition of the springs waters in relation to their location along the arc. The relationship between  $\delta^{37}\text{Cl}$  value of a particular spring and its geographic location/underlying basement rocks is weak, and some variability beyond the limits of analytical uncertainty exist even within a well confined geographic region. In addition, the absence of any cross-arc variation in Cl concentration of the springs is strong indication that the chloride in the springs is probably not directly linked to slab fluid inputs. Correlating the tectonic terrane on which a spring lies to the stable chlorine isotope composition is not a practical approach, but within local areas minor similarities can be teased out, which may offer insight in assessing the influence of different Cl sources. For example in the South Segment,  $\delta^{37}\text{Cl}$  values are well constrained to  $+1.0 \pm 0.3\text{‰}$ , whereas Cl concentrations range from 29-7905 ppm. Cl/B ratios of the five springs are fairly well confined: (19, 18, 23, and 31 with one exception at 203). Differences in Cl concentrations may reflect different degrees of water rock interaction, whereas the spring with elevated Cl/B ratio indicates some Cl contribution from a comparably more chlorine rich source than the other four. Similar patterns are observed in other areas of the arc between proximal springs, and likely illustrate a similar

Cl source and its equivalent Cl contribution. For example, Belknap and Bigelow are located only 5 km from one another and are characterized by Cl concentrations,  $\delta^{37}\text{Cl}$  values, and Cl/B ratios of 1354 and 1251 ppm, +1‰ and +0.8‰, and 215 and 223, respectively, essentially indistinguishable. However just 20 km to the southeast, Sphynx is quite the opposite with a Cl concentration,  $\delta^{37}\text{Cl}$  value, and Cl/B ratio of 6 ppm, -0.1‰, and 30, respectively. The change in chemistry could be explained by a change in Cl source or the extent of water-rock interaction. Lower water-rock interaction and or different dominant Cl source at Sphynx could explain its lower Cl/B ratio and Cl concentration as well as mantle-like  $\delta^{37}\text{Cl}$  value. Even though these major differences in water chemistries exist between proximal springs with very different discharge temperatures, thermal water temperature cannot easily be invoked in order to explain the  $\delta^{37}\text{Cl}$  variation as there is no significant correlation between temperature and Cl concentration or  $\delta^{37}\text{Cl}$  value (Figure 25).

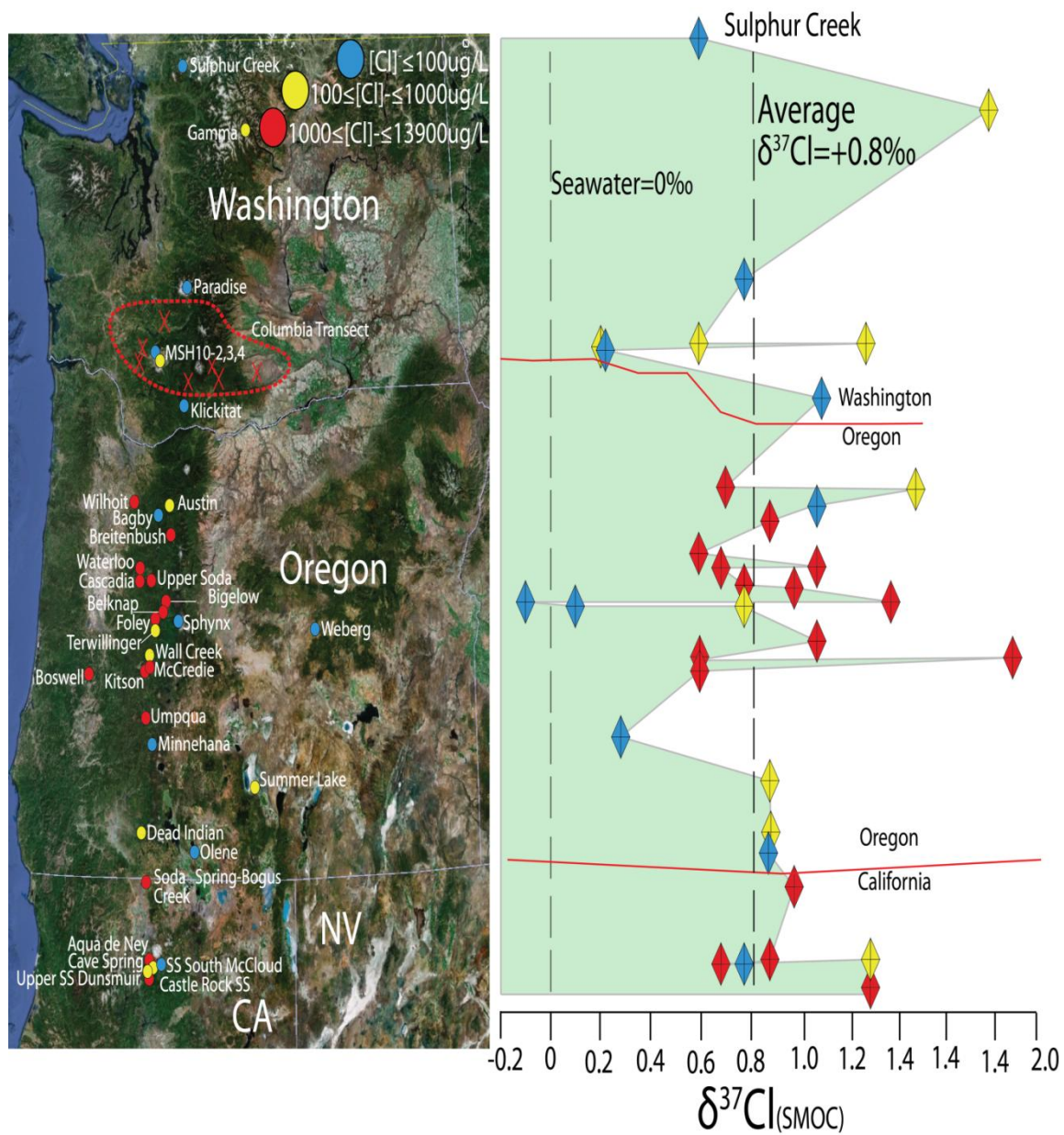


Figure 24:  $\delta^{37}\text{Cl}$  and Cl concentration variation in thermal springs plotted along full extent of the arc. Color of symbols represents the measured Cl concentration in the spring. Dashed red oval represents the arc of the Columbia Transect with "X"'s indicating lava sample locations.

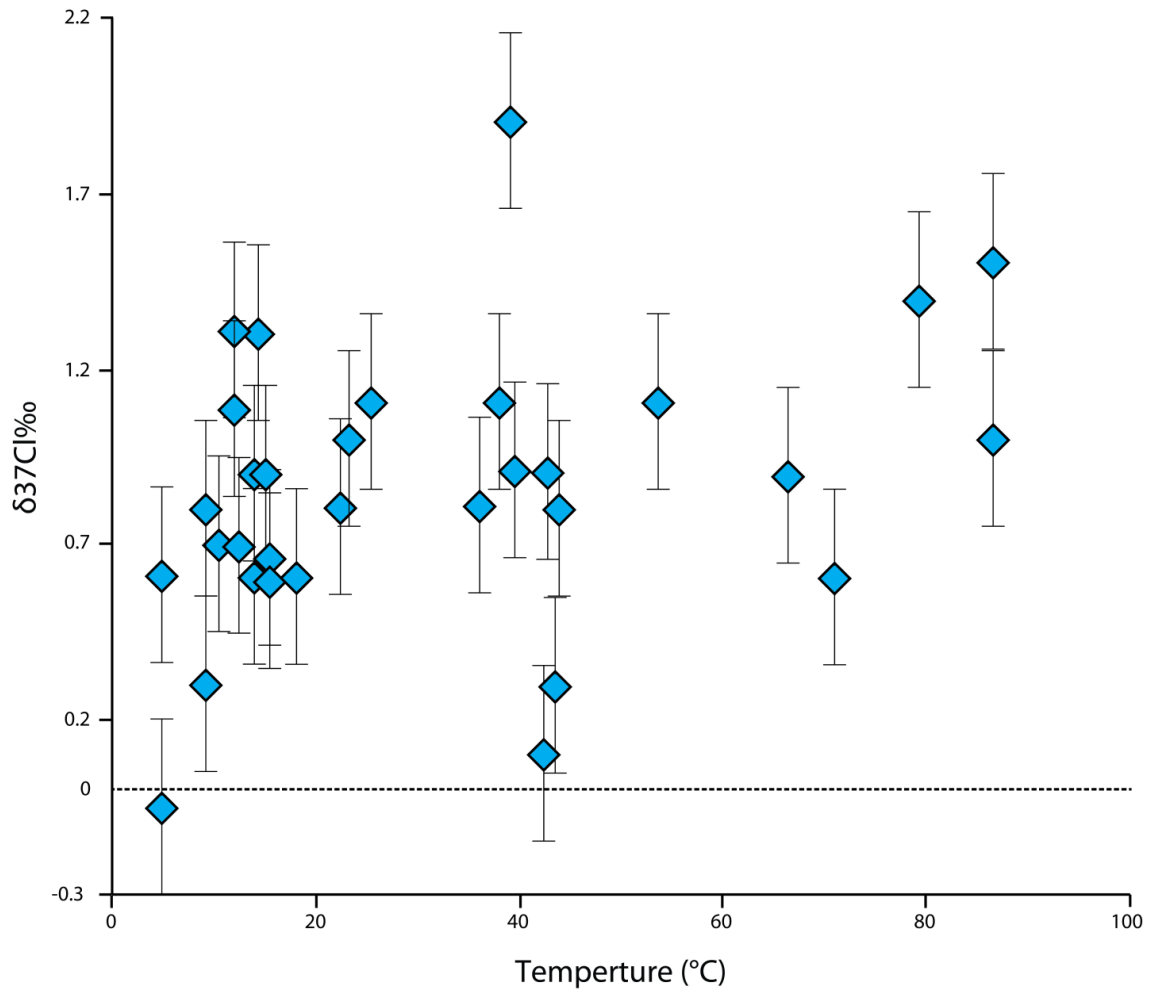


Figure 25:  $\delta^{37}\text{Cl}$  value vs. discharged water temperature of the thermal springs.

### 6.3 Assessing Cl transport through the Cascade Subduction Zone

Hurwitz et al. (2005) previously estimated Cl flux in the central Oregon Cascade subduction zone to be between  $3 \times 10^7$  kg to  $2 \times 10^8$  kg of Cl subducted annually, assuming Cl is hosted in altered oceanic crust only or altered oceanic crust and sediments, respectively. Serpentinites are also significant hosts of Cl in subduction zones (Sharp and Barnes, et al., 2004, Barnes and Sharp, 2006; Kendrick et al., 2013, Scambelluri et al., 2004, 2001). If serpentinites are included in the subducted flux calculations (assuming a 5 km thick 2.5% partially serpentinitized lithospheric mantle with Cl concentration of 1000 ppm), then an additional  $3 \times 10^6$  kg Cl/yr is contributed along this 260 km segment of the arc. Of that amount,  $5 \times 10^6$  kg/yr is thought to discharge through the springs. With an intrusion rate between 9-33 km<sup>3</sup>/km My, and assuming all Cl is retained in magmatic intrusions with an average initial concentration of 1000 ppm, the amount of total Cl added to the crust due to magmatism is between  $6.8 \times 10^6$  kg to  $2.5 \times 10^7$  kg/yr; that is ~2.5 to, 8% of the subducted Cl budget. The large discrepancy between the amount of Cl subducted compared to the maximum amount calculated to be brought back to the surface suggests that the majority of subducted Cl is either lost at shallow levels during subduction, locked up in a serpentinitized mantle wedge, or subducted back into the mantle.

## Chapter 7: Conclusions

Samples from 37 thermal springs from along and across the Cascade Volcanic Arc were analyzed for their Cl concentrations and stable Cl isotopic compositions in order to identify Cl sources and assess volatile cycling through the subduction zone. This effort was augmented by also analyzing the Cl stable isotope compositions and halogen chemistry of representative volcanic rocks from the Columbia Transect. Conclusions of this study are summarized as follows:

1. Primitive basaltic lavas from across the Columbia Transect are characterized by an average  $\delta^{37}\text{Cl}$  value of  $+0.4 \pm 0.3\text{‰}$  and have chlorine concentrations between 17 to 160 ppm. The Mt. St. Helens Dacite has the highest  $\delta^{37}\text{Cl}$  value of  $+0.8\text{‰}$  and comparable Cl concentration to the rest of the primitive basalts suggesting  $\delta^{37}\text{Cl}$  value and Cl composition is relatively resistant to the evolution of a closed system magma. However it appears halogen concentrations, especially Cl are highly susceptible to alteration by degassing. Halogen ratios vary systematically along the arc transect, with the highest I/Nb and F/Nb ratios in the forearc, and lowest I/Nb and F/Nb ratios in the backarc. The Cl in the lavas is likely derived from a locally modified mantle in addition to minor amounts from accreted oceanic crustal

material and lower crustal mafic and ultramafic material that has been incorporated into the magma.

2. Based on oxygen and hydrogen isotope data, all thermal waters with the exception of Boswell Spring, are meteoric in origin and are recharged at comparable to slightly higher elevations to their points of discharge, with the exception of two springs (Boswell and Klickitat).
3. The narrow range and average  $\delta^{37}\text{Cl}$  value (-0.1‰ to +1.9‰ ave = +0.8‰) of the thermal springs suggests that the Cl is dominantly derived from hydrothermal interaction with the surrounding host volcanic rocks. Deviations in Cl concentration can be attributed to differences in fluid-rock ratios between springs; whereas major differences in  $\delta^{37}\text{Cl}$  values may reflect Cl contributions from a different source and/or operation of distinct Cl isotopic fractionation processes, such as invoked to explain the mantle-like  $\delta^{37}\text{Cl}$  value at the Sphynx spring.
4. No spatial correlation is observed throughout the arc with respect to  $\delta^{37}\text{Cl}$  value or Cl concentration in the springs. The decoupled nature of Cl systematics in the springs to their spatial distribution along the arc suggests the Cl inventories are not directly related to the fluid inputs from the subducted slab.

5. Despite previous estimates to the contrary, the observed Cl discharge from Cascadia springs can be reconciled with leaching of Cl from the local volcanic rocks assuming sufficiently high magmatic fluxes and higher Cl concentration in partially degassed magmas, or significantly more youthful thermal spring ages.

APPENDIX A: THERMAL SPRINGWATER AQUEOUS GEOCHEMICAL  
DATA

Table A1: Geochemical data for thermal springwaters.

| Name                                 | Cave Spring <sup>a</sup> | Upper Soda Spring Dunsmuir <sup>a</sup> | Soda Spring S. McCloud <sup>a</sup> | Castle Rock Soda Spring <sup>a</sup> | Aqua de Ney | Analytical LOD <sub>(ppm)</sub> /Uncertainty (±%) |
|--------------------------------------|--------------------------|---|-------------------------------------|--------------------------------------|-------------|---|
| pH                                   | 6.0                      | 6.0                                     | 6.0                                 | 6.5                                  | 11.9        |   |
| Temp(°C)                             | 11.9                     | 12.3                                    | 9.3                                 | 14.4                                 | 15.1        |   |
| HCO <sub>3</sub>                     | 1260                     | 1032                                    | 992                                 | 2461                                 | 17348       | 1   |
| Cl                                   | 370.6                    | 3725.5                                  | 29.1                                | 1020.1                               | 7905.3      | 0.2   |
| SO <sub>4</sub>                      | 1.0                      | 1.0                                     | 1.0                                 | 1.0                                  | 561.6       | 0.2   |
| Br <sup>b</sup>                      | 1.00                     | 0.96                                    | 0.12                                | 2.86                                 | 13.00       | 0.2   |
| F <sup>b</sup>                       | 0.16                     | 0.12                                    | 0.08                                | 0.44                                 | 2.00        | 0.2   |
| I <sup>b</sup>                       | n.d.                     | n.d.                                    | n.d.                                | n.d.                                 | n.d.        | 0.2   |
| δ <sup>37</sup> Cl <sub>(SMOC)</sub> | 1.2‰<br>1.4‰             | 0.7‰<br>0.7‰                            | 0.8‰                                | 1.3‰                                 | 0.9‰        | ±0.2‰   |
| δ <sup>18</sup> O <sub>(SMOW)</sub>  | n.d.                     | n.d.                                    | n.d.                                | n.d.                                 | -10.1       | ±0.3‰   |
| δD <sub>(SMOW)</sub>                 | n.d.                     | n.d.                                    | n.d.                                | n.d.                                 | -21         | ±3‰   |
| B                                    | 19.792                   | 18.372                                  | 1.616                               | 43.490                               | 251.319     | 0.006   |
| Na                                   | 398.914                  | 385.545                                 | 59.254                              | 914.312                              | 10512.771   | 0.007   |
| Mg                                   | 82.060                   | 77.719                                  | 41.224                              | 197.441                              | b.d.1       | 0.001   |
| Al                                   | <0.01                    | <0.012                                  | <0.01                               | <0.022                               | b.d.1       | 0.00009   |
| Si                                   | 35.564                   | 37.642                                  | 33.447                              | 41.034                               | 896.927     | 0.039   |
| P                                    | <0.01                    | <0.01                                   | <0.01                               | <0.01                                | 2.414       | 0.005   |
| K                                    | 21.227                   | 19.809                                  | 4.255                               | 23.116                               | 142.608     | 0.005   |
| Ca                                   | 113.450                  | 98.390                                  | 204.276                             | 171.612                              | 5.634       | 0.007   |
| Ti                                   | n.d.                     | n.d.                                    | n.d.                                | n.d.                                 | 0.0971      | 0.00003   |
| V <sub>(ppb)</sub>                   | n.d.                     | n.d.                                    | n.d.                                | n.d.                                 | 0.2903      | 0.00002   |
| Cr                                   | 0.0054                   | <0.006                                  | 0.0130                              | <0.011                               | b.d.1       | 0.00008   |
| Mn                                   | 0.3578                   | 0.3084                                  | 0.5853                              | 0.3031                               | b.d.1       | 0.00002   |
| Fe                                   | 7.102                    | 4.867                                   | 18.679                              | <0.033                               | b.d.1       | 0.001   |
| Co                                   | <0.005                   | <0.006                                  | <0.005                              | <0.011                               | b.d.1       | 0.00004   |
| Ni                                   | <0.005                   | <0.006                                  | <0.005                              | <0.011                               | 0.0003      | 0.00002   |
| Cu                                   | <0.005                   | <0.006                                  | <0.005                              | <0.011                               | 0.0894      | 0.00002   |
| Zn                                   | 0.0111                   | <0.012                                  | <0.01                               | <0.022                               | b.d.1       | 0.00007   |
| As                                   | 0.0114                   | <0.006                                  | 0.0058                              | <0.011                               | 0.0047      | 0.00003   |
| Se                                   | <0.025                   | <0.03                                   | <0.025                              | <0.055                               | b.d.1       | 0.00003   |
| Rb                                   | <0.05                    | <0.06                                   | <0.05                               | <0.11                                | 0.1301      | 0.00001   |
| Sr                                   | 1.3092                   | 1.2302                                  | 1.1298                              | 2.7090                               | b.d.1       | 0.00008   |
| Zr                                   | n.d.                     | n.d.                                    | n.d.                                | n.d.                                 | b.d.1       | 0.00007   |
| Mo                                   | <0.005                   | <0.006                                  | <0.005                              | <0.011                               | 0.1835      | 0.00003   |
| Ag                                   | n.d.                     | n.d.                                    | n.d.                                | n.d.                                 | 0.0062      | 0.00005   |
| Cd                                   | <0.005                   | <0.006                                  | <0.005                              | <0.011                               | b.d.1       | 0.00001   |
| Sb                                   | n.d.                     | n.d.                                    | n.d.                                | n.d.                                 | b.d.1       | 0.00003   |
| Cs                                   | n.d.                     | n.d.                                    | n.d.                                | n.d.                                 | 0.0118      | 0.00001   |
| Ba                                   | 0.072                    | 0.062                                   | 1.941                               | 0.602                                | 0.2500      | 0.00002   |
| Pb                                   | n.d.                     | n.d.                                    | n.d.                                | n.d.                                 | 0.0011      | 0.00001   |
| Li                                   | 0.809                    | 0.788                                   | 0.081                               | 0.948                                | n.d.        | 0.005   |

Table A1 cont.

| Name                                     | Soda Spring Bogus Creek <sup>a</sup> | Olene  | Summer Lake 1 | Summer Lake 2 | Dead Indian <sup>a</sup> | Minnehaha <sup>a</sup> | Analytical LOD <sub>(ppm)</sub> /Uncertainty <sub>(±%)</sub> |
|--|--------------------------------------|--------|---------------|---------------|--------------------------|------------------------|--|
| <b>pH</b>                                | 6.6                                  | 7.9    | 8.5           | 8.3           | 6.0                      | 6.4                    |  |
| <b>Temp<sup>(°C)</sup></b>               | 23.2                                 | 39.5   | 42.8          | 48.0          | 14.0                     | 9.3                    |  |
| <b>HCO<sub>3</sub></b>                   | 3202                                 | 53     | 529           | 416           | 1892                     | 2435                   | 1  |
| <b>Cl</b>                                | 4134.6                               | 35.2   | 292.3         | 334.0         | 347.3                    | 15.0                   | 0.2  |
| <b>SO<sub>4</sub></b>                    | 16.0                                 | 196.1  | 109.1         | 61.3          | 23.7                     | 24.3                   | 0.2  |
| <b>Br<sup>b</sup></b>                    | 5.00                                 | n.d    | n.d           | n.d           | 0.28                     | 0.03                   | 0.2  |
| <b>F<sup>b</sup></b>                     | <0.01                                | n.d    | n.d           | n.d           | 0.08                     | <0.01                  | 0.2  |
| <b>I<sup>b</sup></b>                     | n.d                                  | n.d    | n.d           | n.d           | n.d                      | n.d                    | 0.2  |
| <b>δ<sup>37</sup>Cl<sub>(SMOC)</sub></b> | 1.0                                  | 0.9    | 0.9           | n.d           | 0.3<br>1.5               | 0.3                    | ±0.2‰  |
| <b>δ<sup>18</sup>O<sub>(SMOW)</sub></b>  | n.d.                                 | -11.6  | -13.4         | -13.6         | -12.5                    | -14.3                  | ±0.3‰  |
| <b>δD<sub>(SMOW)</sub></b>               | n.d.                                 | -103   | -113          | -120          | -98                      | -110                   | ±3‰  |
| <b>B</b>                                 | 97.376                               | 0.506  | 7.300         | 6.876         | 17.406                   | 0.189                  | 0.006  |
| <b>Na</b>                                | 3484.491                             | 99.747 | 453.339       | 391.473       | 435.483                  | 115.540                | 0.007  |
| <b>Mg</b>                                | 55.367                               | 2.003  | 0.118         | 0.098         | 156.765                  | 261.678                | 0.001  |
| <b>Al</b>                                | <0.1                                 | 0.0948 | b.d.l         | 0.0100        | <0.012                   | <0.012                 | 0.00009  |
| <b>Si</b>                                | 34.639                               | 33.490 | 40.507        | 42.555        | 41.027                   | 34.968                 | 0.039  |
| <b>P</b>                                 | <0.01                                | 0.140  | 0.075         | b.d.l         | <0.01                    | <0.01                  | 0.005  |
| <b>K</b>                                 | 99.190                               | 4.521  | 6.368         | 4.827         | 15.901                   | 27.035                 | 0.005  |
| <b>Ca</b>                                | 165.810                              | 24.614 | 2.068         | 2.585         | 168.650                  | 304.944                | 0.007  |
| <b>Ti</b>                                | n.d.                                 | 0.0066 | 0.0042        | 0.0046        | n.d.                     | n.d.                   | 0.00003  |
| <b>V<sub>(ppb)</sub></b>                 | n.d.                                 | 9.5796 | b.d.l         | b.d.l         | n.d.                     | n.d.                   | 0.00002  |
| <b>Cr</b>                                | <0.05                                | 0.0005 | b.d.l         | b.d.l         | <0.006                   | 0.0067                 | 0.00008  |
| <b>Mn</b>                                | 0.1697                               | 0.0294 | 0.0087        | 0.0114        | 0.4884                   | 4.7460                 | 0.00002  |
| <b>Fe</b>                                | <0.15                                | 0.060  | 0.005         | 0.009         | 2.840                    | 8.170                  | 0.001  |
| <b>Co</b>                                | <0.05                                | b.d.l  | b.d.l         | b.d.l         | <0.006                   | 0.0110                 | 0.00004  |
| <b>Ni</b>                                | <0.05                                | 0.0010 | b.d.l         | b.d.l         | 0.0079                   | 0.0197                 | 0.00002  |
| <b>Cu</b>                                | <0.05                                | 0.0015 | 0.0032        | 0.0029        | <0.006                   | <0.006                 | 0.00002  |
| <b>Zn</b>                                | 0.0339                               | 0.0052 | b.d.l         | b.d.l         | <0.012                   | <0.012                 | 0.00007  |
| <b>As</b>                                | 0.0729                               | 0.0344 | 0.0038        | 0.0327        | 0.5320                   | <0.006                 | 0.00003  |
| <b>Se</b>                                | <0.25                                | b.d.l  | b.d.l         | b.d.l         | <0.03                    | <0.03                  | 0.00003  |
| <b>Rb</b>                                | <0.5                                 | 0.0092 | 0.0074        | 0.0069        | <0.06                    | <0.06                  | 0.00001  |
| <b>Sr</b>                                | 8.6238                               | 0.2426 | 0.1081        | 0.0884        | 1.5125                   | 1.7598                 | 0.00008  |
| <b>Zr</b>                                | n.d.                                 | b.d.l  | b.d.l         | b.d.l         | n.d.                     | n.d.                   | 0.00007  |
| <b>Mo</b>                                | <0.05                                | 0.0117 | 0.0320        | 0.0395        | <0.006                   | <0.006                 | 0.00003  |
| <b>Ag</b>                                | n.d.                                 | b.d.l  | b.d.l         | b.d.l         | n.d.                     | n.d.                   | 0.00005  |
| <b>Cd</b>                                | <0.05                                | 0.0003 | b.d.l         | b.d.l         | <0.006                   | <0.006                 | 0.00001  |
| <b>Sb</b>                                | n.d.                                 | 0.0010 | b.d.l         | b.d.l         | n.d.                     | n.d.                   | 0.00003  |
| <b>Cs</b>                                | n.d.                                 | 0.0062 | 0.0040        | 0.0044        | n.d.                     | n.d.                   | 0.00001  |
| <b>Ba</b>                                | 0.275                                | 0.0085 | 0.0102        | 0.0101        | 0.113                    | 0.208                  | 0.00002  |
| <b>Pb</b>                                | n.d.                                 | 0.0001 | 0.0001        | 0.0002        | n.d.                     | n.d.                   | 0.00001  |
| <b>Li</b>                                | 5.631                                | n.d.   | n.d.          | n.d.          | 0.584                    | 0.096                  | 0.005  |

Table A1 cont.

| Name                                     | Umpqua   | Kitson   | McCredie   | Wall Creek | Terwillinger | Foley   | Analytical LOD <sub>(ppm)</sub> /Uncertainty <sub>(±%)</sub> |
|--|----------|----------|------------|------------|--------------|---------|--|
| <b>pH</b>                                | 6.2      | 7.5      | 7.2        | 7.9        | 8.5          | 6.1     |  |
| <b>Temp<sup>(°C)</sup></b>               | 43.5     | 39.0     | 71.0       | 38.0       | 43.8         | 79.2    |  |
| <b>HCO<sub>3</sub></b>                   | 1308     | 30       | 24         | 43         | 24           | 22      | 1  |
| <b>Cl</b>                                | 3546.2   | 2918.5   | 2332.6     | 1194.0     | 818.3        | 1399.6  | 0.2  |
| <b>SO<sub>4</sub></b>                    | 194.0    | 174.2    | 279.6      | 146.8      | 253.0        | 557.0   | 0.2  |
| <b>Br<sup>b</sup></b>                    | 5.50     | 7.00     | 5.00       | 2.70       | 1.82         | 3.54    | 0.2  |
| <b>F<sup>b</sup></b>                     | 1.00     | 2.50     | 2.50       | 8.60       | 0.80         | 0.40    | 0.2  |
| <b>I<sup>b</sup></b>                     | 436      | 390      | 239        | 72         | 180          | 220     | 0.2  |
| <b>δ<sup>37</sup>Cl<sub>(SMOC)</sub></b> | 0.3      | 1.9      | 0.0<br>1.2 | 1.1        | 0.9<br>0.7   | 1.4     | ±0.2‰  |
| <b>δ<sup>18</sup>O<sub>(SMOW)</sub></b>  | -12.0    | -11.9    | -12.4      | -12.7      | -12.1        | -11.6   | ±0.3‰  |
| <b>δD<sub>(SMOW)</sub></b>               | -101     | -94      | -96        | -96        | -92          | -91     | ±3‰  |
| <b>B</b>                                 | 40.837   | 19.737   | 17.903     | 6.541      | 5.222        | 8.506   | 0.006  |
| <b>Na</b>                                | 2243.795 | 1189.471 | 983.807    | 330.822    | 389.096      | 530.678 | 0.007  |
| <b>Mg</b>                                | 41.097   | 1.992    | 0.915      | 0.240      | 0.072        | 0.081   | 0.001  |
| <b>Al</b>                                | b.d.1    | 0.0096   | 0.0108     | 0.0426     | 0.0072       | 0.0153  | 0.00009  |
| <b>Si</b>                                | 37.527   | 18.397   | 31.155     | 29.434     | 20.867       | 27.625  | 0.039  |
| <b>P</b>                                 | b.d.1    | b.d.1    | 0.165      | b.d.1      | b.d.1        | b.d.1   | 0.005  |
| <b>K</b>                                 | 62.780   | 20.904   | 23.895     | 8.880      | 6.378        | 8.887   | 0.005  |
| <b>Ca</b>                                | 346.816  | 601.489  | 474.411    | 113.478    | 212.487      | 514.164 | 0.007  |
| <b>Ti</b>                                | 0.0050   | 0.0028   | 0.0042     | 0.0041     | 0.0026       | 0.0037  | 0.00003  |
| <b>V<sub>(ppb)</sub></b>                 | b.d.1    | b.d.1    | b.d.1      | b.d.1      | b.d.1        | b.d.1   | 0.00002  |
| <b>Cr</b>                                | b.d.1    | b.d.1    | b.d.1      | b.d.1      | b.d.1        | b.d.1   | 0.00008  |
| <b>Mn</b>                                | 0.2215   | 0.0848   | 0.1071     | 0.0409     | 0.0029       | 0.0063  | 0.00002  |
| <b>Fe</b>                                | 1.921    | 0.015    | 0.012      | 0.032      | 0.010        | 0.008   | 0.001  |
| <b>Co</b>                                | b.d.1    | b.d.1    | b.d.1      | b.d.1      | b.d.1        | b.d.1   | 0.00004  |
| <b>Ni</b>                                | 0.0050   | 0.0059   | 0.0046     | 0.0014     | 0.0022       | 0.0053  | 0.00002  |
| <b>Cu</b>                                | 0.0189   | 0.0089   | 0.0073     | 0.0024     | 0.0029       | 0.0036  | 0.00002  |
| <b>Zn</b>                                | b.d.1    | b.d.1    | b.d.1      | b.d.1      | b.d.1        | b.d.1   | 0.00007  |
| <b>As</b>                                | 3.1197   | 0.2302   | 0.1643     | 0.0970     | 0.0705       | 0.1455  | 0.00003  |
| <b>Se</b>                                | b.d.1    | b.d.1    | b.d.1      | b.d.1      | b.d.1        | 0.0005  | 0.00003  |
| <b>Rb</b>                                | 0.2033   | 0.0871   | 0.0922     | 0.0305     | 0.0245       | 0.0219  | 0.00001  |
| <b>Sr</b>                                | 10.0790  | 5.5271   | 4.7441     | 1.2412     | 1.4001       | 2.9643  | 0.00008  |
| <b>Zr</b>                                | b.d.1    | b.d.1    | b.d.1      | b.d.1      | b.d.1        | b.d.1   | 0.00007  |
| <b>Mo</b>                                | b.d.1    | 0.0098   | 0.0178     | 0.0131     | 0.0125       | 0.0185  | 0.00003  |
| <b>Ag</b>                                | b.d.1    | b.d.1    | b.d.1      | b.d.1      | b.d.1        | b.d.1   | 0.00005  |
| <b>Cd</b>                                | b.d.1    | b.d.1    | b.d.1      | b.d.1      | b.d.1        | b.d.1   | 0.00001  |
| <b>Sb</b>                                | 0.0010   | 0.0011   | 0.0020     | 0.0003     | 0.0003       | 0.0007  | 0.00003  |
| <b>Cs</b>                                | 0.1950   | 0.0631   | 0.0878     | 0.0214     | 0.0142       | 0.0089  | 0.00001  |
| <b>Ba</b>                                | 0.1985   | 0.1592   | 0.1715     | 0.0533     | 0.0098       | 0.0788  | 0.00002  |
| <b>Pb</b>                                | 0.0006   | 0.0006   | 0.0004     | 0.0002     | 0.0002       | 0.0003  | 0.00001  |
| <b>Li</b>                                | n.d.     | n.d.     | n.d.       | n.d.       | n.d.         | n.d.    | 0.005  |

Table A1: cont.

| Name                                 | Sphynx <sup>a</sup> | Belknap | Bigelow | Waterloo <sup>a</sup> | Cascadia <sup>a</sup> | Upper Soda Spring <sup>a</sup> | Analytical LOD <sub>(ppm)</sub> /Uncertainty <sub>(±%)</sub> |
|--------------------------------------|---------------------|---------|---------|-----------------------|-----------------------|--------------------------------|--|
| pH                                   | 8.5                 | 7.5     | 7.0     | 6.1                   | 6.1                   | 6.1                            |  |
| Temp <sub>(°C)</sub>                 | 4.9                 | 86.5    | 36.3    | 15.4                  | 15.7                  | 12.2                           |  |
| HCO <sub>3</sub>                     | 61                  | 24      | 20      | 1385                  | 1348                  | 1618                           | 1  |
| Cl                                   | 5.8                 | 1354.5  | 1251.2  | 1636.3                | 2794.1                | 3725.5                         | 0.2  |
| SO <sub>4</sub>                      | 3.4                 | 172.2   | 144.7   | 19.5                  | 47.1                  | 117.4                          | 0.2  |
| Br <sup>b</sup>                      | 0.03                | 3.60    | 2.60    | 5.00                  | 9.00                  | 8.00                           | 0.2  |
| F <sup>b</sup>                       | 0.15                | 1.20    | 3.20    | 1.00                  | 1.00                  | 1.00                           | 0.2  |
| I <sup>b</sup>                       | n.d.                | 103     | 200     | n.d.                  | n.d.                  | n.d.                           | 0.2  |
| δ <sup>37</sup> Cl <sub>(SMOC)</sub> | -0.1                | 1.0     | 0.8     | 0.6                   | 0.5                   | 1.1                            | ±0.2‰  |
|                                      | 0.0                 |         |         |                       | 0.8                   |                                |  |
| δ <sup>18</sup> O <sub>(SMOW)</sub>  | -13.5               | -11.8   | -11.4   | -8.3                  | -8.6                  | n.d.                           | ±0.3‰  |
| δD <sub>(SMOW)</sub>                 | -96                 | -99     | -95     | -68                   | -72                   | n.d.                           | ±3‰  |
| B                                    | 0.195               | 6.309   | 5.603   | 27.443                | 39.548                | 28.082                         | 0.006  |
| Na                                   | 21.651              | 661.645 | 633.881 | 1200.153              | 1597.520              | 2154.861                       | 0.007  |
| Mg                                   | 3.099               | 0.263   | 0.917   | 62.532                | 99.558                | 48.240                         | 0.001  |
| Al                                   | 0.0041              | 0.0017  | 0.0068  | <0.05                 | 0.0872                | <0.05                          | 0.00009  |
| Si                                   | 13.283              | 40.795  | 32.294  | 35.284                | 16.711                | 20.351                         | 0.039  |
| P                                    | 0.080               | b.d.1   | b.d.1   | <0.01                 | <0.01                 | <0.01                          | 0.005  |
| K                                    | 2.017               | 16.208  | 16.135  | 21.833                | 31.779                | 68.548                         | 0.005  |
| Ca                                   | 4.038               | 219.258 | 190.754 | 190.385               | 348.193               | 600.730                        | 0.007  |
| Ti                                   | n.d.                | 0.0053  | 0.0042  | n.d.                  | n.d.                  | n.d.                           | 0.00003  |
| V <sub>(ppb)</sub>                   | n.d.                | 0.0006  | 0.0014  | n.d.                  | n.d.                  | n.d.                           | 0.00002  |
| Cr                                   | <0.001              | 0.0077  | b.d.1   | <0.025                | <0.025                | <0.025                         | 0.00008  |
| Mn                                   | <0.001              | 0.0111  | 0.0550  | 0.5126                | 2.3520                | 0.7273                         | 0.00002  |
| Fe                                   | <0.003              | 0.022   | 0.027   | 8.977                 | 24.421                | 6.882                          | 0.001  |
| Co                                   | <0.001              | b.d.1   | b.d.1   | <0.025                | <0.025                | <0.025                         | 0.00004  |
| Ni                                   | <0.001              | 0.0072  | 0.0021  | <0.025                | <0.025                | <0.025                         | 0.00002  |
| Cu                                   | <0.001              | 0.0046  | 0.0045  | <0.025                | <0.025                | <0.025                         | 0.00002  |
| Zn                                   | <0.002              | b.d.1   | b.d.1   | <0.05                 | 0.0534                | <0.05                          | 0.00007  |
| As                                   | 0.0360              | 0.4293  | 0.2703  | 0.6621                | 0.2868                | 0.5192                         | 0.00003  |
| Se                                   | <0.005              | b.d.1   | b.d.1   | <0.125                | <0.125                | <0.125                         | 0.00003  |
| Rb                                   | <0.01               | 0.0379  | 0.0439  | <0.25                 | <0.25                 | 0.2830                         | 0.00001  |
| Sr                                   | 0.0296              | 1.3883  | 1.2907  | 4.1611                | 5.5583                | 8.4117                         | 0.00008  |
| Zr                                   | n.d.                | b.d.1   | b.d.1   | n.d.                  | n.d.                  | n.d.                           | 0.00007  |
| Mo                                   | 0.0030              | 0.0219  | 0.0157  | <0.025                | <0.025                | <0.025                         | 0.00003  |
| Ag                                   | n.d.                | b.d.1   | b.d.1   | n.d.                  | n.d.                  | n.d.                           | 0.00005  |
| Cd                                   | <0.001              | b.d.1   | b.d.1   | <0.025                | <0.025                | <0.025                         | 0.00001  |
| Sb                                   | n.d.                | 0.0034  | 0.0026  | n.d.                  | n.d.                  | n.d.                           | 0.00003  |
| Cs                                   | n.d.                | 0.0267  | 0.0338  | n.d.                  | n.d.                  | n.d.                           | 0.00001  |
| Ba                                   | <0.001              | 0.0837  | 0.0348  | 0.175                 | 0.187                 | 0.121                          | 0.00002  |
| Pb                                   | n.d.                | 0.0002  | 0.0002  | n.d.                  | n.d.                  | n.d.                           | 0.00001  |
| Li                                   | 0.006               | n.d.    | n.d.    | 1.615                 | 2.356                 | 3.594                          | 0.005  |

Table A1: cont.

| Name                                      | Boswell    | Weberg  | Breitenbush | Bagby  | Austin  | Wilhoit    | Analytical LOD <sub>(ppm)</sub><br>/Uncertainty <sub>(±‰)</sub> |
|---|------------|---------|-------------|--------|---------|------------|---|
| <b>pH</b>                                 | 8.6        | 6.8     | 7.6         | 9.0    | 7.5     | 6.2        |   |
| <b>Temp</b> <sub>(°C)</sub>               | 14.2       | 42.5    | 66.5        | 53.8   | 86.5    | 10.7       |   |
| <b>HCO<sub>3</sub></b>                    | 27         | 1823    | 135         | 67     | 56      | 2142       | 1   |
| <b>Cl</b>                                 | 13848.5    | 62.9    | 1085.1      | 17.9   | 406.2   | 2647.5     | 0.2   |
| <b>SO<sub>4</sub></b>                     | n.d.       | 2.3     | 136.8       | 41.3   | 141.9   | 25.0       | 0.2   |
| <b>Br<sup>b</sup></b>                     | 48.00      | n.d.    | 3.00        | n.d.   | 20.00   | 4.50       | 0.2   |
| <b>F<sup>b</sup></b>                      | 0.00       | n.d.    | 3.80        | 0.70   | 1.30    | 1.00       | 0.2   |
| <b>I<sup>b</sup></b>                      | 7004       | n.d.    | 80          | n.d.   | 1       | n.d.       | 0.2   |
| <b>δ<sup>37</sup>Cl</b> <sub>(SMOC)</sub> | 0.5<br>0.7 | 0.1     | 0.9         | 1.1    | 1.5     | 0.3<br>1.1 | ±0.2‰   |
| <b>δ<sup>18</sup>O</b> <sub>(SMOW)</sub>  | -2.3       | -14.6   | -12.3       | -12.8  | -12.4   | -8.2       | ±0.3‰   |
| <b>δD</b> <sub>(SMOW)</sub>               | -15        | -121    | -102        | -92    | -100    | -72        | ±3‰   |
| <b>B</b>                                  | 6.775      | 17.664  | 3.854       | 0.068  | 2.585   | 34.878     | 0.006   |
| <b>Na</b>                                 | 3922.369   | 707.000 | 680.997     | 52.257 | 299.730 | 1799.831   | 0.007   |
| <b>Mg</b>                                 | 0.408      | 8.261   | 0.853       | 0.065  | 0.118   | 110.678    | 0.001   |
| <b>Al</b>                                 | b.d.1      | 0.0139  | 0.0057      | 1.2638 | 0.0196  | <0.05      | 0.00009   |
| <b>Si</b>                                 | b.d.1      | 40.090  | 68.692      | 36.087 | 37.806  | 31.877     | 0.039   |
| <b>P</b>                                  | 0.823      | 0.025   | b.d.1       | b.d.1  | b.d.1   | <0.01      | 0.005   |
| <b>K</b>                                  | 11.469     | 39.314  | 30.130      | 1.108  | 6.992   | 20.341     | 0.005   |
| <b>Ca</b>                                 | 6890.330   | 37.512  | 100.578     | 3.857  | 36.883  | 369.152    | 0.007   |
| <b>Ti</b>                                 | b.d.1      | 0.0075  | 0.0076      | 0.0132 | 0.0043  | n.d.       | 0.00003   |
| <b>V</b> <sub>(ppb)</sub>                 | b.d.1      | b.d.1   | b.d.1       | b.d.1  | b.d.1   | n.d.       | 0.00002   |
| <b>Cr</b>                                 | b.d.1      | b.d.1   | b.d.1       | 0.0008 | b.d.1   | <0.025     | 0.00008   |
| <b>Mn</b>                                 | 0.0102     | 0.0452  | 0.2164      | 0.0024 | 0.0100  | 0.3310     | 0.00002   |
| <b>Fe</b>                                 | 0.039      | 0.089   | 0.073       | 0.440  | 0.013   | 11.201     | 0.001   |
| <b>Co</b>                                 | 0.0066     | b.d.1   | b.d.1       | b.d.1  | b.d.1   | <0.025     | 0.00004   |
| <b>Ni</b>                                 | 0.0797     | 0.0007  | 0.0024      | 0.0003 | 0.0007  | <0.025     | 0.00002   |
| <b>Cu</b>                                 | 0.0314     | 0.0055  | 0.0050      | 0.0006 | 0.0022  | <0.025     | 0.00002   |
| <b>Zn</b>                                 | b.d.1      | 0.0022  | b.d.1       | 0.0107 | b.d.1   | <0.05      | 0.00007   |
| <b>As</b>                                 | b.d.1      | 0.0013  | 0.4618      | 0.0184 | 0.5007  | 0.3227     | 0.00003   |
| <b>Se</b>                                 | b.d.1      | b.d.1   | 0.0005      | b.d.1  | b.d.1   | <0.125     | 0.00003   |
| <b>Rb</b>                                 | 0.0132     | 0.0751  | 0.1257      | 0.0042 | 0.0228  | <0.25      | 0.00001   |
| <b>Sr</b>                                 | 47.4844    | 1.8886  | 0.7718      | 0.0256 | 0.3448  | 3.3227     | 0.00008   |
| <b>Zr</b>                                 | b.d.1      | b.d.1   | b.d.1       | b.d.1  | b.d.1   | n.d.       | 0.00007   |
| <b>Mo</b>                                 | 0.0155     | b.d.1   | 0.0156      | 0.0162 | 0.0281  | <0.025     | 0.00003   |
| <b>Ag</b>                                 | b.d.1      | b.d.1   | b.d.1       | b.d.1  | b.d.1   | n.d.       | 0.00005   |
| <b>Cd</b>                                 | b.d.1      | b.d.1   | b.d.1       | 0.0001 | b.d.1   | <0.025     | 0.00001   |
| <b>Sb</b>                                 | b.d.1      | b.d.1   | 0.0137      | 0.0005 | 0.0058  | n.d.       | 0.00003   |
| <b>Cs</b>                                 | b.d.1      | 0.0159  | 0.0878      | 0.0020 | 0.0243  | n.d.       | 0.00001   |
| <b>Ba</b>                                 | 0.2207     | 5.5570  | 0.0706      | 0.0086 | 0.0218  | 0.053      | 0.00002   |
| <b>Pb</b>                                 | 0.0024     | 0.0003  | 0.0003      | 0.0006 | 0.0002  | n.d.       | 0.00001   |
| <b>Li</b>                                 | n.d.       | n.d.    | n.d.        | n.d.   | n.d.    | 2.860      | 0.005   |

Table A1: cont.

| Name                                     | Klickitat | MSH10<br>02 | MSH10<br>03 | MSH10<br>04 | Carbonate<br>Spring <sup>a</sup> | Paradise<br>Warm<br>Spring <sup>a</sup> | Analytical LOD <sub>(ppm)</sub><br>/Uncertainty <sub>(±%)</sub> |
|--|-----------|-------------|-------------|-------------|----------------------------------|---|---|
| <b>pH</b>                                | 5.8       | n.d.        | n.d.        | n.d.        | 6.7                              | 6.3                                     |   |
| <b>Temp<sup>(°C)</sup></b>               | 25.4      | n.d.        | n.d.        | n.d.        | 18.1                             | 22.4                                    |   |
| <b>HCO<sub>3</sub></b>                   | 1096      | n.d.        | n.d.        | n.d.        | n.d.                             | n.d.                                    | 1   |
| <b>Cl</b>                                | 20.7      | 250.0       | 300.0       | 250.0       | 50.9                             | 64.5                                    | 0.2   |
| <b>SO<sub>4</sub></b>                    | 2.0       | n.d.        | n.d.        | n.d.        | 180.0                            | 187.9                                   | 0.2   |
| <b>Br<sup>b</sup></b>                    | n.d.      | n.d.        | n.d.        | n.d.        | n.d.                             | n.d.                                    | 0.2   |
| <b>F<sup>b</sup></b>                     | n.d.      | n.d.        | n.d.        | n.d.        | n.d.                             | n.d.                                    | 0.2   |
| <b>I<sup>b</sup></b>                     | n.d.      | n.d.        | n.d.        | n.d.        | n.d.                             | n.d.                                    | 0.2   |
| <b>δ<sup>37</sup>Cl<sub>(SMOC)</sub></b> | 1.1       | 1.3         | 0.6         | 0.2         | 0.6                              | 0.8                                     | ±0.2‰   |
| <b>δ<sup>18</sup>O<sub>(SMOW)</sub></b>  | -15.3     | n.d.        | n.d.        | n.d.        | n.d.                             | n.d.                                    | ±0.3‰   |
| <b>δD<sub>(SMOW)</sub></b>               | -114      | n.d.        | n.d.        | n.d.        | n.d.                             | n.d.                                    | ±3‰   |
| <b>B</b>                                 | 0.090     | n.d.        | n.d.        | n.d.        | n.d.                             | 0.852                                   | 0.006   |
| <b>Na</b>                                | 66.540    | n.d.        | n.d.        | n.d.        | n.d.                             | 13.100                                  | 0.007   |
| <b>Mg</b>                                | 110.883   | n.d.        | n.d.        | n.d.        | n.d.                             | 32.490                                  | 0.001   |
| <b>Al</b>                                | 0.0038    | n.d.        | n.d.        | n.d.        | n.d.                             | >.005                                   | 0.00009   |
| <b>Si</b>                                | 74.057    | n.d.        | n.d.        | n.d.        | n.d.                             | n.d.                                    | 0.039   |
| <b>P</b>                                 | 0.382     | n.d.        | n.d.        | n.d.        | n.d.                             | n.d.                                    | 0.005   |
| <b>K</b>                                 | 10.507    | n.d.        | n.d.        | n.d.        | n.d.                             | 17.530                                  | 0.005   |
| <b>Ca</b>                                | 132.997   | n.d.        | n.d.        | n.d.        | n.d.                             | 42.960                                  | 0.007   |
| <b>Ti</b>                                | 0.0078    | n.d.        | n.d.        | n.d.        | n.d.                             | n.d.                                    | 0.00003   |
| <b>V<sub>(ppb)</sub></b>                 | b.d.l     | n.d.        | n.d.        | n.d.        | n.d.                             | n.d.                                    | 0.00002   |
| <b>Cr</b>                                | b.d.l     | n.d.        | n.d.        | n.d.        | n.d.                             | n.d.                                    | 0.00008   |
| <b>Mn</b>                                | 0.2371    | n.d.        | n.d.        | n.d.        | n.d.                             | n.d.                                    | 0.00002   |
| <b>Fe</b>                                | 14.514    | n.d.        | n.d.        | n.d.        | n.d.                             | n.d.                                    | 0.001   |
| <b>Co</b>                                | b.d.l     | n.d.        | n.d.        | n.d.        | n.d.                             | n.d.                                    | 0.00004   |
| <b>Ni</b>                                | 0.0016    | n.d.        | n.d.        | n.d.        | n.d.                             | n.d.                                    | 0.00002   |
| <b>Cu</b>                                | 0.0002    | n.d.        | n.d.        | n.d.        | n.d.                             | n.d.                                    | 0.00002   |
| <b>Zn</b>                                | b.d.l     | n.d.        | n.d.        | n.d.        | n.d.                             | n.d.                                    | 0.00007   |
| <b>As</b>                                | b.d.l     | n.d.        | n.d.        | n.d.        | n.d.                             | 0.0070                                  | 0.00003   |
| <b>Se</b>                                | b.d.l     | n.d.        | n.d.        | n.d.        | n.d.                             | n.d.                                    | 0.00003   |
| <b>Rb</b>                                | 0.0232    | n.d.        | n.d.        | n.d.        | n.d.                             | n.d.                                    | 0.00001   |
| <b>Sr</b>                                | 0.2616    | n.d.        | n.d.        | n.d.        | n.d.                             | 0.2500                                  | 0.00008   |
| <b>Zr</b>                                | b.d.l     | n.d.        | n.d.        | n.d.        | n.d.                             | n.d.                                    | 0.00007   |
| <b>Mo</b>                                | b.d.l     | n.d.        | n.d.        | n.d.        | n.d.                             | n.d.                                    | 0.00003   |
| <b>Ag</b>                                | 0.0005    | n.d.        | n.d.        | n.d.        | n.d.                             | n.d.                                    | 0.00005   |
| <b>Cd</b>                                | b.d.l     | n.d.        | n.d.        | n.d.        | n.d.                             | n.d.                                    | 0.00001   |
| <b>Sb</b>                                | b.d.l     | n.d.        | n.d.        | n.d.        | n.d.                             | n.d.                                    | 0.00003   |
| <b>Cs</b>                                | 0.0005    | n.d.        | n.d.        | n.d.        | n.d.                             | n.d.                                    | 0.00001   |
| <b>Ba</b>                                | 0.0517    | n.d.        | n.d.        | n.d.        | n.d.                             | 0.002                                   | 0.00002   |
| <b>Pb</b>                                | 0.0001    | n.d.        | n.d.        | n.d.        | n.d.                             | n.d.                                    | 0.00001   |
| <b>Li</b>                                | n.d.      | n.d.        | n.d.        | n.d.        | n.d.                             | 0.124                                   | 0.005   |

Table A1: cont.

| Name                                 | Gamma | Sulphur Creek <sup>a</sup> | Analytical<br>LOD <sub>(ppm)</sub><br>/Uncertainty <sub>(±%)</sub> |
|--------------------------------------|-------|----------------------------|--|
| pH                                   | n.d.  | 6.2                        |  |
| Temp <sup>(°C)</sup>                 | n.d.  | 5.1                        |  |
| HCO <sub>3</sub>                     | n.d.  | n.d.                       | 1  |
| Cl                                   | 736.0 | 5.9                        | 0.2  |
| SO <sub>4</sub>                      | n.d.  | 61.5                       | 0.2  |
| Br <sup>b</sup>                      | n.d.  | n.d.                       | 0.2  |
| F <sup>b</sup>                       | n.d.  | n.d.                       | 0.2  |
| I <sup>b</sup>                       | n.d.  | n.d.                       | 0.2  |
| δ <sup>37</sup> Cl <sub>(SMOC)</sub> | 1.8   | 0.6                        | ±0.2‰  |
| δ <sup>18</sup> O <sub>(SMOW)</sub>  | n.d.  | n.d.                       | ±0.3‰  |
| δD <sub>(SMOW)</sub>                 | n.d.  | n.d.                       | ±3‰  |
| B                                    | n.d.  | 0.113                      | 0.006  |
| Na                                   | n.d.  | 13.100                     | 0.007  |
| Mg                                   | n.d.  | 6.500                      | 0.001  |
| Al                                   | n.d.  | 0.0070                     | 0.00009  |
| Si                                   | n.d.  | 20.280                     | 0.039  |
| P                                    | n.d.  | n.d.                       | 0.005  |
| K                                    | n.d.  | 3.460                      | 0.005  |
| Ca                                   | n.d.  | 9.140                      | 0.007  |
| Ti                                   | n.d.  | n.d.                       | 0.00003  |
| V <sub>(ppb)</sub>                   | n.d.  | n.d.                       | 0.00002  |
| Cr                                   | n.d.  | n.d.                       | 0.00008  |
| Mn                                   | n.d.  | n.d.                       | 0.00002  |
| Fe                                   | n.d.  | n.d.                       | 0.001  |
| Co                                   | n.d.  | n.d.                       | 0.00004  |
| Ni                                   | n.d.  | n.d.                       | 0.00002  |
| Cu                                   | n.d.  | n.d.                       | 0.00002  |
| Zn                                   | n.d.  | n.d.                       | 0.00007  |
| As                                   | n.d.  | 0.0010                     | 0.00003  |
| Se                                   | n.d.  | n.d.                       | 0.00003  |
| Rb                                   | n.d.  | n.d.                       | 0.00001  |
| Sr                                   | n.d.  | 0.0640                     | 0.00008  |
| Zr                                   | n.d.  | n.d.                       | 0.00007  |
| Mo                                   | n.d.  | n.d.                       | 0.00003  |
| Ag                                   | n.d.  | n.d.                       | 0.00005  |
| Cd                                   | n.d.  | n.d.                       | 0.00001  |
| Sb                                   | n.d.  | n.d.                       | 0.00003  |
| Cs                                   | n.d.  | n.d.                       | 0.00001  |
| Ba                                   | n.d.  | 0.002                      | 0.00002  |
| Pb                                   | n.d.  | n.d.                       | 0.00001  |
| Li                                   | n.d.  | 0.003                      | 0.005  |

All values reported in (mg/L) unless otherwise denoted  
(n.d.) not determined  
(b.d.l) below detection limit

<sup>a</sup>(All data with exception off Cl,  $\delta^{37}\text{Cl}$  from USGS)  
<sup>b</sup>(Data from Mariner et al., 2003)

APPENDIX B: WHOLE ROCK MAJOR, TRACE, AND ISOTOPE  
GEOCHEMISTRY

Table B1: Whole rock major, trace, and isotope geochemistry

| <b>Group 1 Lavas</b>                     |                              |                               |                               |                               |                              |
|--|------------------------------|-------------------------------|-------------------------------|-------------------------------|------------------------------|
| <b>Name</b>                              | L01-17                       | L01-25                        | L01-24                        | L83-91                        | L83-57                       |
| <b>Location</b>                          | 46°12'36.00"<br>122°15'0.00" | 46° 3'36.00"<br>121°19'48.00" | 45°58'12.00"<br>121°23'24.00" | 45°54'28.80"<br>121°42'39.60" | 46° 0'14.40"<br>121° 9'7.20" |
| <b>Type</b>                              | Alk                          | OIB                           | OIB                           | Alk                           | LKT                          |
| <b>SiO<sub>2</sub></b>                   | 51.82                        | 51.85                         | 51.55                         | 48.17                         | 50.21                        |
| <b>TiO<sub>2</sub></b>                   | 1.76                         | 1.34                          | 1.42                          | 2.56                          | 1.30                         |
| <b>Al<sub>2</sub>O<sub>3</sub></b>       | 16.93                        | 16.99                         | 16.76                         | 17.53                         | 17.09                        |
| <b>FeO</b>                               | 9.15                         | 9.20                          | 8.95                          | 11.77                         | 10.33                        |
| <b>MnO</b>                               | 0.14                         | 0.16                          | 0.15                          | 0.17                          | 0.16                         |
| <b>MgO</b>                               | 6.57                         | 7.50                          | 7.54                          | 6.34                          | 7.50                         |
| <b>CaO</b>                               | 8.39                         | 8.71                          | 8.99                          | 8.38                          | 9.84                         |
| <b>Na<sub>2</sub>O</b>                   | 3.87                         | 3.33                          | 3.49                          | 3.39                          | 3.09                         |
| <b>K<sub>2</sub>O</b>                    | 1.00                         | 0.64                          | 0.84                          | 1.23                          | 0.35                         |
| <b>P<sub>2</sub>O<sub>5</sub></b>        | 0.36                         | 0.28                          | 0.31                          | 0.45                          | 0.13                         |
| <b>Mg#</b>                               | 56.1                         | 59.3                          | 60.0                          | 49.0                          | 56.4                         |
| <b>Cl</b>                                | 141.210                      | 139.582                       | 156.727                       | 18.792                        | 64.718                       |
| <b>Br</b>                                | 0.2647                       | 0.2219                        | 0.3082                        | 0.0547                        | 0.0585                       |
| <b>I</b>                                 | 0.0180                       | 0.0267                        | 0.0280                        | 0.0221                        | 0.0211                       |
| <b>F</b>                                 | 136.3                        | 155.5                         | 197.2                         | 164.1                         | 75.1                         |
| <b>B</b>                                 | 3.0                          | 3.2                           | 3.7                           | 1.3                           | 2.7                          |
| <b>Ba</b>                                | 267                          | 235                           | 245                           | 410                           | 102                          |
| <b>Rb</b>                                | 17.4                         | 10.7                          | 12.9                          | 22.0                          | 5.3                          |
| <b>Sr</b>                                | 496                          | 447                           | 578                           | 590                           | 295                          |
| <b>Y</b>                                 | 23.8                         | 24.9                          | 24.4                          | 27.0                          | 21.8                         |
| <b>Zr</b>                                | 152                          | 137                           | 150                           | 196                           | 107                          |
| <b>Nb</b>                                | 20.10                        | 12.09                         | 12.65                         | 33.00                         | 8.17                         |
| <b>Li</b>                                | n.d.                         | n.d.                          | n.d.                          | 6.49                          | 5.93                         |
| <b>La</b>                                | 18.17                        | 16.42                         | 20.37                         | n.d.                          | 7.35                         |
| <b>Gd</b>                                | 5.27                         | 4.89                          | 4.80                          | n.d.                          | 3.29                         |
| <b>Tb</b>                                | 0.83                         | 0.80                          | 0.78                          | n.d.                          | 0.61                         |
| <b>Yb</b>                                | 1.96                         | 2.19                          | 2.12                          | n.d.                          | 2.03                         |
| <b>Hf</b>                                | 3.83                         | 3.56                          | 3.83                          | n.d.                          | 2.43                         |
| <b>Ta</b>                                | 1.29                         | 0.77                          | 0.81                          | n.d.                          | 0.48                         |
| <b>Pb</b>                                | 3.49                         | 3.85                          | 3.76                          | n.d.                          | 1.36                         |
| <b>Th</b>                                | 1.98                         | 1.87                          | 2.62                          | n.d.                          | 0.78                         |
| <b>U</b>                                 | 0.63                         | 0.57                          | 0.72                          | n.d.                          | 0.27                         |
| <b>Ni</b>                                | 95                           | 124                           | 123                           | 50                            | 43                           |
| <b>Cr</b>                                | 180                          | 214                           | 227                           | 72                            | 325                          |
| <b>Sc</b>                                | 26.2                         | 29.4                          | 30.5                          | n.d.                          | 31.0                         |
| <b>V</b>                                 | 190                          | 191                           | 183                           | 194                           | 183                          |
| <b>δ<sup>18</sup>O<sub>rock</sub></b>    | 5.88                         | n.d.                          | 5.53                          | 6.11                          | n.d.                         |
| <b>δ<sup>18</sup>O<sub>olivine</sub></b> | 5.38                         | n.d.                          | 5.03                          | n.d.                          | n.d.                         |
| <b>δ<sup>37</sup>Cl</b>                  | 0.5                          | -0.1                          | 0.7                           | 0.5                           | 0.1                          |
| <b>δ<sup>11</sup>B</b>                   | n.d.                         | n.d.                          | n.d.                          | -9.09                         | -7.98                        |
| <b>δ<sup>7</sup>Li7</b>                  | n.d.                         | n.d.                          | n.d.                          | 2.86                          | 3.39                         |

Table B1 cont.

|                                   |      |      |      |                 |                 |
|-----------------------------------|------|------|------|-----------------|-----------------|
| $\text{Sr}^{87}/\text{Sr}^{86}$   | n.d. | n.d. | n.d. | <b>0.703110</b> | <b>0.702940</b> |
| $\text{Nd}^{143}/\text{Nd}^{144}$ | n.d. | n.d. | n.d. | 0.512915        | 0.513017        |
| $\text{Pb}^{206}/\text{Pb}^{204}$ | n.d. | n.d. | n.d. | 18.790          | 18.969          |
| $\text{Pb}^{207}/\text{Pb}^{204}$ | n.d. | n.d. | n.d. | 15.541          | 15.606          |
| $\text{Pb}^{208}/\text{Pb}^{204}$ | n.d. | n.d. | n.d. | 38.347          | 38.632          |

Table B1 cont.

| Name                                     | Group 2 Lavas                 |                               |                               | Hi Crustal Melt               |
|--|-------------------------------|-------------------------------|-------------------------------|-------------------------------|
|  | V457                          | V348                          | L00-10                        | MSH-33                        |
| <b>Location</b>                          | 46° 5'52.80"<br>122°20'31.20" | 46° 3'46.80"<br>122°25'51.60" | 45°32'24.00"<br>122°33'36.00" | 46°13'12.00"<br>122°11'13.20" |
| <b>Type</b>                              | HKCA                          | CA                            | CA                            | D                             |
| <b>SiO<sub>2</sub></b>                   | 50.72                         | 52.97                         | 54.37                         | 63.19                         |
| <b>TiO<sub>2</sub></b>                   | 1.28                          | 0.92                          | 1.23                          | 0.64                          |
| <b>Al<sub>2</sub>O<sub>3</sub></b>       | 16.03                         | 16.21                         | 17.41                         | 18.11                         |
| <b>FeO</b>                               | 7.87                          | 7.74                          | 7.19                          | 4.42                          |
| <b>MnO</b>                               | 0.14                          | 0.13                          | 0.12                          | 0.07                          |
| <b>MgO</b>                               | 8.04                          | 9.18                          | 6.23                          | 2.19                          |
| <b>CaO</b>                               | 9.74                          | 8.83                          | 7.84                          | 5.37                          |
| <b>Na<sub>2</sub>O</b>                   | 3.44                          | 3.21                          | 4.10                          | 4.60                          |
| <b>K<sub>2</sub>O</b>                    | 2.19                          | 0.62                          | 1.18                          | 1.26                          |
| <b>P<sub>2</sub>O<sub>5</sub></b>        | 0.55                          | 0.19                          | 0.35                          | 0.14                          |
| <b>Mg#</b>                               | 64.6                          | 67.9                          | 60.7                          | 47.0                          |
| <b>Cl</b>                                | 16.761                        | 81.468                        | 65.931                        | 119.130                       |
| <b>Br</b>                                | 0.0782                        | 0.1312                        | 0.1524                        | 0.2444                        |
| <b>I</b>                                 | 0.0919                        | 0.0994                        | 0.0255                        | 0.0157                        |
| <b>F</b>                                 | 599.9                         | 143.7                         | 317.1                         | 120.6                         |
| <b>B</b>                                 | 8.2                           | 12.2                          | 4.1                           | 18.0                          |
| <b>Ba</b>                                | 552                           | 189                           | 359                           | 287                           |
| <b>Rb</b>                                | 17.0                          | 6.8                           | 15.6                          | 28.9                          |
| <b>Sr</b>                                | 1302                          | 633                           | 837                           | 466                           |
| <b>Y</b>                                 | 19.0                          | 18.0                          | 18.5                          | 12.2                          |
| <b>Zr</b>                                | 149                           | 115                           | 165                           | 120                           |
| <b>Nb</b>                                | 7.20                          | 5.38                          | 8.35                          | 4.92                          |
| <b>Li</b>                                | 9.55                          | 8.93                          | n.d.                          | n.d.                          |
| <b>La</b>                                | n.d.                          | 12.57                         | 21.76                         | 11.19                         |
| <b>Gd</b>                                | n.d.                          | 3.29                          | 4.85                          | n.d.                          |
| <b>Tb</b>                                | n.d.                          | 0.55                          | 0.67                          | 0.40                          |
| <b>Yb</b>                                | n.d.                          | 1.53                          | 1.43                          | 1.02                          |
| <b>Hf</b>                                | n.d.                          | 2.78                          | 4.39                          | 2.94                          |
| <b>Ta</b>                                | n.d.                          | 0.31                          | 0.50                          | 0.33                          |
| <b>Pb</b>                                | n.d.                          | 3.01                          | 4.62                          | 6.63                          |
| <b>Th</b>                                | n.d.                          | 0.97                          | 2.71                          | 2.13                          |
| <b>U</b>                                 | n.d.                          | 0.35                          | 0.91                          | 0.85                          |
| <b>Ni</b>                                | 112                           | 178                           | 131                           | 9                             |
| <b>Cr</b>                                | 258                           | 393                           | 178                           | 13                            |
| <b>Sc</b>                                | n.d.                          | 24.6                          | 20.9                          | 12.8                          |
| <b>V</b>                                 | 212                           | 188                           | 145                           | 80                            |
| <b>δ<sup>18</sup>O<sub>rock</sub></b>    | 5.53                          | n.d.                          | 5.63                          | 6.60                          |
| <b>δ<sup>18</sup>O<sub>olivine</sub></b> | 5.03                          | n.d.                          | 5.13                          | n.d.                          |
| <b>δ<sup>37</sup>Cl</b>                  | 0                             | n.d.                          | 0.6                           | 0.8                           |
| <b>δ<sup>11</sup>B</b>                   | -2.74                         | -1.43                         | n.d.                          | -2.67                         |

Table B1 contd.

|                                   |             |             |             |             |
|-----------------------------------|-------------|-------------|-------------|-------------|
| $\delta^7\text{Li}$               | <b>3.43</b> | <b>2.94</b> | <b>n.d.</b> | <b>n.d.</b> |
| $\text{Sr}^{87}/\text{Sr}^{86}$   | 0.703577    | 0.703460    | 0.703425    | 0.703650    |
| $\text{Nd}^{143}/\text{Nd}^{144}$ | 0.512896    | 0.512915    | n.d.        | 0.512910    |
| $\text{Pb}^{206}/\text{Pb}^{204}$ | 18.934      | 18.942      | 18.749      | 18.800      |
| $\text{Pb}^{207}/\text{Pb}^{204}$ | 15.586      | 15.568      | 15.552      | 15.550      |
| $\text{Pb}^{208}/\text{Pb}^{204}$ | 38.611      | 38.471      | 38.353      | 38.430      |

(n.d.) Not determined

All data from Leeman et al., 2004, 2005, unpublished data with the exception of (CL, Br, F, I,  $\delta^{37}\text{Cl}$  this study)

Element Oxides reported as wt % recalculated to 100% totals

Minor and trace elements reported in ppm

(HKCA) High potassium calc alkaline, (CA) Calc alkaline, (D) Dacite

## REFERENCES

- Abers, G. A., van Keken, P. E., Kneller, E. A., Ferris, A., and Stachnik, J. C., 2006, The thermal structure of subduction zones constrained by seismic imaging: Implications for slab dehydration and wedge flow: *Earth and Planetary Science Letters*, v. 241, no. 3, p. 387-397.
- Arcuri, T., and Brimhall, G., 2003, The chloride source for atacamite mineralization at the Radomiro Tomic porphyry copper deposit, Northern Chile: *Economic Geology*, v. 98, no. 8, p. 1667-1681.
- Bacon, C. R., Bruggman, P. E., Christiansen, R. L., Clyne, M. A., Donnelly-Nolan, J. M., and Hildreth, W., 1997, Primitive magmas at five Cascade volcanic fields; melts from hot, heterogeneous sub-arc mantle: *The Canadian Mineralogist*, v. 35, no. 2, p. 397-423.
- Baldwin, E. M., 1981, *Geology of Oregon*. Kendall, Hunt Publishing Co., Dubuque, Iowa.
- Barnes, H., 1954, Some tables for the ionic composition of sea water: *Journal of experimental biology*, v. 31, no. 4, p. 582-588.
- Barnes, I., and O'Neil, J. R., 1969, The Relationship between Fluids in Some Fresh Alpine-Type Ultramafics and Possible Modern Serpentinization, Western United States: *Geological Society of America Bulletin*, v. 80, no. 10, p. 1947-1960.
- Barnes, J., and Sharp, Z., 2006, Achlorine isotope study of DSDP/ODP serpentinized ultramafic rocks: Insights into the serpentinization process: *Chemical Geology*, v. 228, no. 4, p. 246-265.

- Barnes, J. D., and Cisneros, M., 2012, Mineralogical control on the chlorine isotope composition of altered oceanic crust: *Chemical Geology*, v. 326–327, no. 0, p. 51-60.
- Barnes, J. D., Sharp, Z. D., and Fischer, T. P., 2008, Chlorine isotope variations across the Izu-Bonin-Mariana arc: *Geology*, v. 36, no. 11, p. 883-886.
- Barnes, J. D., Sharp, Z. D., Fischer, T. P., Hilton, D. R., and Carr, M. J., 2009, Chlorine isotope variations along the Central American volcanic front and back arc: *Geochemistry, Geophysics, Geosystems*, v. 10, no. 11, p. Q11S17.
- Barnes, J. D., and Stefansson, A., 2012, Chlorine Isotope Geochemistry of Icelandic Geothermal Waters *Mineralogical Magazine*, v. 76, no. 6, p. 1456.
- Barnes, J. D., and Stefánsson, A., 2012, Chlorine isotope geochemistry of Icelandic geothermal waters. 22nd Annual Goldschmidt Conference. .
- Barnes, J. D., and Straub, S. M., 2010, Chlorine stable isotope variations in Izu Bonin tephra: Implications for serpentinite subduction: *Chemical Geology*, v. 272, no. 1–4, p. 62-74.
- Bebout, G. E., 1996, Volatile transfer and recycling at convergent margins: mass-balance and insights from high-P/T metamorphic rocks: *Geophysical Monograph Series*, v. 96, p. 179-193.
- Bergfeld, D., Evans, W. C., Mcgee, K. A., and Spicer, K. R., 2008, Pre-and post-eruptive investigations of gas and water samples from Mount St. Helens, Washington, 2002 to 2005: US Geological Survey professional paper, no. 1750, p. 523-542.

- Blackwell, D. D., and Steele, J. I., 1985, Heat flow of the Cascades Range in Guffanti, Marianne, and Muffler, L.J.P., eds.: Proceedings of the workshop on geothermal resources of the Cascade range, U.S. Geological Survey Open-File Report, v. 85-521, p. 20-23.
- Blackwell, D. D., Steele, J. L., Kelley, S., and Korosec, M. A., 1990, Heat flow in the state of Washington and thermal conditions in the Cascade Range: *Journal of Geophysical Research: Solid Earth* (1978–2012), v. 95, no. B12, p. 19495-19516.
- Bonifacie, M., Busigny, V., Mével, C., Philippot, P., Agrinier, P., Jendrzejewski, N., Scambelluri, M., and Javoy, M., 2008, Chlorine isotopic composition in seafloor serpentinites and high-pressure metaperidotites. Insights into oceanic serpentinization and subduction processes: *Geochimica et Cosmochimica Acta*, v. 72, no. 1, p. 126-139.
- Bonifacie, M., Charlou, J. L., Jendrzejewski, N., Agrinier, P., and Donval, J. P., 2005, Chlorine isotopic compositions of high temperature hydrothermal vent fluids over ridge axes: *Chemical Geology*, v. 221, no. 3–4, p. 279-288.
- Bonifacie, M., Monnin, C., Jendrzejewski, N., Agrinier, P., and Javoy, M., 2007, Chlorine stable isotopic composition of basement fluids of the eastern flank of the Juan de Fuca Ridge (ODP Leg 168): *Earth and Planetary Science Letters*, v. 260, no. 1, p. 10-22.
- Brook, C., Mariner, R., Mabey, D., Swanson, J., Guffanti, M., and Muffler, L., 1979, Hydrothermal convection systems with reservoir temperatures > 90°C: Assessment

- of geothermal resources of the United States-1978: US Geological Survey Circular, v. 790, p. 18-85.
- Brown, E., 1987, Structural geology and accretionary history of the Northwest Cascades system, Washington and British Columbia: Geological Society of America Bulletin, v. 99, no. 2, p. 201-214.
- Bu, X., Wang, T., and Hall, G., 2003, Determination of halogens in organic compounds by high resolution inductively coupled plasma mass spectrometry (HR-ICP-MS): J. Anal. At. Spectrom., v. 18, no. 12, p. 1443-1451.
- Bureau, H., Keppler, H., and Métrich, N., 2000, Volcanic degassing of bromine and iodine: Experimental fluid/melt partitioning data and applications to stratospheric chemistry: Earth and Planetary Science Letters, v. 183, no. 1, p. 51-60.
- Cameron, B., Walker, J., Carr, M., Patino, L., Matias, O., and Feigenson, M., 2003, Flux versus decompression melting at stratovolcanoes in southeastern Guatemala: Journal of Volcanology and Geothermal Research, v. 119, no. 1, p. 21-50.
- Carroll, M. R., and Webster, J. D., 1994, Solubilities of sulfur, noble gases, nitrogen, chlorine, and fluorine in magmas: Reviews in Mineralogy and Geochemistry, v. 30, no. 1, p. 231-279.
- Clynne, M. A., 1984, Stratigraphy and major element geochemistry of the Lassen Volcanic Center, California: U.S. Geological Survey Open File Report, p. 84-224.
- Clynne, M. A., and Muffler, L. J. P., 2010, Geologic map of Lassen Volcanic National Park and vicinity, California.

- Conrey, R. M., Sherrod, D. R., Hooper, P. R., and Swanson, D. A., 1997, Diverse primitive magmas in the Cascade arc, northern Oregon and southern Washington: *Canadian Mineralogist*, v. 35, p. 367-396.
- Coplen, T. B., Kendall, C., and Hopple, J., 1983, Comparison of stable isotope reference samples: *Nature*, v. 302, no. 5905, p. 236-238.
- Cotton, F. A., Wilkinson, G., Murillo, C. A., and Bochmann, M., 1988, *Advanced inorganic chemistry*, Wiley New York.
- Couch, R., and Riddihough, R., 1989, The crustal structure of the western continental margin of North America: *Geophysical Framework of the Continental United States*, v. 172, p. 103-128.
- Crider, J. G., 2001, Oblique slip and the geometry of normal-fault linkage: mechanics and a case study from the Basin and Range in Oregon: *Journal of Structural Geology*, v. 23, no. 12, p. 1997-2009.
- Crowley, T. J., 2000, Causes of Climate Change Over the Past 1000 Years: *Science*, v. 289, no. 5477, p. 270-277.
- Davies, J. H., and Stevenson, D., 1992, Physical model of source region of subduction zone volcanics: *Journal of Geophysical Research: Solid Earth (1978–2012)*, v. 97, no. B2, p. 2037-2070.
- Donath, F. A., 1962, Analysis of Basin-Range structure, south-central Oregon: *Geological Society of America Bulletin*, v. 73, no. 1, p. 1-16.

- du Bray, E. A., and John, D. A., 2011, Petrologic, tectonic, and metallogenic evolution of the Ancestral Cascades magmatic arc, Washington, Oregon, and northern California: *Geosphere*, v. 7, no. 5, p. 1102-1133.
- Duncan, R. A., 1982, A captured island chain in the coast range of Oregon and Washington: *Journal of Geophysical Research: Solid Earth*, v. 87, no. B13, p. 10827-10837.
- Duncan, R. A., and Kulm, L., 1989, Plate tectonic evolution of the Cascades arc-subduction complex: *The Eastern Pacific Ocean and Hawaii*, v. 1, p. 413-438.
- Eastoe, C., Long, A., Land, L. S., and Kyle, J. R., 2001, Stable chlorine isotopes in halite and brine from the Gulf Coast Basin: brine genesis and evolution: *Chemical Geology*, v. 176, no. 1, p. 343-360.
- Eastoe, C., and Peryt, T., 1999, Stable chlorine isotope evidence for non-marine chloride in Badenian evaporites, Carpathian mountain region: *Terra Nova*, v. 11, no. 2-3, p. 118-131.
- Eastoe, C., Peryt, T., Petrychenko, O. Y., and Geisler-Cussey, D., 2007, Stable chlorine isotopes in Phanerozoic evaporites: *Applied Geochemistry*, v. 22, no. 3, p. 575-588.
- Eggenkamp, H., Kreulen, R., and Koster van Groos, A., 1995, Chlorine stable isotope fractionation in evaporites: *Geochimica et Cosmochimica Acta*, v. 59, no. 24, p. 5169-5175.

- Fischer, T. P., 2008, Fluxes of volatiles (H<sub>2</sub>O, CO<sub>2</sub>, N<sub>2</sub>, Cl, F) from arc volcanoes: *Geochemical Journal*, v. 42, no. 1, p. 21-38.
- Gaschnig, R. M., Vervoort, J. D., Lewis, R. S., and McClelland, W. C., 2010, Migrating magmatism in the northern US Cordillera: in situ U–Pb geochronology of the Idaho batholith: *Contributions to Mineralogy and Petrology*, v. 159, no. 6, p. 863-883.
- Giggenbach, W., 1992, Isotopic shifts in waters from geothermal and volcanic systems along convergent plate boundaries and their origin: *Earth and Planetary Science Letters*, v. 113, no. 4, p. 495-510.
- Godon, A., Jendrzewski, N., Castrec-Rouelle, M., Dia, A., Pineau, F., Boulègue, J., and Javoy, M., 2004, Origin and evolution of fluids from mud volcanoes in the Barbados accretionary complex: *Geochimica et Cosmochimica Acta*, v. 68, no. 9, p. 2153-2165.
- Green, N. L., and Harry, D. L., 1999, On the relationship between subducted slab age and arc basalt petrogenesis, Cascadia subduction system, North America: *Earth and planetary science letters*, v. 171, no. 3, p. 367-381.
- Grove, T. L., Chatterjee, N., Parman, S. W., and Médard, E., 2006, The influence of H<sub>2</sub>O on mantle wedge melting: *Earth and Planetary Science Letters*, v. 249, no. 1, p. 74-89.

- Hacker, B. R., Abers, G. A., and Peacock, S. M., 2003, Subduction factory 1. Theoretical mineralogy, densities, seismic wave speeds, and H<sub>2</sub>O contents: *Journal of Geophysical Research*, v. 108, no. B1, p. 2029.
- Hedenquist, J. W., and Lowenstern, J. B., 1994, The role of magmas in the formation of hydrothermal ore deposits: *Nature*, v. 370, no. 6490, p. 519-527.
- Hervig, R. L., Moore, G. M., Williams, L. B., Peacock, S. M., Holloway, J. R., and Roggensack, K., 2002, Isotopic and elemental partitioning of boron between hydrous fluid and silicate melt: *American Mineralogist*, v. 87, no. 5-6, p. 769-774.
- Hildreth, W., 2007, Quaternary magmatism in the Cascades-geologic perspectives: US Geological Survey professional paper, no. 1744, p. 1-125.
- Hilton, D., Hammerschmidt, K., Teufel, S., and Friedrichsen, H., 1993, Helium isotope characteristics of Andean geothermal fluids and lavas: *Earth and Planetary Science Letters*, v. 120, no. 3, p. 265-282.
- Hilton, D. R., Fischer, T. P., and Marty, B., 2002, Noble gases and volatile recycling at subduction zones: *Reviews in mineralogy and geochemistry*, v. 47, no. 1, p. 319-370.
- Honda, S., 1985, Thermal structure beneath Tohoku, northeast Japan: *Tectonophysics*, v. 112, no. 1, p. 69-102.
- Hooper, P. R., 1997, The Columbia River flood basalt province: current status: *Geophysical Monograph Series*, v. 100, p. 1-27.

- Hurwitz, S., Mariner, R. H., Fehn, U., and Snyder, G. T., 2005, Systematics of halogen elements and their radioisotopes in thermal springs of the Cascade Range, Central Oregon, Western USA: *Earth and Planetary Science Letters*, v. 235, no. 3, p. 700-714.
- Ingebritsen, S., Sherrod, D., and Mariner, R., 1989, Heat flow and hydrothermal circulation in the Cascade Range, north-central Oregon: *Science*, v. 243, no. 4897, p. 1458-1462.
- Ingebritsen, S. E., Mariner, R. H., and Sherrod, D. R., 1991, Hydrothermal systems of the Cascade Range, north-central Oregon: Available from Books and Open Files Reports Section, USGS Box 25425, Denver, CO 80225. USGS Open File Report 91-69, 1991. 217 p, 33 fig, 10 tab, 168 ref, append.
- Irwin, W. P., 1972, Terranes of the western Paleozoic and Triassic belt in the southern Klamath Mountains, California: *US Geol. Surv. Prof. Pap.*, v. 800, p. 103-111.
- Irwin, W. P., 1985, Age and tectonics of plutonic belts in accreted terranes of the Klamath Mountains, California and Oregon.
- Iwamori, H., 1998, Transportation of H<sub>2</sub>O and melting in subduction zones: *Earth and Planetary Science Letters*, v. 160, no. 1, p. 65-80.
- James, E. R., Manga, M., and Rose, T. P., 1999, CO<sub>2</sub> degassing in the Oregon Cascades: *Geology*, v. 27, no. 9, p. 823-826.

- John, T., Layne, G. D., Haase, K. M., and Barnes, J. D., 2010, Chlorine isotope evidence for crustal recycling into the Earth's mantle: *Earth and Planetary Science Letters*, v. 298, no. 1–2, p. 175-182.
- John, T., Scambelluri, M., Frische, M., Barnes, J. D., and Bach, W., 2011, Dehydration of subducting serpentinite: Implications for halogen mobility in subduction zones and the deep halogen cycle: *Earth and Planetary Science Letters*, v. 308, no. 1–2, p. 65-76.
- Kaufmann, R., Frapé, S., Fritz, P., and Bentley, H., 1987, Chlorine stable isotope composition of Canadian Shield brines: Saline water and gases in crystalline rocks, *Special Paper—Geological Association of Canada*, v. 33, p. 89-93.
- Kaufmann, R., Long, A., Bentley, H., and Davis, S., 1984, Natural chlorine isotope variations: *Nature*, v. 309, no. 5966, p. 338-340.
- Kaufmann, R. S., Frapé, S., McNutt, R., and Eastoe, C., 1993, Chlorine stable isotope distribution of Michigan Basin formation waters: *Applied geochemistry*, v. 8, no. 4, p. 403-407.
- Kendrick, M. A., Woodhead, J. D., and Kamenetsky, V. S., 2012, Tracking halogens through the subduction cycle: *Geology*, v. 40, no. 12, p. 1075-1078.
- Kilinc, I. A., and Burnham, C. W., 1972, Partitioning of Chloride Between a Silicate Melt and Coexisting Aqueous Phase from 2 to 8 Kilobars: *Economic Geology*, v. 67, no. 2, p. 231-235.

- Kodolányi, J., and Pettke, T., 2011, Loss of trace elements from serpentinites during fluid-assisted transformation of chrysotile to antigorite—an example from Guatemala: *Chemical Geology*, v. 284, no. 3, p. 351-362.
- Leeman, W. P., Lewis, J. F., Evarts, R. C., Conrey, R. M., and Streck, M. J., 2005, Petrologic constraints on the thermal structure of the Cascades arc: *Journal of Volcanology and Geothermal Research*, v. 140, no. 1-3, p. 67-105.
- Leeman, W. P., Smith, D. R., Hildreth, W., Palacz, Z., and Rogers, N., 1990, Compositional diversity of late Cenozoic basalts in a transect across the southern Washington Cascades: implications for subduction zone magmatism: *Journal of Geophysical Research*, v. 95, no. B12, p. 19561-19519,19582.
- Leeman, W. P., Tonarini, S., Chan, L. H., and Borg, L. E., 2004, Boron and lithium isotopic variations in a hot subduction zone - the southern Washington Cascades: *Chemical Geology*, v. 212, no. 1-2, p. 101-124.
- Magill, J. R., Wells, R. E., Simpson, R. W., and Cox, A. V., 1982, Post 12 my rotation of southwest Washington: *Journal of Geophysical Research: Solid Earth (1978–2012)*, v. 87, no. B5, p. 3761-3776.
- Manning, C. E., 2004, The chemistry of subduction-zone fluids: *Earth and Planetary Science Letters*, v. 223, no. 1, p. 1-16.
- Mariner, R., Presser, T., Evans, W., and Pringle, M., 1990, Discharge rates of fluid and heat by thermal springs of the Cascade Range, Washington, Oregon, and northern

- California: *Journal of Geophysical Research: Solid Earth* (1978–2012), v. 95, no. B12, p. 19517-19531.
- Mariner, R., Swanson, J., Orris, G., Presser, T., and Evans, W., 1981, Chemical and isotopic data for water from thermal springs and wells of Oregon: Geological Survey, Menlo Park, CA (USA).
- Mariner, R. H., Evans, W. C., Presser, T. S., and White, L. D., 2003, Excess nitrogen in selected thermal and mineral springs of the Cascade Range in northern California, Oregon, and Washington: sedimentary or volcanic in origin?: *Journal of Volcanology and Geothermal Research*, v. 121, no. 1–2, p. 99-114.
- McBirney, A. R., 1978, Volcanic Evolution of Cascade Range: *Annual Review of Earth and Planetary Sciences*, v. 6, p. 437-456.
- Miller, K. C., Keller, G. R., Gridley, J. M., Luetgert, J. H., Mooney, W. D., and Thybo, H., 1997, Crustal structure along the west flank of the Cascades, western Washington: *Journal of Geophysical Research: Solid Earth*, v. 102, no. B8, p. 17857-17873.
- Miller, R. B., 1989, The Mesozoic Rimrock Lake inlier, southern Washington Cascades: Implications for the basement to the Columbia Embayment: *Geological Society of America Bulletin*, v. 101, no. 10, p. 1289-1305.
- Musashi, M., Oi, T., Eggenkamp, H. G., and Matsuo, M., 2008, Chlorine isotope fractionation associated with volcanic activity at the Kusatsu-Bandaiko hot spring in Japan: *Isotopes in environmental and health studies*, v. 44, no. 3, p. 305-313.

- Nicholls, I., and Ringwood, A., 1973, Effect of water on olivine stability in tholeiites and the production of silica-saturated magmas in the island-arc environment: *The Journal of Geology*, p. 285-300.
- Norris, R. M., and Webb, R. W., 1990, *Geology of California*, New York, John Wiley & Sons, Inc.
- Palmer, M., London, D., Morgan, G., and Babb, H., 1992, Experimental determination of fractionation of  $^{11}\text{B} / ^{10}\text{B}$  between tourmaline and aqueous vapor: A temperature- and pressure-dependent isotopic system: *Chemical Geology: Isotope Geoscience section*, v. 101, no. 1, p. 123-129.
- Peacock, S. A., 1990, Fluid processes in subduction zones: *Science*, v. 248, no. 4953, p. 329-337.
- Peacock, S. M., 1996, Thermal and petrologic structure of subduction zones: *Geophysical Monograph Series*, v. 96, p. 119-133.
- Pinti, D., Castro, M., Shoaukar-Stash, O., Tremblay, A., Garduño, V., Hall, C., Hélie, J., and Ghaleb, B., 2012, Evolution of the geothermal fluids at Los Azufres, Mexico, as traced by noble gas isotopes,  $\delta^{18}\text{O}$ ,  $\delta\text{D}$ ,  $\delta^{13}\text{C}$  and  $^{87}\text{Sr} / ^{86}\text{Sr}$ : *Journal of Volcanology and Geothermal Research*.
- Priest, G. R., 1990, Volcanic and tectonic evolution of the Cascade Volcanic Arc, central Oregon: *Journal of Geophysical Research: Solid Earth*, v. 95, no. B12, p. 19583-19599.

- Ransom, B., Spivack, A. J., and Kastner, M., 1995, Stable Cl isotopes in subduction-zone pore waters: Implications for fluid-rock reactions and the cycling of chlorine: *Geology*, v. 23, no. 8, p. 715-718.
- Reiners, P. W., Hammond, P. E., McKenna, J. M., and Duncan, R. A., 2000, Young basalts of the central Washington Cascades, flux melting of the mantle, and trace element signatures of primary arc magmas: *Contributions to Mineralogy and Petrology*, v. 138, no. 3, p. 249-264.
- Riley, J. P., and Chester, R., 1971, *Introduction to marine chemistry*.
- Rizzo, A. L., Caracausi, A., Liotta, M., Paonita, A., Barnes, J. D., Corsaro, R. A., and Martelli, M., 2013, Chlorine isotope composition of volcanic gases and rocks at Mount Etna (Italy) and inferences on the local mantle source: *Earth and Planetary Science Letters*.
- Robock, A., 2000, Volcanic eruptions and climate: *Reviews of Geophysics*, v. 38, no. 2, p. 191-219.
- Rondenay, S., Abers, G. A., and van Keken, P. E., 2008, Seismic imaging of subduction zone metamorphism: *Geology*, v. 36, no. 4, p. 275-278.
- Rowe, M. C., Kent, A. J., and Nielsen, R. L., 2009, Subduction influence on oxygen fugacity and trace and volatile elements in basalts across the Cascade Volcanic Arc: *Journal of Petrology*, v. 50, no. 1, p. 61-91.

- Rüpke, L. H., Morgan, J. P., Hort, M., and Connolly, J. A., 2004, Serpentine and the subduction zone water cycle: *Earth and Planetary Science Letters*, v. 223, no. 1, p. 17-34.
- Ruscitto, D., Wallace, P., Johnson, E., Kent, A., and Bindeman, I., 2010, Volatile contents of mafic magmas from cinder cones in the Central Oregon High Cascades: Implications for magma formation and mantle conditions in a hot arc: *Earth and Planetary Science Letters*, v. 298, no. 1, p. 153-161.
- Ruscitto, D., Wallace, P., and Kent, A., 2011, Revisiting the compositions and volatile contents of olivine-hosted melt inclusions from the Mount Shasta region: implications for the formation of high-Mg andesites: *Contributions to Mineralogy and Petrology*, v. 162, no. 1, p. 109-132.
- Saar, M. O., Castro, M. C., Hall, C. M., Manga, M., and Rose, T. P., 2005, Quantifying magmatic, crustal, and atmospheric helium contributions to volcanic aquifers using all stable noble gases: Implications for magmatism and groundwater flow: *Geochemistry, Geophysics, Geosystems*, v. 6, no. 3, p. Q03008.
- Schmidt, M. E., Grunder, A. L., and Rowe, M. C., 2008, Segmentation of the Cascade Arc as indicated by Sr and Nd isotopic variation among diverse primitive basalts: *Earth and Planetary Science Letters*, v. 266, no. 1–2, p. 166-181.
- Schmidt, M. W., and Poli, S., 1998, Experimentally based water budgets for dehydrating slabs and consequences for arc magma generation: *Earth and Planetary Science Letters*, v. 163, no. 1, p. 361-379.

- Schnetger, B., and Muramatsu, Y., 1996, Determination of halogens, with special reference to iodine, in geological and biological samples using pyrohydrolysis for preparation and inductively coupled plasma mass spectrometry and ion chromatography for measurement: *Analyst*, v. 121, no. 11, p. 1627-1631.
- Sharp, Z., Barnes, J., Brearley, A., Chaussidon, M., Fischer, T., and Kamenetsky, V., 2007, Chlorine isotope homogeneity of the mantle, crust and carbonaceous chondrites: *Nature*, v. 446, no. 7139, p. 1062-1065.
- Sharp, Z., Barnes, J., Fischer, T., and Halick, M., 2010, An experimental determination of chlorine isotope fractionation in acid systems and applications to volcanic fumaroles: *Geochimica et Cosmochimica Acta*, v. 74, no. 1, p. 264-273.
- Sharp, Z., Mercer, J., Jones, R., Brearley, A., Selverstone, J., Bekker, A., and Stachel, T., 2013, The chlorine isotope composition of chondrites and Earth: *Geochimica et Cosmochimica Acta*, v. 107, p. 189-204.
- Sherrod, D. R., and Smith, J. G., 2000, Geologic map of upper Eocene to Holocene volcanic and related rocks of the Cascade Range, Oregon, US Geological Survey.
- Shouakar-Stash, O., Alexeev, S., Frape, S., Alexeeva, L., and Drimmie, R., 2007, Geochemistry and stable isotopic signatures, including chlorine and bromine isotopes, of the deep groundwaters of the Siberian Platform, Russia: *Applied geochemistry*, v. 22, no. 3, p. 589-605.
- Smith, J. G., 1993, Geologic map of upper Eocene to Holocene volcanic and related rocks in the Cascade Range, Washington, U.S. Geological Survey Miscellaneous

Investigations Series Map I-2005, scale 1:500,000.

Snoke, A. W., and Barnes, C. G., 2006, The development of tectonic concepts for the Klamath Mountains province, California and Oregon: Special Papers-Geological Society of America, v. 410, p. 1.

Spivack, A. J., Kastner, M., and Ransom, B., 2002, Elemental and isotopic chloride geochemistry and fluid flow in the Nankai Trough: Geophysical research letters, v. 29, no. 14, p. 1661.

Stanley, W. D., Finn, C., and Plesha, J. L., 1987, Tectonics and conductivity structures in the Southern Washington Cascades: Journal of Geophysical Research: Solid Earth, v. 92, no. B10, p. 10179-10193.

Stern, R. J., 2002, Subduction zones: Reviews of Geophysics, v. 40, no. 4, p. 3-1-3-38.

Stewart, M. A., and Spivack, A. J., 2004, The stable-chlorine isotope compositions of natural and anthropogenic materials: Reviews in mineralogy and geochemistry, v. 55, no. 1, p. 231-254.

Syracuse, E. M., van Keken, P. E., and Abers, G. A., 2010, The global range of subduction zone thermal models: Physics of the Earth and Planetary Interiors, v. 183, no. 1, p. 73-90.

Tatsumi, Y., 2005, The subduction factory: How it operates in the evolving Earth: GSA today, v. 15, no. 7, p. 4.

- Taylor, E. M., 1990, Volcanic history and tectonic development of the central High Cascade Range, Oregon: *Journal of Geophysical Research*, v. 95, no. B12, p. 19611-19619,19622.
- Vengosh, A., Starinsky, A., Kolodny, Y., and Chivas, A. R., 1991, Boron isotope geochemistry as a tracer for the evolution of brines and associated hot springs from the Dead Sea, Israel: *Geochimica et cosmochimica acta*, v. 55, no. 6, p. 1689-1695.
- Verplanck, E. P., and Duncan, R. A., 1987, Temporal variations in plate convergence and eruption rates in the Western Cascades, Oregon: *Tectonics*, v. 6, no. 2, p. 197-209.
- Villemant, B. t., and Boudon, G., 1999, H<sub>2</sub>O and halogen (F, Cl, Br) behaviour during shallow magma degassing processes: *Earth and Planetary Science Letters*, v. 168, no. 3, p. 271-286.
- von Huene, R., and Scholl, D. W., 1991, Observations at convergent margins concerning sediment subduction, subduction erosion, and the growth of continental crust: *Reviews of Geophysics*, v. 29, no. 3, p. 279-316.
- Vong, R. J., Hansson, H.-C., Ross, H. B., Covert, D. S., and Charlson, R. J., 1988, Northeastern Pacific submicrometer aerosol and rainwater composition: A multivariate analysis: *Journal of Geophysical Research*, v. 93, no. D2, p. 1625-1637.
- Wallace, P. J., 2005, Volatiles in subduction zone magmas: concentrations and fluxes based on melt inclusion and volcanic gas data: *Journal of Volcanology and Geothermal Research*, v. 140, no. 1, p. 217-240.

- Waring, G. A., Blankenship, R. R., and Bentall, R., 1965, Thermal springs of the United States and other countries of the world: a summary, US Government Printing Office Washington, DC.
- Weaver, C. S., and Baker, G. E., 1988, Geometry of the Juan de Fuca plate beneath Washington and northern Oregon from seismicity: *Bulletin of the Seismological Society of America*, v. 78, no. 1, p. 264-275.
- Wells, R. E., 1990, Paleomagnetic rotations and the cenozoic tectonics of the Cascade Arc, Washington, Oregon, and California: *Journal of Geophysical Research: Solid Earth*, v. 95, no. B12, p. 19409-19417.
- Wilson, D. S., 1988, Tectonic history of the Juan de Fuca Ridge over the last 40 million years: *Journal of Geophysical Research: Solid Earth (1978–2012)*, v. 93, no. B10, p. 11863-11876.
- Wilson, D. S., 2002, The Juan de Fuca plate and slab: Isochron structure and Cenozoic plate motions: *The Cascadia Subduction Zone and Related Subduction Systems—Seismic Structure, Intraslab Earthquakes and Processes, and Earthquake Hazards*, v. 2, p. 9.
- Yeats, R. S., Graven, E. P., Werner, K. S., Goldfinger, C., and Popowski, T., 1996, Tectonics of the Willamette Valley, Oregon: Assessing earthquake hazards and reducing risk in the Pacific Northwest: *US Geological Survey Professional Paper*, v. 1560, p. 183-222.

Zajacz, Z., Candela, P. A., Piccoli, P. M., and Sanchez-Valle, C., 2012, The partitioning of sulfur and chlorine between andesite melts and magmatic volatiles and the exchange coefficients of major cations: *Geochimica et Cosmochimica Acta*, v. 89, no. 0, p. 81-101.

Zhang, M., Hobbs, M.Y., Frapé, S.K., Nordstrom, D.K., Ball, J.W., and McCleskey, R.B., 2004, Stable chlorine isotopic composition of geothermal waters from Yellowstone National Park, in Wany, R.B., and Seal, R.R., eds.: *Water-Rock Interactions: Proceedings of the Eleventh International Symposium on water-rock interaction*, v. Volume 1, p. p. 233-236.